TECHNISCHE UNIVERSITÄT MÜNCHEN

Fakultät für Elektrotechnik und Informationstechnik

Lehrstuhl für Nanoelektronik

Solution-Processable Carbon Nanotube Devices for Biosensing Applications

Vijay Deep Bhatt

Vollständiger Abdruck der von der Fakultät für Elektrotechnik und Informationstechnik

der Technischen Universität München zur Erlangung des akademischen Grades eines

Doktor-Ingenieurs (Dr.-Ing.)

genehmigten Dissertation.

Vorsitzende(r):   Prof. Dr.-Ing. Klaus Diepold

Prüfer der Dissertation:

      1. Prof. Paolo Lugli, Ph.D.

      2. Prof. Dr. Oliver Hayden

Die Dissertation wurde am 18.04.2018 bei der Technischen Universität München

eingereicht und durch die Fakultät für Elektrotechnik und Informationstechnik

am 06.08.2018 angenommen.

Abstract

Research in the field of flexible and printed electronics has led to continuous decrease in the production costs of electronic devices. Simultaneously, significant advances have been made in sensor technologies based on solution-processable novel nanomaterials. Combination of these technologies has paved the path for the production of disposable biosensors that can be used in early diagnosis of several diseases, hence improving the quality of life.

In the present work, development of electrolyte-gated carbon nanotube field effect transistor (CNTFET) for biosensing applications was carried out. Towards this aim carbon nanotubes (CNT) were initially tested for their biocompatibility and use as an electrode material. After they were proven to be biocompatible, CNT electrodes were employed for impedance measurements. To achieve integration of spray deposited CNT electrodes with 3D printing, test chips were produced which combine these additive technologies. An entirely solution processable electrolyte gated CNTFET was developed next, with the aim of lowering the overall device cost. To understand the impact of geometrical factors and materials used for transistor fabrication, different architectures were studied. This led to the development of multi-analyte sensor array. Devices with a single gate to control multiple semiconducting channels or multiple gates for controlling single semiconducting channels were developed. Using functionalisation schemes towards sensing of specific ions, arrays capable of simultaneous detection of multiple ions were demonstrated.

Using these transistors as the sensing platform, biosensors for different classes of biochemicals were developed. Ion sensors for Na^+, K^+, NH_4^+, Mg^{2+}, $H_2PO_4^-$, NO_3^- were demonstrated. Further, enzymaztic sensors were explored. Enzymes like glucose oxidase and lactate oxidase were used for the detection of glucose and lactate. Detection of organophosphate pesticide is demonstrated by monitoring the activity of enzyme acetylcholinesterase. Dopamine sensors based on modulation of charge in double layer capacitor were developed with sensitivity up to 10 fM. To isolate carbon nanotubes from unknown chemical environment extended gate architecture was explored and its use as DNA sensor was demonstrated. The electrolyte gated CNTFET platform for biosensors offers a unique prospect to realize the goal of cost-effective point-of-care diagnostics.

Zusammenfassung

Forschung im Feld von flexible und gedruckte Elektronik führte zu einer kontinuierlichen Senkung der Produktionskosten von elektronischen Geräten. Gleichzeitig wurden Fortschritte im Bereich der Sensortechnologien erzielt basierend auf neuartigen Nanomaterialien. Die Kombination dieser Technologien hat den Weg für die Herstellung von Einweg-Biosensoren geebnet, die zur Früherkennung verschiedener Krankheiten eingesetzt werden können und somit die Lebensqualität verbessern.

In dieser Arbeit wurde ein elektrolytgesteuerter Kohlenstoff-Nanoröhren-Feld-Effekt-Transistor (CNTFET) für biosensorische Anwendungen entwickelt. Dazu wurden zunächst Kohlenstoff-Nanoröhren (CNT) auf ihre Biokompatibilität getestet und als Elektrodenmaterial eingesetzt. Nachdem sie sich als biokompatibel erwiesen hatten, wurden CNT-Elektroden für die Impedanzmessungen eingesetzt. Um eine erfolgreiche Integration von sprühbeschichteten CNT-Elektroden mit 3D-Druck zu erreichen, wurden Testchips hergestellt, die diese Additivtechnologien kombinieren. Als nächster Schritt wurde ein vollständig lösungsverarbeitbarer elektrolytgesteuerter CNTFET entwickelt, mit dem Ziel, die Gesamtkosten des Gerätes zu senken. Um die Auswirkungen von geometrischen Faktoren und Materialien für die Transistorfertigung zu verstehen, wurden verschiedene Architekturen untersucht. Dies führte zur Entwicklung eines Multi-Analyten-Sensorarrays. Es wurden Geräte mit einem einzigen Gate zur Steuerung mehrerer halbleitender Kanäle oder mehreren Gates zur Steuerung einzelner halbleitender Kanäle entwickelt. Mit Hilfe von Funktionalisierungsschemata zur Erfassung von spezifischen Ionen wurden Arrays demonstriert, die in der Lage sind, mehrere Ionen gleichzeitig zu detektieren.

Mit diesen Transistoren als Sensorplattform wurden Biosensoren für verschiedene Klassen von Biochemikalien entwickelt. Ionen Sensoren für Na^+, K^+, NH_4^+, Mg^{2+}, $H_2PO_4^-$, NO_3^- wurden bewiesen. Weitere enzymbasierte Sensoren wurden untersucht. Enzyme wie Glucoseoxidase und Laktatoxidase wurden für die Erkennung von Glucose und Laktat benutzt. Der Nachweis von phosphororganischen Pestiziden ist durch die Beobachtung der Enzymaktivität Acetylcholinesterase bewiesen. Der Dopamin Sensor basiert auf die Ladungsänderung der Doppelschichtkapazität und weist eine Empfindlichkeit bis zu 10 fM auf. Um Kohlenstoff-Nanoröhren aus unbekannter chemischer Umgebung zu isolieren, wurde eine erweiterte Gate-Architektur erforscht und deren nutzen als DNA Sensor gezeigt. Die elektrolytgesteuerte CNTFET-Plattform für Biosensoren bietet eine einzigartige Möglichkeit, das Ziel der kostengünstige Point-of-Care Diagnostik zu realisieren.

Contents

List of Figures

List of Tables

Chapter 1

Introduction

1.1 Introduction

Human endeavour to continuously improve the quality of life, and understanding the ever-changing environment demands sensory input. This need has lead to the development of various sensing technologies empowering us to measure the physical surroundings. From the days of doctors tasting urine for diagnosis of diabetes to modern glucose meters, sensors capable of detecting chemicals have progressed tremendously. Despite this technological progress, world health organisation estimates around 400 million people lack essential medical care. With such a large number of people without appropriate medical care, there is much to improve. A medical practitioner can recommend medication only after a successful diagnosis of illness. Assisted by imaging techniques and blood tests many diseases can be cured with small expense if diagnosed in early stage. However, with high test costs, and unavailability of the immediate test report it is often not done. By the time the diagnosis report is available the disease might have progressed towards a worse state. This situation can be vastly improved by developing low-cost sensors which can provide immediate test results. Not only it saves test costs but brings benefits of fast treatment leading to better life quality and mortality rate.

Novel nanomaterials help to achieve the goal of affordable diagnostic devices. New devices are under continuous research, and many such systems are proposed by academic and research institutions. These sensors combined with telemedicine or perhaps one day with an artificially intelligent health monitoring system have

potential to improve human health and enable better environment globally. Sophisticated sensing devices capable of determining trace levels of chemicals exist but are incredibly expensive and outside the reach of most of the population. Even if they were affordable, they are still bulky and would not be practical to use near a patient. Nanomaterial-based sensors have risen as a viable alternative to traditional sensors; they promise low cost, high sensitivity and small form factor to quantify a large class of chemicals. Their sphere of influence range from environmental monitoring, industrial use, wastewater management and of course a medical point of care device. In this work, as nanomaterial carbon nanotube is used for fabrication of biosensors. Transistor fabricated using random carbon nanotube network and gated by an aqueous electrolyte forms the biosensing platform. Its use in monitoring cell proliferation, as an ion sensor, or as a glucose and lactate sensor is examined. The same platform is further used for detection of neurotransmitters dopamine and acetylcholine. DNA detection is also tested with a so-called extended gate architecture.

Chapter 2 presents state-of-art of biosensors and various methods with promising future. Chapter 3 introduces electrolyte gated carbon nanotube transistor their working and its use as a biosensor. Material properties and fabrication techniques are also introduced which were used during this thesis. Chapter 4 demonstrates a transistor fabricated entirely from carbon nanotubes. Their use as an electrode material for monitoring cell cultures is presented. An extended gate device architecture and its advantages are also de discussed. Various biosensors developed during this work are presented in chapter 5. Finally, chapter 6 presents views of the author regarding challenges faced in bringing these sensors from academic laboratories to clinical use and hurdles that must be overcome for achieving a real point-of-care diagnostic device.

Chapter 2

BioSensors: State of Art

International Union of Pure and Applied Chemistry (IUPAC) defines biosensor as *"A device that uses specific biochemical reactions mediated by isolated enzymes, immunosystems, tissues, organelles or whole cells to detect chemical compounds usually by electrical, thermal or optical signals "* [8].

In general, the major requisites of a biosensors are

1. There should be a biochemical reaction.

2. Biological mediator should be part of it.

3. A transduction mechanism should be involved in detection of chemical composition and the final readout.

Five major components of the biosensors are shown in Figure 2.1. Further, a biosensor can be broadly classified according to the type of analyte, reaction mediating agent, and transduction mechanism used. In the below sections we discuss the different biosensors and the sensing mechanisms in detail.

2.1   Transduction Principles

Word "Transducer" implies a device responsible for the conversion of a physical quantity from one form to another. In case of a biosensor, the physical parameters converted are typically charge, mass, light intensity, heat, pH, material property such as resistivity or dielectric constant. For easy data processing and storage, final

3
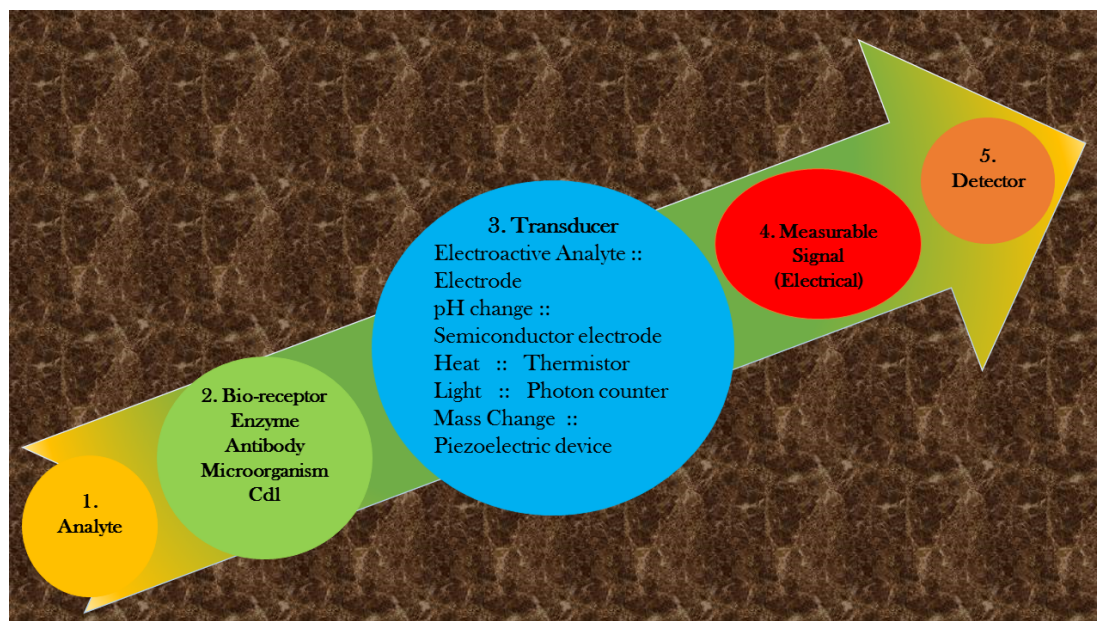
FIGURE 2.1: Different stages of a biosensor

output in the form of electronic signal is often desired. We will review further the sensors based on the following major transducing categories.

1. Charge

2. Light intensity

3. Mass

4. Dielectric constant

2.1.1 Charge based biosensor

Sensors based on detection of charged species in a chemical environment represent one of the important class of biosensors. Further progress in field of electrochemistry led to the production of one of the earliest chemical sensor, i.e. the pH sensor [9], which was a charge based sensor. Such biosensors fall into three major categories

1. Potentiometric: to detect the influence of charge in such a way that the biorecognition event is in direct correlation with voltage measured.

2. Amperometric: measuring the change of electric current between two electrodes upon the alteration in the concentration of biochemical. One of the

earliest biosensor, i.e. glucose meter introduced by Leland C. Clark at the New York Academy of Sciences Symposium in 1962 is based on such electrochemical technique [10].

3. Conductometric: It utilises the variation in the electrical conductivity of the sample as an indicator of change in the concentration of biochemical.

As in any electrochemical cell, a minimum of two electrodes are separated by an electrolyte and either a voltage is applied and resulting current is measured (amperometric sensor), or directly the cell voltage is measured (potentiometric sensors). In all of these methods, two rules must always be obeyed.

1. At interface the charges can separate but, overall the electrochemical cell remains neutral.

2. The electrical circuit should always form a closed loop, i.e. at least two electrodes are present and form the closed path for the signal. In this arrangement, depending on nature of interfaces, steady state current can be conditionally present.

2.1.1.1 Potentiometric sensors

The property which forms the basis for these sensors is the chemical potential μ and is related to the free energy G, a thermodynamic property given by equation 2.1

$$\mu_i = \left(\frac{\delta G}{\delta n}\right)_{T,P,j\neq i} = RT ln a_i \tag{2.1}$$

where n is the quantity of species i with activity a_i. If these chemical species are charged then, the relation also includes term contributing electrical work, and it can be re-written as equation 2.2

$$\tilde{\mu}_i = \mu_i \pm zF\varphi \tag{2.2}$$

At equilibrium, dG = 0, therefore

$$dG = \Sigma\tilde{\mu}_i dn_i = 0. \tag{2.3}$$

This is the Gibbs equation, and it explains the interfacial potential π given as

$$\pi = \varphi^m - \varphi^S = \frac{\mu_i^{0,S} - \mu_i^{0,m}}{z_i F} + \frac{RT}{z_i F} ln \frac{a_i^S}{a_i^m} \qquad (2.4)$$

Here a_i^m is the activity of the species i in the metallic phase and a_i^S is the activity in the solution phase . Thus rewriting 2.4 we obtain the Nernst equation.

$$\pi = \pi^0 + \frac{RT}{z_i F} ln a_i^S \qquad (2.5)$$

If a metal separates a solution (which contains the corresponding metallic ions i) in two sections such that each solution section has a different concentration of i then there exists a potential difference between the two sections of solutions given by

$$\pi = \frac{RT}{z F} ln \frac{a_i^1}{a_1^2}. \qquad (2.6)$$

Here 1, 2 represent the two sections separated by the metal which can exchange species i (typically metal cation). If we select any other permeable membrane instead of the metal to separate the solutions, we will get the same potential given that the species i can move across the membrane. This principle enables ion selective electrodes and ion selective field effect transistor based sensors. If the activity of species i on one side of the membrane is fixed, then the measured potential directly correlates to the concentration of i on other side. It should be noted that such sensors are logarithmically related to concentration change. At 25^oC, the sensitivity is around 60mV for monovalent species.

This idea has been extended to the field effect transistors where effective gate voltage becomes a function of ion activity, due to above mentioned Nernst potential. The drain current then becomes a measure of the ion concentration. This idea was introduced by P. Bergveld [11], and one of the first ion sensitive ion selective field effect transistor using membrane was introduced by Moss et al. [12]. They used transistor gate potential as the function of potassium concentration which results in the drain current variation. More detail on ISFET and their adaptation to sense biological substances will be discussed in chapter 3. However before continuing to other sensing principles few important observations about potentiometric sensors are listed below,

1. There is no specific constraint on the response time of the sensor. The only necessary requirement is that of thermodynamic equilibrium.

2. There is no restriction on the size of the sensor.

Thus in principle, miniaturised devices with fast response time are indeed a possibility. Ion-selective sensors constitute majority of potentiometric sensors. A typical example is pH sensor, where doped glass membrane acts as a selective membrane for H^+ ion. However strictly speaking pH sensor by itself cannot be considered as biosensor unless it involves the use of a biochemical reaction.

Building on the principle of ion-selective electrodes, several bioreactions which produce ions as a byproduct has been used for fabrication of biosensors. Zhybak et al. used NH_4^+ as the reporter ion for detection of urea, as well as creatinine [13]. Several groups have used H^+ ion, which is often, a byproduct of reactions catalysed by enzymes, to quantify initial substrate concentration [14, 15]. Chemical reactions given below presents reaction paths for various biosensors based on potentiometric techniques.

Hydrogen ion based reaction paths

$$penicillin \xrightarrow{\text{penicillinase}} penicilloicacid + H^+ \tag{2.7}$$

$$D - glucose + O_2 \xrightarrow{glucose\,oxidase + H_2O} D - gluconate + H^+ \tag{2.8}$$

$$lipids \xrightarrow{\text{lipase}} glycerol + fattyacids + H^+ \tag{2.9}$$
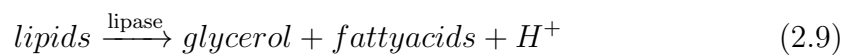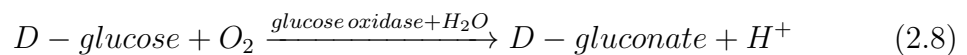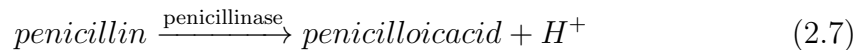
Ammonium cation based reaction paths

$$Urea \xrightarrow{Urease} 2.NH_4^+ + CO_3^{2-} \tag{2.10}$$

$$L - aminoacid + O_2 + H_2O \xrightarrow{L-aminoacidoxidase} Ketoacid + NH_4^+ + H_2O_2 \tag{2.11}$$
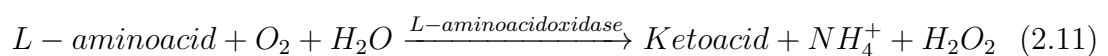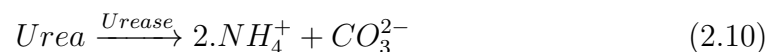
Cyanide anion based reaction paths

$$amygdalin + 2H_2O \xrightarrow{\beta glucosidase} 2glucose + benzaldehyde + H^+ + CN^- \quad (2.12)$$
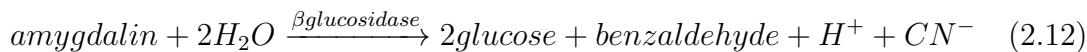
Potentiometric sensors based on ion concentration have also been used for DNA sequencing [16, 17]. Protein sensing demonstrated by Wang et al. used protein adsorption on a molecularly imprinted surface to detect the potential change which is proportional to the quantity of adsorbed protein [18]. Duzgun et al. used aptamer as a binding molecule and identified the potential difference between electrodes due to the capture of target protein [19]. DNA hybridisation has also been successfully measured using potentiometric Cd^{2+} ion sensors [20].

Potentiometric sensors have few limiting requirements; the foremost being need of a stable reference electrode relative to which all the potential measurements are done [21]. Potentiometric sensors based on the charged macromolecules such as proteins and DNA further suffer from shielding of their charge due to double layer formation [22]. Additionally, Nernst equation dictates the sensitivity of potentiometric sensors; thus they have a logarithmic response. This further limits the achievable practical resolution.

In the next section, we will discuss amperometric sensors which attempts to overcome some of the above mentioned issues of potentiometric sensors.

2.1.1.2 Amperometric sensors

In case of potentiometric sensors, we were concerned only with measurements at electrochemical equilibrium conditions and dynamic processes were not considered. However a wealth of information is hidden in the dynamics of how a chemical reaction proceeds. Generally upon conversion of reactant A into product B the reaction is possible in both directions, forward and backward [23]. The rate of conversion from reactants to products is measured using ν [M/s] and is given as ν_f and ν_b for forward, and backward reaction respectively,

$$\nu_f = k_f C_A \quad (2.13)$$

$$\nu_b = k_b C_B \tag{2.14}$$

Intuitively it implies that rate of conversion is dependent on concentration C and conversion factor k. At equilibrium, the final concentrations of A and B becomes constant thus the rate of the forward reaction equals that of the backward reaction [24]. Hence for the reaction given in equation 2.15,

$$\text{A} \underset{k_b}{\overset{k_f}{\rightleftharpoons}} \text{B} \tag{2.15}$$

$$k_f C_A = k_b C_B \implies \frac{k_f}{k_b} = K = \frac{C_B}{C_A} \tag{2.16}$$

Arrhenius equation is used to explain rate constants k as

$$k = A' e^{-\frac{E_A}{RT}} \tag{2.17}$$

Here E_A is equivalent to energy barrier which must be overcome for the reaction to proceed, also known as activation energy [25]. Rewriting equation 2.17 in terms of ΔG

$$k = A^{"} e^{-\Delta G/RT}. \tag{2.18}$$

Extending this idea to electrochemical reactions let us consider reaction 2.19, with reagent O being reduced using n electrons into reagent R.

$$\text{O} + \text{ne} \underset{k_b}{\overset{k_f}{\rightleftharpoons}} \text{R} \tag{2.19}$$

Since this is related to current i, it can be broken into two components cathodic current density j_c, i.e. electrons given into the solution, and anodic current density j_a, i.e. electrons exiting the solution [26]. The rate of conversion of O into a reduced compound R is given as

$$\nu_f = k_f C_O(0, t) = \frac{j_c}{nF} \tag{2.20}$$

and similarly, for the backward reaction, it is given as

$$\nu_b = k_b C_R(0,t) = \frac{j_a}{nF} \tag{2.21}$$

thus total current is given as

$$j = j_c - j_a = nF[k_f C_O(0,t) - k_b C_R(0,t)] \tag{2.22}$$

here $C_O(0,t)$ and $C_R(0,t)$ are the concentrations of oxidised and reduced species, respectively at time t. Thus if we relate rate constants k with the applied potential, we can predict the concentration.

If the potential of the electrode is changed by E volts the energy of one mole of electrons is changed by $-FE$. If we use the relation of free energy to electric work, we can state that

$$\Delta Ga = \Delta G_{0a} - (1-\alpha)F(E - E^0) \tag{2.23}$$

here ΔG_a is the free energy change at equilibrium for the anodic process. When F(E - E^0) is positive, the barrier for anodic process decreases from its equilibrium state ΔG_{0a}. Similarly, the cathodic barrier increases to

$$\Delta Gc = \Delta G_{0c} + \alpha F(E - E^0) \tag{2.24}$$

here E^0 is the formal potential. Using equations 2.18, 2.22, 2.23 and 2.24, we get

$$j = Fk^0[C_O(0,t)e^{-\alpha \frac{F(E-E^0)}{RT}} - C_R(0,t)e^{(1-\alpha)\frac{F(E-E^0)}{RT}}]. \tag{2.25}$$

Equation 2.25 dictates sensor response and can be used for various electrochemical processes. In cases when a high potential is applied, the reaction becomes limited by mass transfer. In that scenario, all the molecules coming at surface get converted much faster than the rate at which they arrive. Thus total current density becomes

$$j = nFm_o[C_{O,bulk} - C_o(0,t)]. \tag{2.26}$$

In this situation the current is called mass limited current, given as $j_l = nFm_oC_{O,bulk}$. The surface concentration can be given as

$$C_o(0, t) = C_{O,bulk}\left(1 - \frac{j}{j_l}\right). \tag{2.27}$$

In a typical amperometric sensor, if the applied potential is such that mass transfer limits the reaction, we obtain a linear relation of current measured with the concentration of the analyte.

Amperometric sensors compared to potentiometric sensors have higher sensitivity (linear compared to logarithmic). They do not suffer from Debye length screening effects. However similar to potentiometric sensors they also require a reference electrode and either the analyte itself should be electro-active or it should be converted into an electrically active compound. Several sensors based on amperometric technique have been proposed, including the highly acclaimed the glucose sensor.

The first generation glucose sensors were based on amperometric detection of hydrogen peroxide [27]. Need of platinum restricted their use to laboratories only. Since it was based on amperometric detection of peroxide produced, it required higher potentials for greater selectivity. The second generation eliminated the need for oxygen and use of peroxide for detection. Instead, they introduced redox mediators [28, 29]. They further eliminated the need for platinum and used screen printed electrodes, thus lowering the cost and resulted in mass adoption. The third generation still employs amperometric detection but does not require redox mediators, instead it tries to use organic conducting materials for direct electron transfer from enzyme to the electrode [30].

Amperometric detection has been successfully demonstrated for amino acids such as glutamic acid, lysine, glutamine and histidine; for vitamin sensors such as L-ascorbic acid [31], Vitamin B12 [32], and Nicotinic acid [33]. Either enzyme is used for generation of electroactive compounds to be detected [34], or direct detection has been shown [35]. Based on the same principle sensors for dopamine [36, 37] or catechol [38] does not involve bioreaction as the necessary components of the biosensor, but nevertheless provide information about important biomolecules.

Schematic of a typical strip based amperometric sensors is shown in Figure 2.2. Commercial amperometric sensors intended for single use are usually fabricated using screen printing techniques where reference, working and counter electrodes
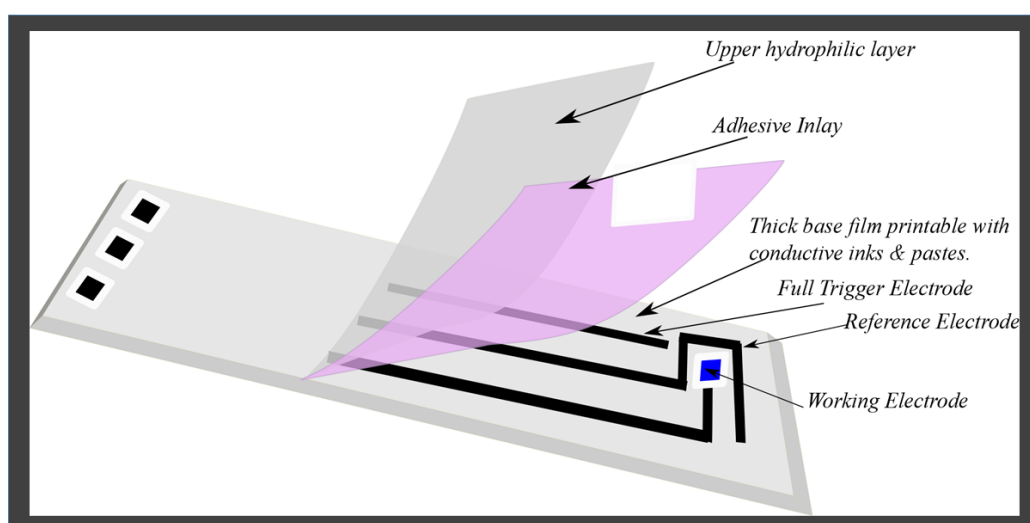
FIGURE 2.2: Pictorial representation of an amperometric strip biosensor.

all are on the same plane. If enzyme as a biocatalyst has to be incorporated, it is immobilised on the working electrode. Most of the electrode area is encapsulated with an insulating material except for the part where the analyte solution is in contact with the electrodes, and the part which is left open for electronic contact [39].

2.1.1.3 Conductometric sensors

Finally, the last class of electrochemical sensors are those which involves modulation of electrical conductivity of an electrochemical cell [40]. Most successful conductometric sensors are gas sensors where the electrochemical cell is composed of a selective material separated by two metal contacts as shown in Figure 2.3.

The adsorption of chemical of interest on the surface causes change in R_s. This changes the total impedance between the two electrodes and can be read out electronically. The equivalent circuit shows the contact resistance of electrodes to the sensing layer as R_C, R_S is the resistance of the surface being modulated by chemical interaction. R_B and R_I represent the bulk and interface resistances respectively.
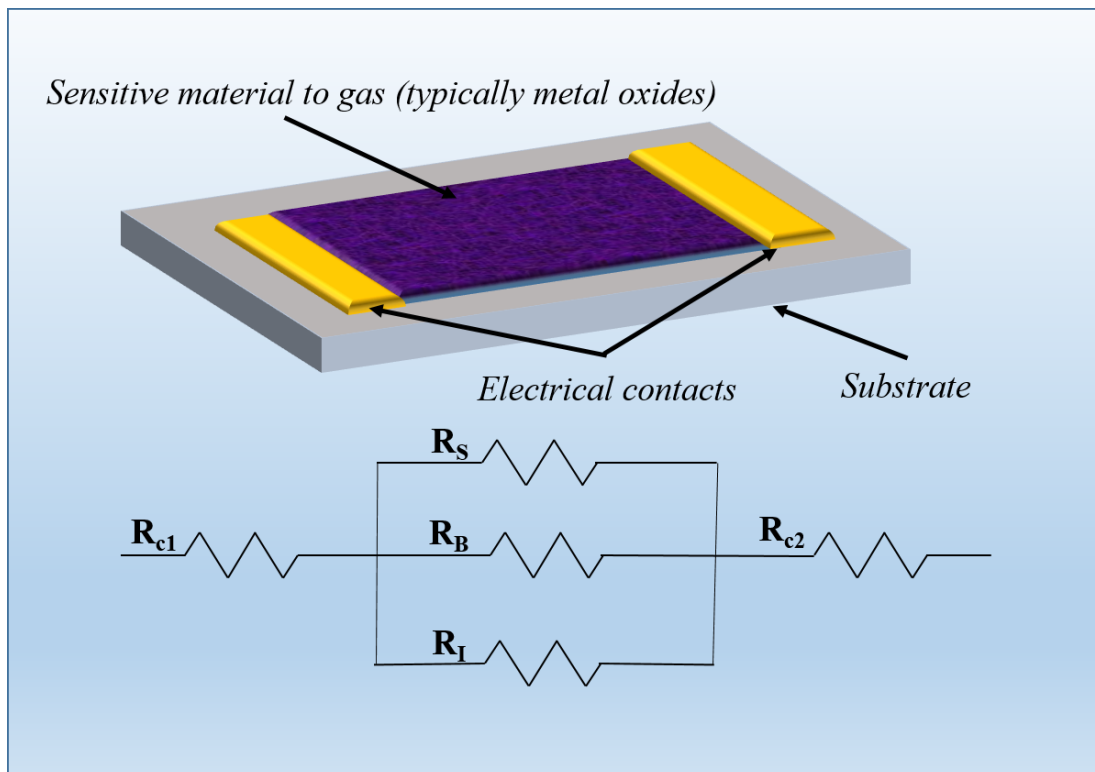
FIGURE 2.3: Schematic Representation of a conductometric biosensor. The major electrical components involved are also shown.

2.1.1.4 Limitation of electrochemical sensors

In the above sections, we saw the working of electrochemical sensors. However, there are several scenarios where such sensors have severe limitations. One such limitation is that only molecules which are electrically active can be detected with electrochemical sensors. Another severe limitation is non-availability of a micro-reference electrode. Even though there have been several attempts [41, 42], a stable micro reference electrode which would maintain its potential in different situations just remains elusive. In amperometric sensors where the requirement of reference electrode can be relaxed are affected by geometrical factors. For sensors with reproducible geometry, the size cannot be reduced below a certain extent, while maintaining the low cost. In miniaturised electrodes, the tolerance would have to be kept tight, and it loses economic benefit due to increased fabrication cost. Perhaps the most significant drawback of these sensors is that they must be brought into contact with the sample. This involuntarily causes contamination of the sensors. This results in extra costs of cleaning them, and issues related to sterilisation and recalibration. One alternative is to keep the price low enough to make disposable sensor.
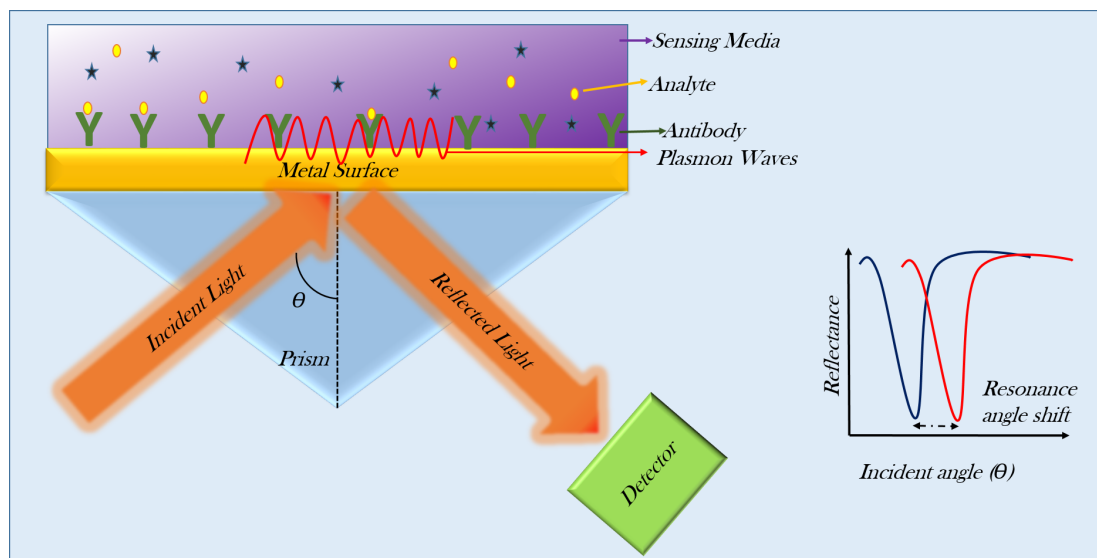
FIGURE 2.4: Schematic Representation of a Surface Plasmon Resonance (SPR) based Sensor.

2.1.2   Optics based biosensors

This class of biosensor utilises optical phenomena to convey biological information. They constitute the second most successful biosensor after glucose, i.e. pregnancy test strips. Essentially a biochemical reaction occurs which alters the colour of the sensor surface. This may be quantitative or qualitative. They typically lack any further signal processing and results are inferred by observing the colour change directly. Optical readers which readout the intensity of colour may infer quantitative information [43].

An important kind of sensor based on optical phenomena are known as Surface Plasmon Resonance (SPR) sensors. Though the research on SPR started in early 1900's its use for sensing purposes was demonstrated much later in the 1980s [44].

The use of nanomaterial and continuous development has shaped SPR based systems into a commercial product. The principle of SPR lies on the change of refractive index at the sensor surface when the analyte binds to the probe molecule. Depending on the amount of analyte bound to the surface the resonance angle shifts and is measured as shown in figure 2.4. By using calibration, quantitative analysis is possible. However this method is based on the change of refractive index, sufficient amount of analyte must bind to the probe molecules for a measurable change. Typically smaller molecules ($MW < 1000Da$), pose challenge for direct detection. In such cases, enzyme based amplification can help to achieve lower detection limit [45].
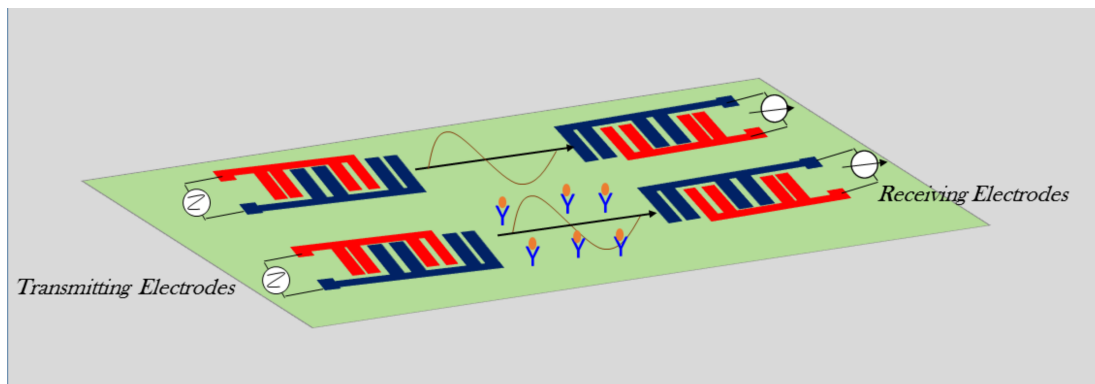
FIGURE 2.5: Schematic representation of a surface acoustic wave (SAW) based sensor.

2.1.3 Microelectromechanical biosensor

A unique class of sensors employing change in mechanical property as an indicator for biorecognition element is discussed in this section. They are mostly based on the information related to change in mass of some part of the system. Hence these sensors are most useful for sensing large biomolecules.

2.1.3.1 Surface acoustic wave based biosensors

The acoustic wave propagating on the surface of a piezoelectric substrate is the major component of these sensors. As shown in Figure 2.5, one end of the sensor transmits the acoustic wave, and the other end receives it. The generation of the acoustic wave is achieved by the use of interdigitated electrodes patterned on a piezoelectric crystal. A similar electrode structure is used to record/sense them. These waves are strongly dependent on the surface properties [46]. When there is a variation in the path of acoustic wave, recorded potential at sensor electrode may vary in phase, amplitude or frequency [47].

To use this sensitive surface as a biosensor, the sensor surface is first primed with capture sites which selectively binds to the target molecules. If an unknown sample contains the target molecule, the surface properties are modified upon binding of these target molecule with capture sites. This influences the transmission of the acoustic wave. Building on this principle, biosensors for penicillin detection has been demonstrated [48]. Several other use cases for gas detection and protein detection have also been demonstrated. For a review on such sensors refer to [49].
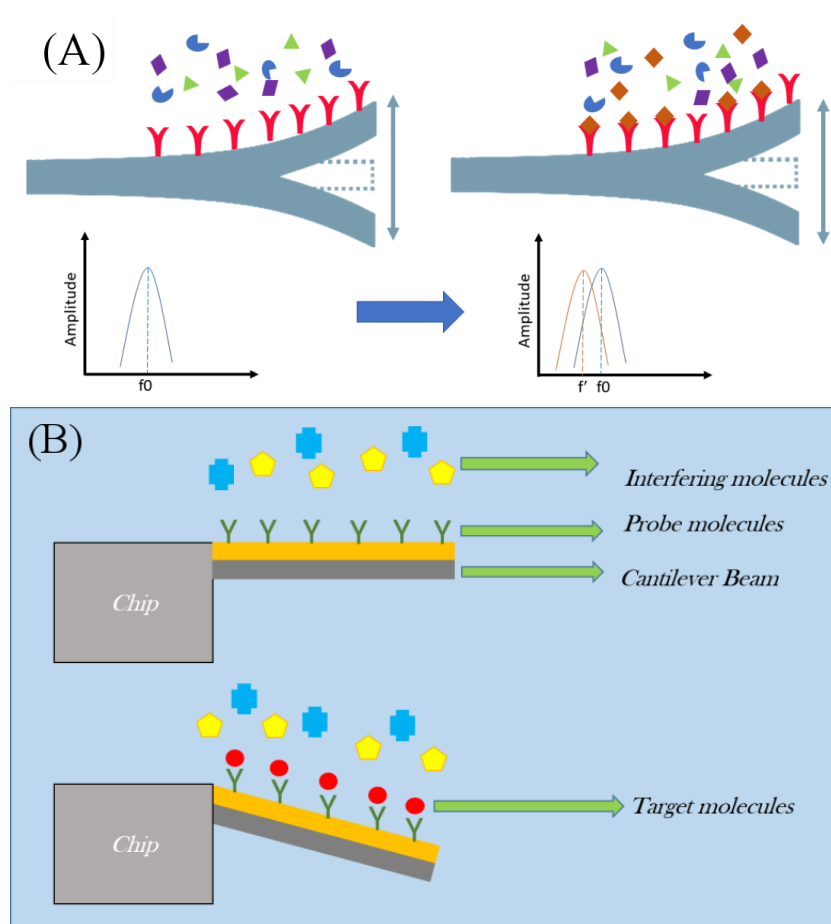
FIGURE 2.6: (A)Illustration of cantilever based sensor working on priciple of resonance frequency shift. (B) Mechanical sensor based on deflection due to surface stress.

2.1.3.2 Cantilever-based devices

Another exciting use of micromechanical devices is in the cantilever configuration. Absorption of molecules on a micro cantilever causes change in its interaction with environment. For example an oscillating cantilever will shift its resonance frequency due to change in its mass. To induce selectivity the surface of cantilever is functionalised with capture probe specific to analyte of interest [50]. Selective reaction on only one side of sensor results in its bending and can be read out using optical deflection. Figure 2.6(A) shows the working principle of such a sensor based on shift in resonance frequency. Figure 2.6(B) shows deflection based micro cantilever biosensor.

2.2 Biosensing systems

Development of biosensor is just one aspect of the determination of target analyte. Like any other system, a usable bio-sensor system must provide result in a comprehensible way to the end user. Not only should the chemical information be transduced to optical or electrical signal, but also appropriately interpreted for the user. For example, the electric current level measured by a glucose meter must be translated to mg/dl or another suitable physiological unit. Depending on the number of modalities a sensor is capable of detecting, we can broadly classify them into single or multiple analyte sensor systems.

2.2.1 Single analyte sensor

These systems are dedicated towards analysis of a single specific chemical entity. Usually, they provide the reading of the sensor directly or translate it to medically relevant units. A typical example would be glucose meters which directly inform about the blood sugar level. Using just one analyte, a medical practitioner may have enough confidence to judge and prescribe suitable treatment for the patient. However such scenarios are limited, and often the decision is made based on multiple tests for unambiguous diagnosis [51].

2.2.2 Multi-analyte sensor systems

The need of sensing numerous entities usually stems from medical requirements. For correct diagnosis of several symptoms, a medical practitioner may require information about more than one analyte. A solution to such situation calls for the multi-analyte sensor system, similar to shown in Figure 2.7. The effort in development of such multi-analyte sensor is increasing. The number of analytes being sensed is targeted to diagnose the illness successfully [52]. However, there are not many commercial examples of reliable multi-analyte sensor outside research environment.

Another possible use of multiple target sensor is in simultaneous fingerprinting of various analytes [53–55]. In these systems combination of sensors with selectivity towards different analytes are used. The strict requirement of high sensitivity may be relaxed. Instead, data-driven approach to quantify analyte can be used [56]. The response towards different compounds is recorded and grouped using
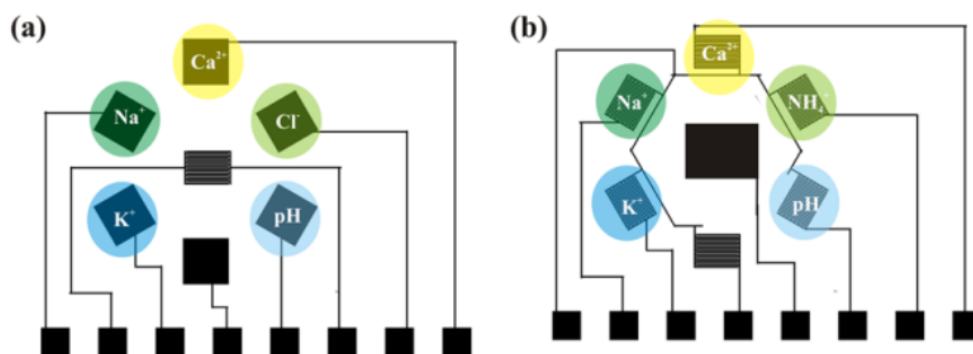
FIGURE 2.7: Two different layouts of the multi-analyte sensor are shown. (a) Five different ion-selective membranes are placed on five different gates which all share the same channel. (b) Five different ion-selective membranes are placed on five different channels which all share the same gates. In both cases one place is unfunctionalised of reference measurement.

statistical techniques. These techniques are aptly called fingerprinting as a match between response pattern with known compounds is used for classification.

2.3 Biosensor application areas

Based on the application requirements biosensor systems may be classified into following categories.

2.3.1 Qualitative assessment

Accurate knowledge of analyte concentration is preferred all the times. However, it might not be always achievable due to the complexity of the sample, or shortage of analysis time. In such situations, it might suffice to know qualitatively, the presence or absence of a chemical compound. Such application areas include security and bioterrorism[57], detection of allergen or toxin in food processing plants, or detection of infection in cases where disease which may spread quickly, or when early detection can lead to better prognosis [58].

2.3.2 Quantitative diagnostics

If it is desired to know the absolute amount of analyte present in the sample, it becomes necessary to use biosensors capable of a quantitative assay. Situations

where the mere knowledge of the presence or absence of the analyte is not enough a more detailed quantitative detection of the amount of analyte is required [59]. Outside medical application, industrial sectors such as bioreactors and food quality control requires quantitative sensors.

2.3.3 Point of care testing (PoCT)

A diagnostic test performed near the patient offer advantage of fast turnaround time of the test report, resulting in a better course of treatment for the patient. Demand for such system ranges from patients in big hospitals to those with limited medical facilities or those locked in remote areas. Obvious benefits are fast diagnosis which leads to early treatment simultaneously reducing effort to conduct the test in laboratories [60]. However the exact definition of such point of care testing systems is vague. Thus to be more precise we adopt guideline provided by The World Health Organization Sexually Transmitted Diseases Diagnostics Initiative (SDI) called *ASSURED* [61]. According to this guideline, any proposed PoCT system can be judged based on the following criteria.

- Affordable

- Sensitive

- Specific

- User-friendly

- Rapid and robust

- Equipment-free

- Deliverable to end-users

Apart from fast diagnostic time there are several other criteria which determine if a sensing system qualifies as PoCT system or not. Several sensing platforms based on principles such as antibody-antigen binding, are basis of PoCT systems like lateral flow strip (LFS), paper-based microfluidic devices, etc.

To use the sensors discussed in previous sections in a PoCT systems, engineering solutions are needed for system integration of the sensors and innovative readout

technologies. Several technological fronts have to push the boundaries. Microfluidic systems using micropumps, lab-on-chip, direct CMOS integration with sensors, packaging, and economical production are some of the critical areas. Much of these scientific principles have been understood relatively well, and the underlying structure is well matured. Additionally, with the development of new materials, ways to achieve lower detection limit are continuously being explored but at small pace.

Only after this technological advancement, one can hope for cheap, reliable and fast medical diagnostic systems. Towards this aim, there is already research demonstrations of portable and hand-held sensing systems for field testing and wearable devices for continuous health monitoring. Efforts in this area are much talked about in popular media perhaps due to the involvement of tech giants such as Google notably for eye contact lens incorporating glucose sensor. In fact, according to market predictions, the global market share of wearables will increase to $50 billion in 2021 [62]. Amid the enthusiasm, the reality is that majority of commercialised sensors are from a small pool of sensing systems.

2.4 Common challenges in development of biosensor

2.4.1 Sensor response time

In most of the scenarios, it is desired to have fast sensor response. A typical example is at airports, where screening of passengers is required to contain the spread of diseases. Situations such as sports events or operation room also require results to be available in the matter of tens of seconds to a couple of minutes so that a decision can be made. Such situations require fast sensor response. These scenarios become a challenge when on one hand the level of substance to be detected is small, and on the other hand, a fast sensor response is required. Sensors which respond to the surface interaction of biomolecule must wait for the analyte to diffuse through the sample volume to reach the sensor surface. Alam et al. proposed a model for estimating the time required for a sensor with given geometry to generate the response [63]. Nanomaterial based sensors are poised to have faster response, given same sensitivity for all material and geometries. Apart from the issue of diffusion limits, significant time is consumed for sample

preparation. Recent push towards personalised medicine and wearable sensors have focused on analysis without sample preparation.

2.4.2 Selectivity

Another point to be considered in sensor development is to have sufficient selectivity of sensor towards its target analyte. Most of the sensors which utilise biocatalysts offer sufficient selectivity such as in Immunosensors. However, sometimes an enzyme or protein may also catalyse or bind to unwanted molecules [64, 65]. This lack of absolute selectivity poses a challenge especially if the level of the interfering molecule is unknown. Due to this cross-sensitivity, it might be required to monitor primary known cross contaminant levels [66]. Ion selective electrodes also suffer from such interference and often fail in the presence of high concentrations of cross contaminants [67].

2.4.3 Sensitivity

Sensitivity refers to change in the output of sensor w.r.t change in analyte quantity. Sensors with high sensitivity are required in situations where a small change can have a drastic effect such as pH level in humans [68]. Sensitivity directly affects the resolution of the sensor. Thus in situations where the small changes have to be monitored, the sensor must offer sufficient sensitivity to quantify the results.

2.4.4 Analyte volume requirement

Another essential aspect to consider is the minimum amount of sample necessary to do the analysis. Recently the field of point of care diagnostics has been plagued with false hopes of providing analysis with a minuscule amount of sample [69]. For example, the total number of molecules present in a 1 μl drop with one attomolar concentration of analyte to be sensed is $10^{-18} \times 10^{-6} \times 6.023 \times 10^{23} = 0.6023$. In other words, approximately out of two drops of sample only one can have that molecule! Hence claims made for such low detection limit or small sample volume must be carefully scrutinised.

Chapter 3

Electrolyte Gated Carbon Nanotube Field-Effect Transistor

3.1 Carbon Nanotube: Material properties

In 1952 there were reports and even a patent granted for hollow tubes of carbon [70]. In 1991 Sumio Iijima synthesised and characterised the crystal structure of the so-called "hollow carbon tubes" [71]. His work ignited interest in the newly synthesised nanomaterial now known as carbon nanotubes (CNTs). Since then immense progress has been made in in-depth understanding and investigating potential applications of the CNTs. CNTs represent one of the most studied "nanotubes" [72]. As of early 2018, around 84,000 publications and patents directly mention the words "carbon nanotube" in their title. Additionally, with the onset of physical limitations in keeping up with Moore's law [73], more interest and effort has been directed towards nanomaterials such as nanowires, nanotubes, quantum dots and 2D materials to continue the technological progress.

This work utilises carbon nanotubes as its primary material for the production of sensors and electronic devices. This nanomaterial is composed of a single atomic layer of carbon [74]. It can be viewed as a rolled-up sheet of single layer carbon also called as graphene [75]. These cylinders can be a few nm in diameter and up to several μm in length [76]. The 2D sheet of carbon is easily described using two basis vector given as,

$$\vec{a_1} = \frac{a}{2}(\sqrt{3}, 1) \tag{3.1}$$

$$\vec{a_2} = \frac{a}{2}(\sqrt{3}, 1) \tag{3.2}$$
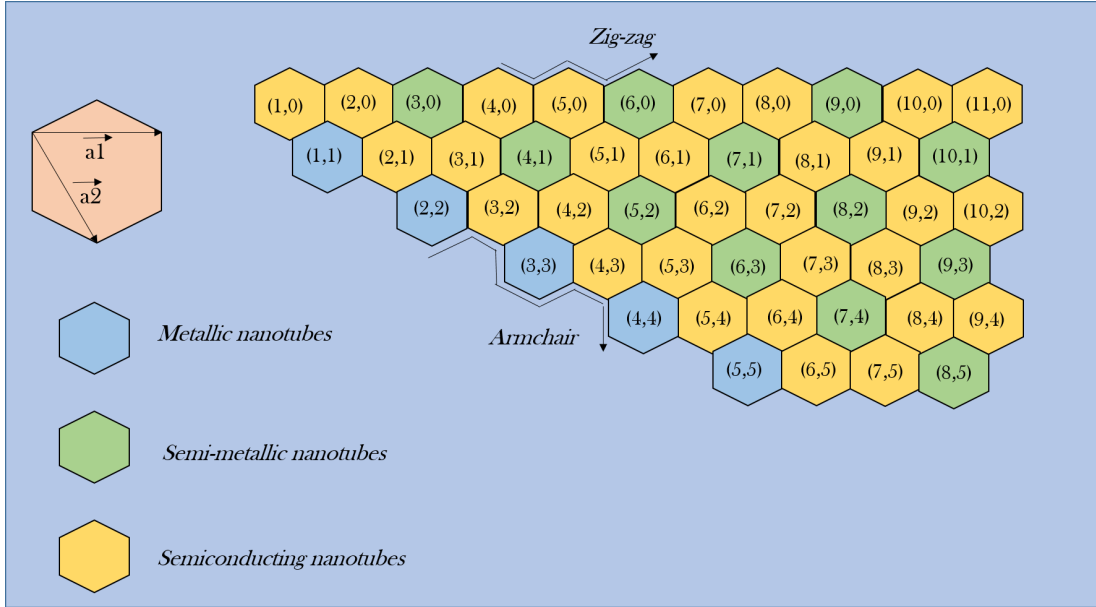
FIGURE 3.1: Figure demonstrating the graphene structure and basis vectors.

Here a is the distance between the pair of two carbon atoms having one atom of carbon in between. This arrangement of carbon is hexagonal, hence a becomes $\sqrt{3} \times 1.42 \mathring{A}$. Figure 3.1 shows the graphene structure and basis vectors. This sheet of graphene can be rolled to form cylinders [77]. However, there are several possibilities to do so.

We can cut graphene into a ribbon, such that $\vec{C}$ given in below equation as a combination of basis vectors $\vec{a_1}$ and $\vec{a_2}$, becomes edge of the cylinder.

$$C = n\vec{a_1} + m\vec{a_2} \tag{3.3}$$

The diameter of carbon nanotubes obtained in this way is given as

$$D = \frac{|C|}{\pi} = \frac{\sqrt{3}}{\pi} a\sqrt{n^2 + nm + m^2} \tag{3.4}$$

Depending on the values of n and m, we achieve following major types of CNTs. [78].

1. (n,0) called as *zigzag*.

2. (m,m) called *armchair*.

3. (n,m) called as *chiral*.

This classification is not only based on geometrical differences but also represents different electrical properties of these nanotubes.

The underlying principle of electrical conduction in carbon nanotubes can be well explained using a simple model based on graphene's hexagonal lattice [79]. The atoms of carbon arranged in a hexagonal manner are present in sp^2 hybridisation state. They form three sigma bonds which are coplanar and separated by 120°. These sigma bonds provide mechanical strength and stability to the lattice [80]. The last remaining electron forms an out of plane π bond. This π bond is a delocalized electron cloud which largely dictates unique electronic properties of the carbon nanotube and graphene sheets.

3.1.1 Carbon Nanotube production

Single sheet of graphene when rolled to form cylinder would produce what is called as single-walled carbon nanotube (SWCNT). Depending on the process parameters used in the production, it is possible to synthesize several such nanotubes which are arranged concentrically. This configuration is called multi-walled carbon nanotubes(MWCNTs) [81].

There exist several methods for production of carbon nanotube, most notable are chemical vapour deposition (CVD) [82, 83], laser ablation [84, 85] and arc discharge [86, 87]. Ijima initially produced carbon nanotubes using DC arc-discharge [71]. In this method, a target is hit with arc generated between two graphite electrode, either metal doped or pure graphite electrodes can be used to produce single or multiple walled carbon nanotubes. Arc discharge has been optimized over the years to produce high-quality carbon nanotubes. Similar to arc discharge, the laser has been used to knock off carbon atoms from a graphite target, and the nanotubes formed are collected. Both of these methods offer moderate production volumes. Chemical vapour deposition (CVD), utilises carbon precursors which are then pyrolysed into atomic carbon. The pyrolysis is carried out in the presence of carrier gases, typically over the hot surfaces. These hot surfaces often contain a catalyst which serves as sites to capture and grow nanotubes. This technique produces CNTs with high throughput but at the cost of purity. Figure 3.2 illustrates the three techniques. Table 3.1 further compares the relative advantages and limitations of the three methods.

To be used as high purity semiconductor material in electronic devices, post processing of CNTs after production is required. During production only $2/3^{rd}$ of
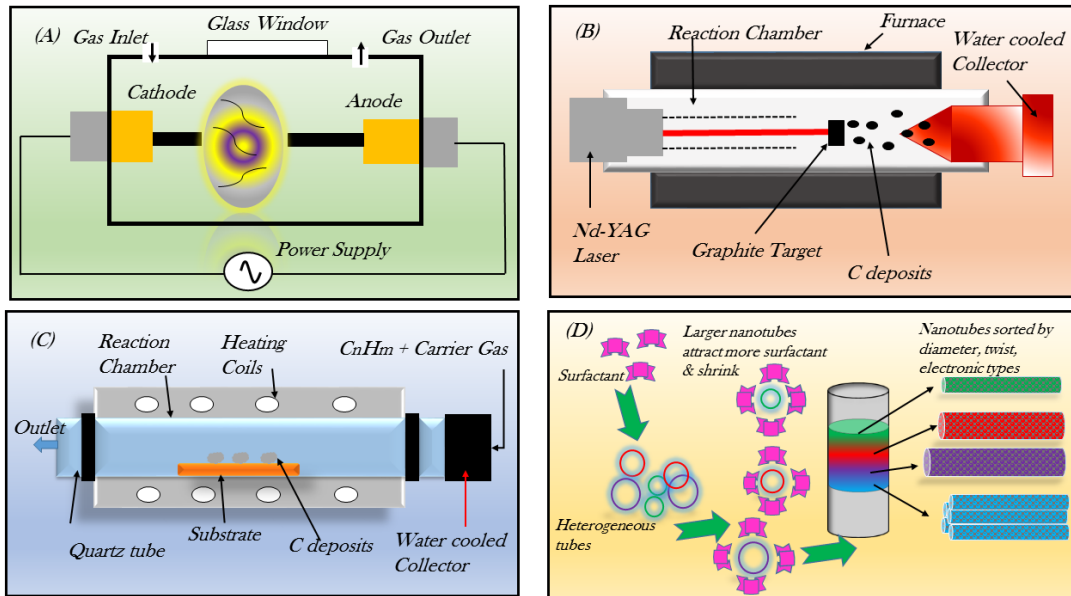
FIGURE 3.2: Figure demonstrating various methods of CNT production. (A)
Arc discharge. (B) Laser Ablation. (C) Chemical Vapour Deposition (CVD)
and (D) Sorting of different types of nanotubes.

	Arc discharge	Laser ablation	Chemical vapor deposition
Purity	High	High	Low
Production control	Low	Medium	High
Production cost	Medium	High	Low
Throughput	Medium	Low	High
Process Temperature	High	Low	Medium

TABLE 3.1: Comparison of different techniques for CNT production.

synthesized CNTs are semiconducting, hence they need to be sorted to obtain
semiconducting CNTs. Moreover other carbonaceous particle impurities and the
metal which was used as catalyst exist in the as-synthesized material and must be
removed.

If CNTs are desired for conducting material then, having multi-walled CNTs
(MWCNTs) is a better choice, as they are mostly metallic and serve as a bet-
ter economic choice. MWCNTs have also been proposed as interconnect material
for silicon industry [88].

Currently, only a few commercial suppliers have hold of the separation techniques
to sort single and multi walled CNTs and they are well guarded with patents or
as trade secrets. Typical methods to sort CNTs involve gradient-based separation
techniques. For example, direct centrifugation of CNTs is used to separate them

by diameter. Organic molecules which selectively wrap around semiconducting CNTs have also been proposed for separation of CNTs [89]. Huge demand of high purity CNTs has led to their extremely high cost. In fact, at the moment highly purified semiconducting CNTs (99.9 %) are around 20,000 times more expensive than gold, of comparable mass. However, it is important to mention that even with such high costs they can be afforded in single use devices, thanks to their high aspect ratio: a sub monolayer of percolating nanotube network is sufficient for device fabrication.

3.1.2 Carbon Nanotube: Process integration

Carbon nanotubes, even with their impressive attributes are of little use if they cannot be integrated into devices and technologies which could benefit from their electrical and mechanical properties. The major application areas of CNTs are listed below:

1. For enhancement of mechanical properties.

2. Use in the fabrication of physical or chemical sensors.

3. Use as an electronic material.

Each of these application areas have to deal with their own challenges. However, few common problems for all of the use cases arise due to the agglomeration of carbon nanotubes into bundles and hydrophobicity of carbon nanotubes [90, 91]. Carbon nanotubes are used as material filler in a polymer matrix to increase the mechanical strength of the polymer [92]. For such application, the as-produced carbon nanotube powder should have low carbonaceous impurities. A homogeneous distribution of carbon nanotubes in large industrial process is desired without use of any additional chemical. However, homogeneous dispersion of CNTs without the use of surfactant is a challenge. Despite this, their continuous use for improving the mechanical strength of modified polymer matrix has been extensively reported [93].

For electronic applications orderly positioned carbon nanotubes are a requirement. However, as discussed above carbon nanotubes are produced in bulk, which means they have to be processed before they can be integrated into devices. This is a rather difficult task given the nano dimensions of individual CNTs. No reliable method exists which can move individual nanotube from one location to another

efficiently, especially at an industrial scale. Some attempts to solve this issue include directly growing patterned carbon nanotube on the silicon substrate [94] or preparing a highly aligned film of nanotubes [95]. Aligning carbon nanotubes using dielectrophoresis has been carried out with some degree of success [96] but is yet to be integrated successfully at commercial scale. Single carbon nanotubes have been demonstrated in sensor or transistors, but the production is mostly academic and for research purposes. It involves identification of single carbon nanotubes using electron microscopes, and then patterning metal contacts using e-beam lithography [97]. It is a very time-consuming process and is not scalable for commercial electronic production where upto billions of transistor per chip are usually required for state-of-art processors. Keeping these hurdles in view probably the most suitable technology for easy integration of carbon nanotubes is random CNT networks [98].

Carbon nanotubes are deposited with the random orientation to form interconnected films on the carrier substrate [99]. It increases the fractal dimension of such films from 1D to quasi 2D film. These films can be visualised as series and a parallel combination of individual nanotubes. Such films offer optimum performance w.r.t effort concerning technological requirements. As the density of carbon nanotubes increases in these films, there is significant improvement in the reproducibility of the films regarding electronic and physical characteristics [100].

For the preparation of such random nanotube network films, CNTs dispersed in the liquid medium are most alluring. Solution based processes offers additional advantages in device fabrication. For example, use of low-temperature processing and a varied choice of substrate material [101]. Water-based dispersions further reduce cost and hazards associated with use of toxic solvents. Thanks to solution processable nature, roll-to-roll production is another significant advantage as it considerably lowers the cost of device fabrication [102]. Thus in recent years solution processed carbon nanotube devices has drawn significant attention of researchers.

Surfactants such as sodium dodecyl sulfate (SDS) [103], carboxymethyl cellulose (CMC) [104], or biomolecules such as deoxyribonucleic acid (DNA) [105] have been used for dispersing carbon nanotubes in the aqueous medium. Often this dispersion is accompanied by sonication process which aids in separation of the carbon nanotube bundles such that the dispersant can wrap around the individual nanotubes [106]. When this mixture is centrifuged, separation of single nanotubes from intact bundles takes place due to the density gradient. In this work, SDS
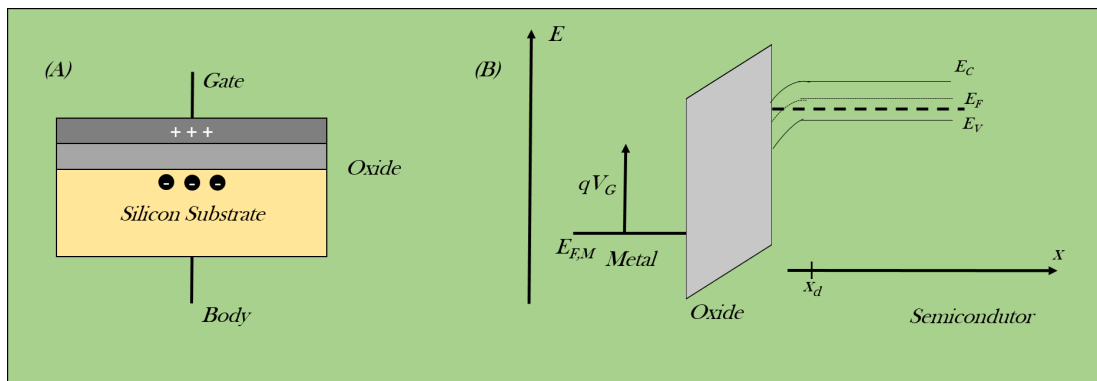
FIGURE 3.3: (A) Typical MOS stack forming a capacitor, charge as well as capacitance is a function of gate voltage. (B) Energy band diagram of MOS capacitor.

around 0.5-1 wt% was mostly used as the dispersant. The formulation (ink) was prepared for 90-95% semiconducting carbon nanotubes as well as multi-walled carbon nanotubes which were primarily used for the electrodes.

3.2 Electrolyte gated field effect transistor: Introduction

Continuing our previous discussion about potentiometric sensors from chapter 2, we will explore here in more detail the working principle of EGFET and sensors based on such devices.

3.2.1 Metal oxide semiconductor capacitor

A typical metal oxide semiconductor (MOS) capacitor is shown in Figure 3.3 (since '70s metal has been mostly replaced by doped polycrystalline silicon) [107]. In simple terms, upon application of gate bias w.r.t substrate, the MOS capacitor accumulates charge in gate metal-oxide interface, as well as at the semiconductor-oxide interface. For such MOS capacitor, the potential profile looks like as shown in Figure 3.3(B). In this capacitor both the oxide interfaces are sealed from any chemical present in the environment. Hence, only the gate bias can modulate the charge of this capacitor.

This capacitor is at the heart of MOSFET. By controlling voltage across this capacitor the charge carrier concentration in the semiconductor channel is modulated. This scheme results in a controllable conductance of the semiconductor interface near the oxide. For state-of-the-art MOS devices, the channel conductance can be varied easily up to 5-8 orders of magnitude. For our discussion, it is sufficient to assume that the transistor drain currents depends on the value of MOS capacitor. This value of MOS capacitor, however, is determined at the time of device fabrication and does not depend on the environmental conditions. For a detailed description on working of MOS transistor, please refer to [107].

It is interesting to consider now, what would happen if instead of oxide we could use an electrolyte, or if we could rearrange the functional parts of MOS transistor. This consideration opens up an opportunity of interfacing environmental factors with the transistor. In an attempt to do so, we must understand what happens when an electrolyte is brought in contact with the metal surface and an electric polarisation is applied. This will be discussed in detail in below sections.

3.2.2 Electric Double layer capacitor

Hermann von Helmholtz was first to propose a model for charge distribution at the liquid metal interface [108]. He proposed that, similar to the metal capacitor where all the charge resides at the interface, charged species in a liquid get accumulated at the metal surface. The separation between metal and the proposed charged layer was determined by the radius of the ions present in the liquid. The capacitance of such system is given by equation 3.5

$$C_H = \frac{\epsilon\epsilon_0}{d} \tag{3.5}$$

ϵ being the dielectric constant of space separating the charge layers, and d is the radius of ion present in solution. Later Gouy and Chapman improved this model. They proposed that unlike metal, charge layer in solution is diffused. If total potential between metal and solution be ϕ_0. Then the differential capacitance is given by equation 3.6 [1].

$$C_{GC} = \left(\frac{2z^2e^2\epsilon\epsilon_0 n^0}{kT}\right)^{1/2} cosh\left(\frac{ze\phi_0}{2kT}\right) \tag{3.6}$$

It can be observed easily that this capacitance, is a function of total number of ions present in the solution, as well as ϕ_0 viz. the applied potential across the
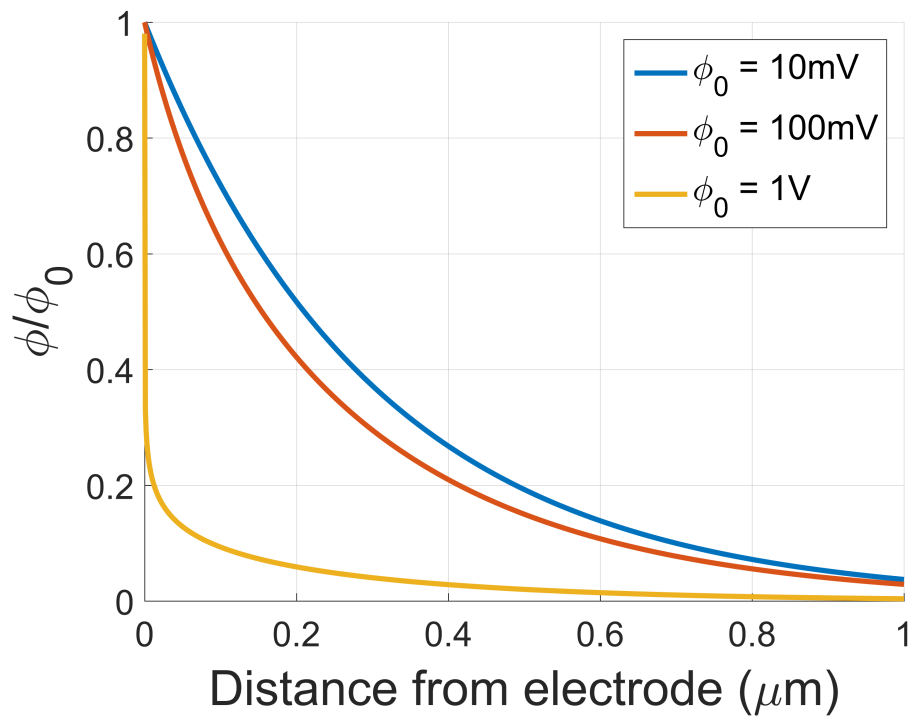
FIGURE 3.4: Potential profiles through the diffuse layer as predicted by the Gouy–Chapman model. Electrolyte concentration is $10^{-2}M$ in aqueous solution of a 1:1 electrolyte at 25^oC. (adapted from [1]).

capacitor. In a typical capacitor the electric field in the insulator is constant, and thus the potential profile is linear. Such is not the case for the electrolyte double layer capacitor. Figure 3.4 shows the potential distribution in diffused layer of double layer capacitor with increase in applied bias.

Similarly 3.5 shows the effect of increasing electrolyte concentration. Hence upon increasing the applied bias as well as the salt concentration, effectively almost all the potential drop happens within few nanometers from the interface. This has a significant effect on the sensors which rely on surface charge detection.

Stern further enhanced this model; he observed that beyond a specific distance ions could not move closer to metal surface due to their physical size [109]. Thus total capacitance can be expressed as series of two capacitances; a Helmholtz capacitance (C_H) given by equation 3.5 and Gouy-Chapman capacitance (C_{GC}) given as equation 3.6. Thus total double layer capacitance C_{dl} is given by

$$\frac{1}{C_{dl}} = \frac{1}{C_H} + \frac{1}{C_{GC}} \tag{3.7}$$
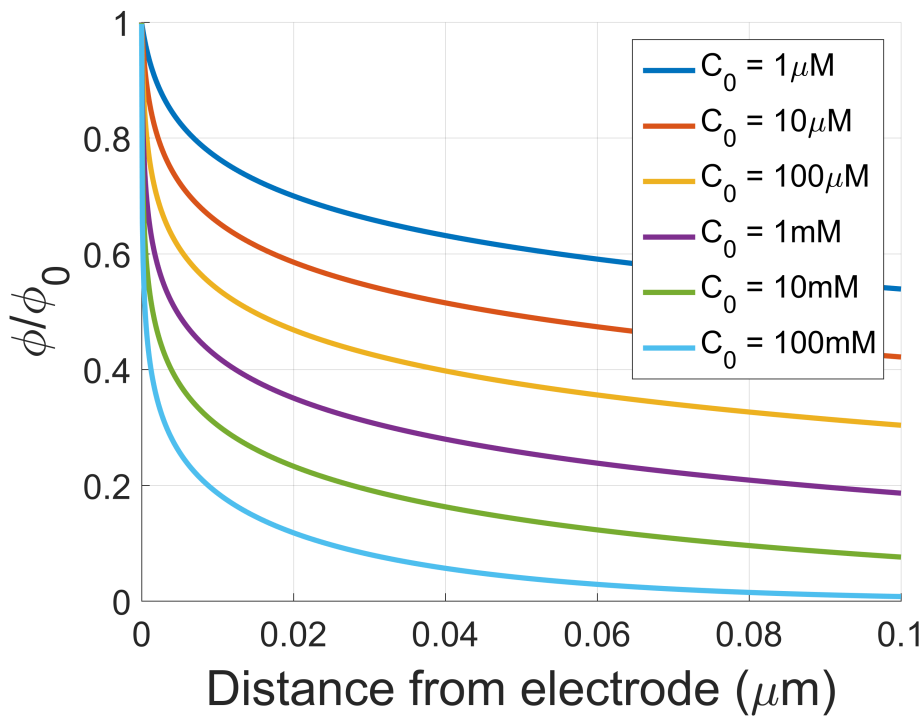
FIGURE 3.5: Potential profiles through the diffuse layer in the Gouy–Chapman model. Calculated for $\phi_0 = 0.5$V in an aqueous solution of a 1:1 electrolyte at 25^oC. (adapted from [1]).

One of the critical parameters that must be taken into account is Debye length (λ_d) [110]. Debye length is defined as

$$\lambda_d = \sqrt{\frac{\epsilon\epsilon_0 kT}{2n^0 z^2 e^2}}. \tag{3.8}$$

It is regarded as the approximate distance from the surface within which the charged particle contributes to the potential at the surface. In a strict sense the effect decays exponentially, and it is only 67% of the total distance. Nevertheless it serves as an excellent measure to check if any charged molecule positioned at a certain distance from the surface can contribute to the potential change or not. The value of double layer capacitor is dependent on multiple parameters. Thus it is essential to maintain all other parameters constant except the primary analyte if such a system is used for sensing of the analyte. In later sections, we will see the impact of ionic concentration on the sensor performance.
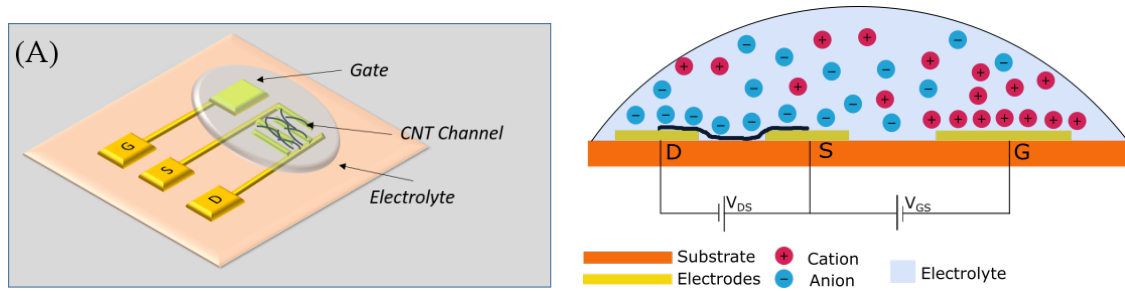
FIGURE 3.6: (A) Schematic of an electrolyte gated FET (EGFET), (B) cross section of EGFET, with applied bias the double layer capacitors accumulate charge at the interfaces.
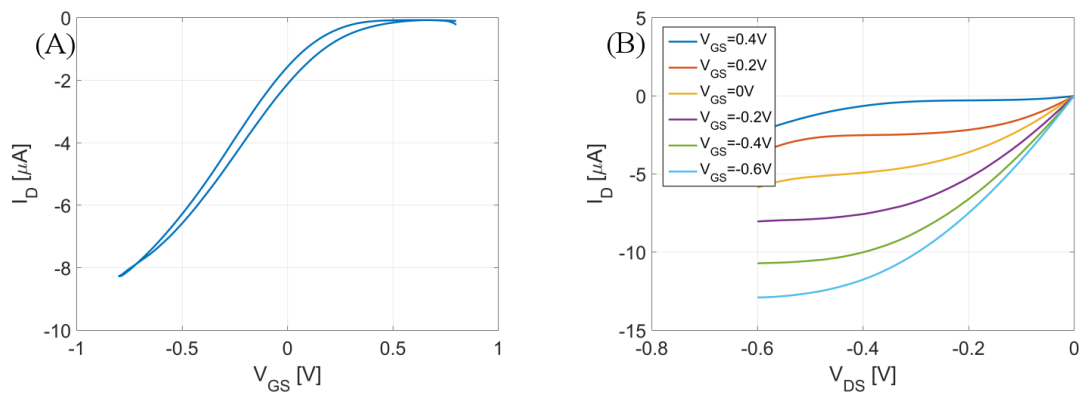
FIGURE 3.7: Transistor Characteristics of an EGFET (A) Transfer Curve, (B) Output Curve.

3.2.3 Electrolyte gated transistor: Working principle

Combining the facts regarding, the existence of capacitor at the metal-electrolyte interface and the use of a capacitor to control the conductivity of semiconducting channel, it becomes possible to envision architecture of electrolyte-gated transistor. Figure 3.6(A) shows a typical schematic of electrolyte-gated transistor used in this thesis. A striking difference with the conventional MOS transistor is the absence of any insulator material protecting the semiconductor. EGFETs with and without an insulating layer have been demonstrated, and in general, the same theory is applicable in both cases [111, 112]. Two double layer capacitors are formed when the gate terminal is polarised w.r.t source electrode. As shown in Figure 3.6(B), the electrolyte maintains the net neutrality. When the external applied voltages i.e. the gate to source voltage and drain to source voltage are varied, we can capture the transistor characteristics as shown in Figure 3.7.

To eliminate the impact of applied polarisation on double layer capacitance, we must use high ion concentration. Figure 3.8 shows the dependence of double layer
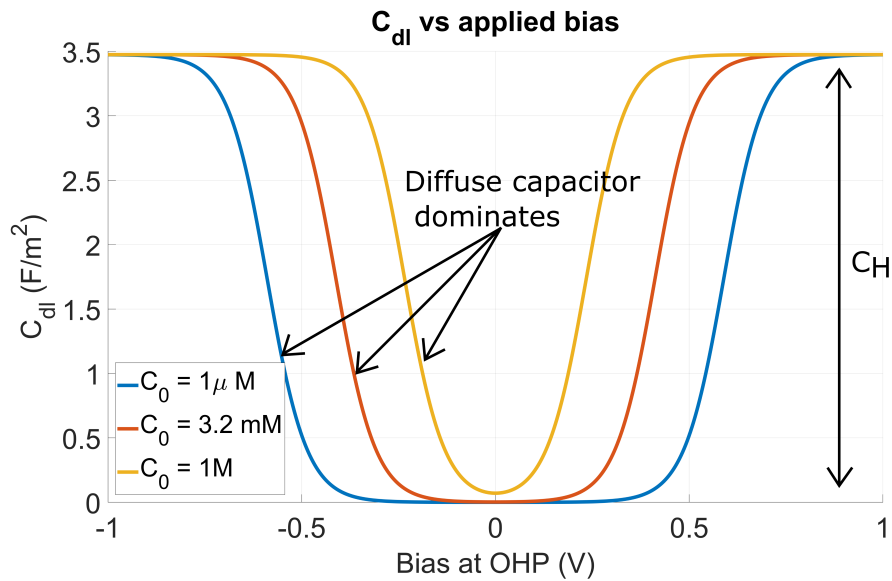
FIGURE 3.8: Variation in electrolyte gate capacitance with ion concentration and applied bias. (adapted from [1])

capacitance on the applied bias and electrolyte concentration [1]. It can be noted that as ionic strength increases the double layer capacitor becomes independent of applied bias and can be approximated equal to Helmholtz capacitor. If one wishes to see the effect of variation in ionic strength, then electrolyte with low ionic strength must be used. The Helmholtz capacitor can be analogously compared to oxide capacitor of traditional MOSFET.

As the electrolyte is in direct contact with the metal surface, and practically no surface is ideally polarizable there always looms an issue of faradic processes occurring at the interfaces. To keep such faradic processes at bay, and satisfying the requirement of gate current to be at least few order of magnitude lower than drain current, only a small gate bias window is available. A similar restriction is applicable to the drain bias w.r.t source [113]. Due to this limitation often the well-known saturation regime in the MOS transistor output characteristic is sparsely visible for EGFETs.

Due to the chemical inertness of carbon nanotubes [114], an aqueous electrolyte solution can be used successfully for gating EG-CNTFETs. However, the polarisation window in this case is limited to $\pm 0.8V$. Using electrolytes which offer wider potential window, it is possible to obtain higher drain currents and also observe saturation effects [115]. Figure 3.9 shows the transfer characteristics of the same transistor, characterised using different electrolytes. Figure 3.9(A) shows transfer curves measured with de-ionised water as electrolyte. The gate voltage is swept from +0.8V to -0.8V w.r.t source. The same device, when gated with the ionic
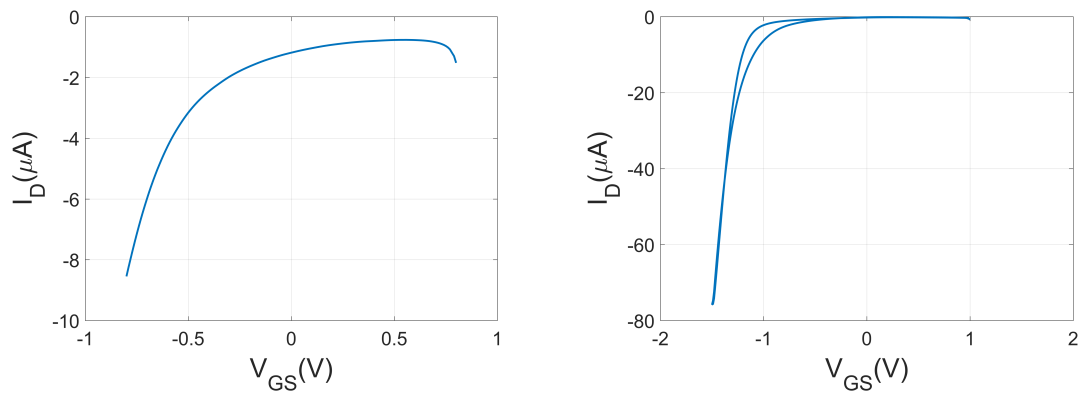
FIGURE 3.9: Transistor Characteristics comparison with different electrolytes (A) DI-water, (B) Ionic Liquid.

liquid, (1-Butyl-3-methylimidazolium hexafluorophosphate) which consist of bulky anion and cation allows a wider gate potential window. The effect on maximum on current is evident (Figure 3.9(B)) and there is one order of magnitude increase in the drain current when the gate voltage is swept from +0.8V to -1.5V w.r.t source.

The work presented in this thesis aims towards the development of biosensors using electrolyte gated transistor, and since virtually all relevant biological analytes are present in aqueous media, all the following results presented in this work were obtained using water-based electrolytes unless mentioned otherwise.

Assuming capacitors at the gate and channel are represented as C_{gate} and $C_{channel}$ respectively, the fraction of total external applied bias V_{GS} available across $C_{channel}$ can be defined as

$$V_{G,channel} = V_{GS}\left(\frac{C_{gate}}{C_{channel} + C_{gate}}\right) \tag{3.9}$$

It is noteworthy that, this is not the only configuration available for electrolyte gated transistors. A non-polarizable electrode that maintains standard potential at all the applied biases is also often used [116]. In case of a non-polarizable electrode, the fraction of gate bias available across the semiconductor-electrolyte interface, is equal to external bias plus the constant offset of the non-polarizable electrode. It is interesting to note that in the latter case, as the gate electrode becomes independent of capacitive effects, there is no effect of gate surface area. This opens up an exciting opportunity for miniaturising the gate electrode as long
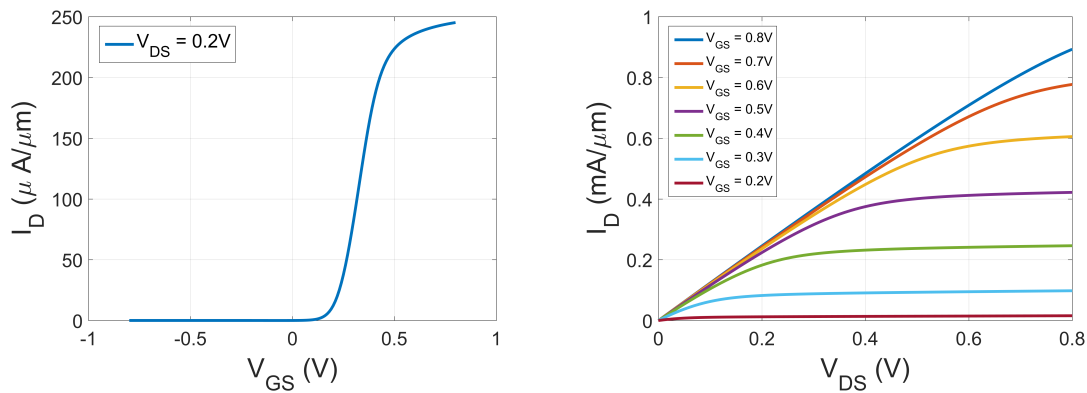
FIGURE 3.10: Simulation of single CNTFET using [2],(A) transfer, (B) output characteristics.

it maintains constant potential drop. In the context of aqueous solutions, Ag/AgCl electrodes are widely used as gate electrode [117].

Carbon nanotube is a hollow cylinder, thus, the classical MOSFET theory of operation cannot be directly applied to CNTFETs. Various researchers have proposed different models with details on topics such as quantum capacitance, ballistic transport, gate coupling, etc. [118, 119]. Overall, a well accepted notion is that the drain current is controlled by gate bias in an EGFET in the same manner as in traditional MOSFETs. As mentioned earlier the saturation region is barely visible in electrolyte gated CNTFETs due to small gate bias available to limit faradic processes; however, this is not the only reason. It has been proposed that due to non-idealities of CNTFETs the ideal saturation region deviates from theoretical prediction [120]. Several models have been developed to describe a carbon nanotube transistor. Most of the models describing a single carbon nanotube transistor with a solid dielectric are updated versions of the models used to describe conventional MOSFET. Figure 3.10 shows the device characteristics of a CNTFET simulated using a model proposed by C S Lee et.al. [2].

To model a CNTFET comprising of random carbon nanotube network, one can assume that it is made up of several individual single nanotube CNTFETs arranged in series and parallel configuration. In this case, one may safely assume that such a CNTFET would produce semantically similar response as a single nanotube transistor. Using a simpler model random carbon nanotube network has been simulated [121]. This lays the foundation for sensors based on electrolyte gated CNTFETs and provides a framework to understand sensor response and parameters to optimise the same.
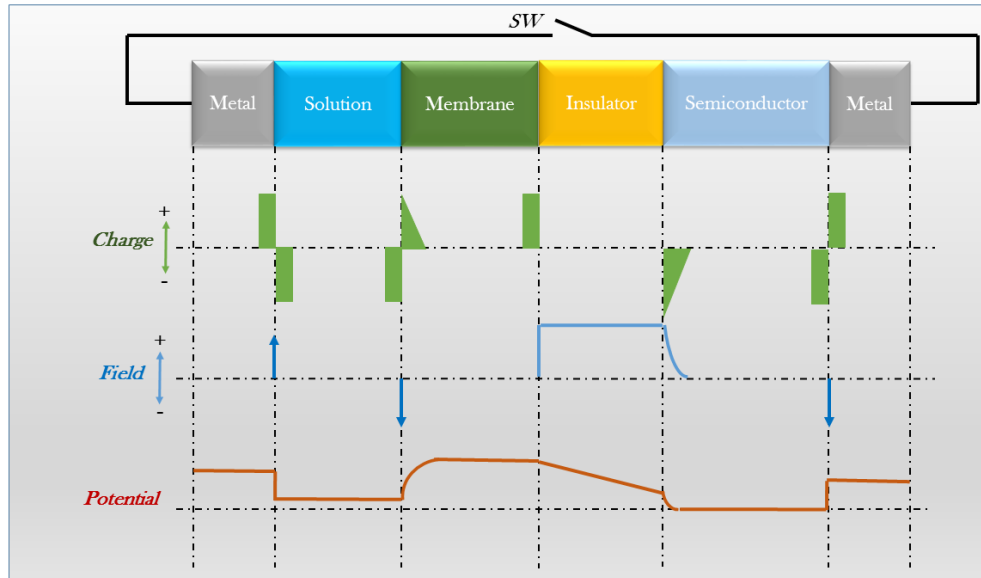
FIGURE 3.11: Profiles of charge, electric field and potential distribution throughout the gate of an EGFET.

With background covered on the functioning of an electrolyte-gated transistor, let us focus on principles to utilise them as sensors and also analyse the merit they offer compared to other sensors.

3.2.4 EGFET as sensors

Bergveld (1970) [11] and Matsuo et al. (1971) [122] independently proposed the idea of ion selective field effect transistor. Similar to an EGFET they observed that the transistor exhibited response towards varying pH. This, later on, gave rise to a whole new class of biosensors, i.e. chemFETs [123].

To begin with, we examine Figure 3.11 which depicts the charge, electric field and potential profiles at different interfaces of a multi layered cross-section system. The membrane shown in Figure 3.11 is a semi-permeable membrane permeable to a specific ion such as H^+.

Comparing this cross-section with the EGFET cross section shown in Figure 3.6(B), it can be noted that only difference is at the membrane insulator interface [123]. It is well known from electrochemistry that any semi-permeable membrane will generate a potential difference based on the activity of the ion present in the two phases, known as Nernst potential (equation 2.6). As this potential term is

in series with externally applied gate potential, it can be included in the gate bias term of the MOSFET equation, which leads to [123].

$$I_D = \frac{\mu C_o W}{L} V_D (V_G - V_T^* - \frac{V_D}{2} + \pi_{ref} + \frac{RT}{z_i F} ln a_2^i) \qquad (3.10)$$

It is clear from the above equation that I_D depends on activity "a" of analyte in the same way as in a classical electrode given by Nernst equation. However now we have additional multiplying factor $\frac{\mu C_o W}{L}$. If the externally applied voltages V_{GS} and V_{DS} are kept constant then the current I_D becomes the function of ion activity. According to equation 3.10, the voltage term $\frac{RT}{z_i F}$ appears at the interface. Thus this presents an opportunity for two interfaces viz. at the gate electrode-electrolyte or semiconducting channel-electrolyte to be functionalized with ion selective membrane. Similar to ion selective electrode it is important to have stable electrode potentials. Due to exposure to unknown chemicals the surface may be contaminated, this necessitates calibration to be performed frequently to obtain reliable results. The term π_{ref} refers to standard electrode potential and is susceptible to drift over time, thus for long term measurements proper care must be taken to avoid significant drift of standard potential.

The gold metal electrode has frequently been used for bio-sensing applications as a pseudo-reference electrode. Thanks to its inert properties it has served the purpose well. However, it has not yet been proven if indeed this pseudo-reference electrode can ever replace standard reference electrode for analytical purposes in sensors based on transistors. Clever use of polymer organic materials are also being explored as a reference electrode [124]. In addition, functionalization to achieve stable reference potential which could work without internal solution over the course of measurement period are also proposed [125].

3.3 Carbon Nanotube Transistor fabrication

In the present work, the main workhorse was electrolyte gated transistor. Several options for device fabrication were explored. In the coming sections, we will briefly examine methods applicable to different steps of transistor fabrication.

3.3.1   Electrode preparation

In a simple field effect transistor, three conducting areas are needed, viz. source, drain, gate. Such an arrangement in a typical electrolyte gated transistor is shown in Figure 3.6. The space between source and drain forms the channel of the transistor and is defined by the channel length, and channel width. A typical requirement for source and drain electrodes is of low contact resistance between the contact pads and semiconductor in the channel. This can be controlled using a material having similar work function as that of semiconductor used. Several materials have been proposed such as gold (Au), palladium (Pd) including others [126, 127]. However due to bio-incompatibility, several of the proposed materials disqualify from being used for the biosensors.

Gold, in this view, turns out to be most promising material, with low contact resistance to carbon nanotubes and its bio-compatible nature [128]. Metallic and multi-walled carbon nanotube offer an excellent alternative with an advantage of better workfunction match to semiconducting carbon nanotubes, and further lowering the overall cost of the biosensor [3]. In following sections, we will go through the commonly used process used in the present work.

3.3.1.1   Lift-off

Patterning of photoresist is a critical step in electronic device fabrication [129]. The lift-off process to pattern the resists is illustrated in Figure 3.12(A). The major advantage of this process is that there is no contact between uncured photoresist and electrode material. This is highly beneficial in case of carbon nanotube electrodes, as removal of uncured resist from nanotubes is difficult. However good adhesion is required as lift-off solvent might remove the electrodes during the process.

3.3.1.2   Etching

The process flow of etching which is another method for photoresists patterning is depicted in Figure 3.12(B). Similar to lift-off, the photoresist is patterned using photon flux and masks. However it differs from the previous process in that, the electrode material layer is covered underneath the resist. This layer of photoresist protects the desired electrode pattern, and the remaining unprotected metal film is etched away using chemical processes, or physical etching such as reactive ion
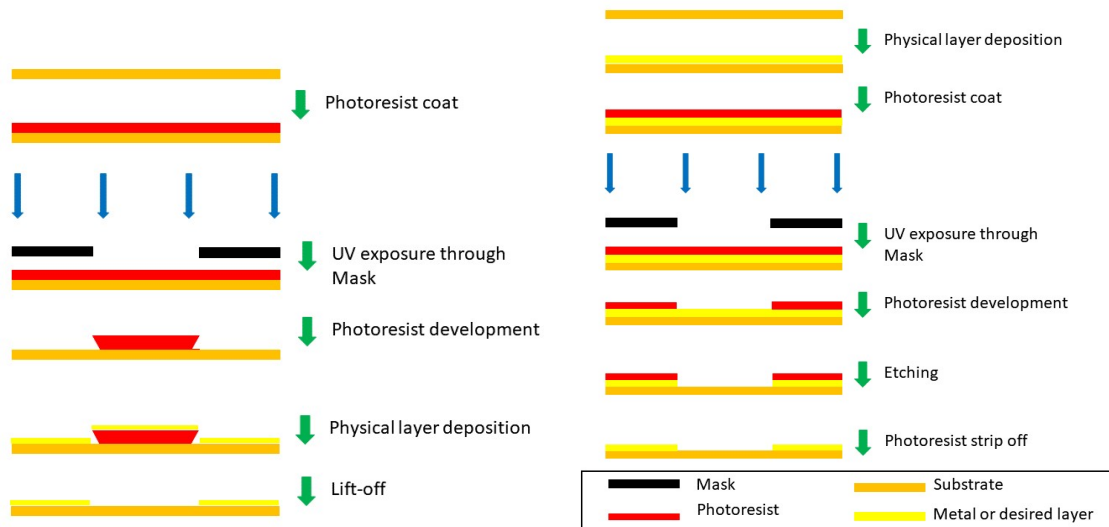
FIGURE 3.12: A stepwise illustration of (A)Lift-off process, (B) Etching process.

etching or plasma ashing. After this step, the patterned photoresist is removed, and the desired electrode pattern is obtained [130].

3.3.1.3 Stencil lithography

This method uses a stencil with desired openings, directly placed over the substrate where electrode pattern is required [131]. Using mechanical methods and support, the stencil and substrate are held together. Finally the electrode material is deposited using techniques like chemical evaporation, sputtering or spray deposition. A general scheme is depicted in Figure 3.13.

A comparison of strength and weakness of each electrode deposition method is presented in table 3.2.

3.3.2 Active layer deposition

Carbon nanotubes dispersed in aqueous media with semiconducting percent ranging from 90% to 99% are used in present work as semiconducting channel. For maximum uniformity, spray deposition was used. Figure 3.13 shows typical spray setup used in the thesis. Stencils were used to deposit random carbon nanotube network selectively [132]. Details of composition used in different sensors will be presented in later chapters.

	Lift-off	Etching	Stencil lithography
Pros	• No photoresist residue left on the electrode.	• No adhesion of particles. • Physical etching for high aspect ratio.	• No need of photoresist. • Reusable stencils makes it very economical and fast.
Cons	• Chances of particles sticking to the substrate during the process. • carbon nanotube network forms an interconnected layer and gets peeled during lift-off	• Difficult to etch away thick carbon nanotube film used for electrodes. • Corrosive chemical are involved.	• Features below few μm are hard to achieve. • Isolated structures can't be fabricated with single stencil mask.

TABLE 3.2: Comparison of different techniques for electrode fabrication.

3.4 Functionalization schemes for bio-molecules

As prepared electrolyte gated transistor is non-selective towards any specific biomolecule. In fact, it shows sensitivity towards various different parameters, for instance ionic concentration, the charge of biomolecule, pH, temperature, bio-molecule adsorption and possibly many more parameters. To utilize it as a sensor for a particular analyte, the EGFET has to be functionalised with specific receptors or selective layers which allow only target molecule to generate a sensor response [133]. Based on this principle, three methods for bio-functionalisation were utilised in this work.

3.4.1 Enzyme Immobilization

Enzymes are macromolecules and play a role of catalyst in biological reactions. They offer very high specificity for only one type of substrate. The word "substrate" in such biochemical reactions is usually used to denote the reactant. The
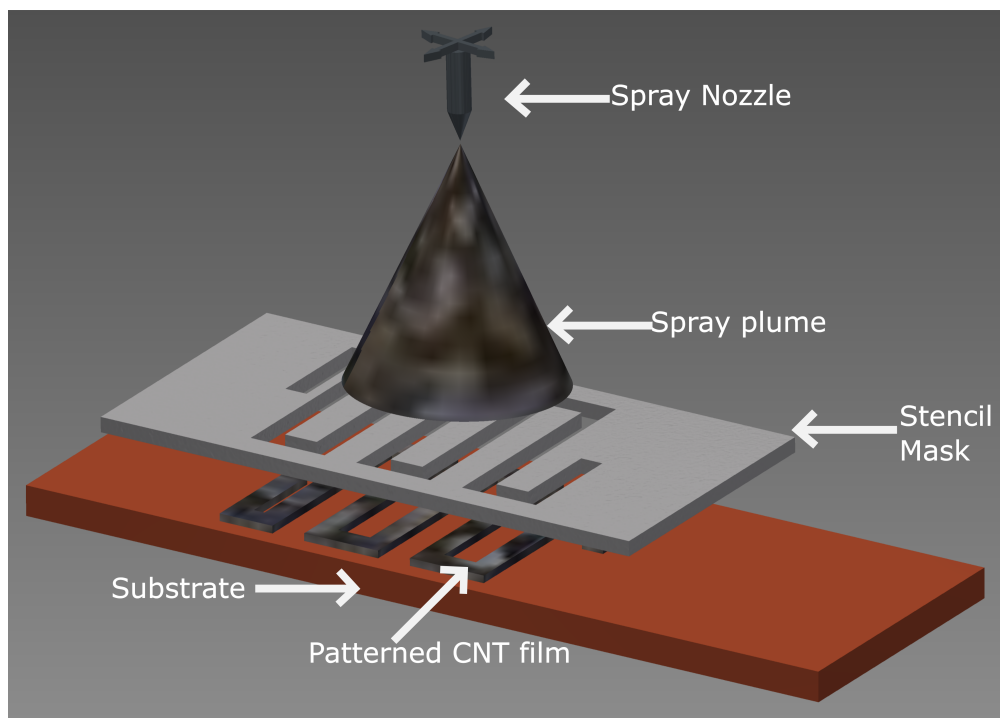
FIGURE 3.13: Carbon nanotube film patterning using stencil and spray deposition technique.

first reported biosensor were enzymatic sensors to indicate the level of oxygen [134]. Field effect transistor based sensors mainly use enzymes for selectivity and are called as enzyme FETs or ENFETs [135]. Usually, the analyte of interest that is to be quantified is the substrate of the biochemical reaction, catalysed by the enzyme. Enzymes convert substrate to reaction product which can be sensed directly by the ENFET. While measurement, the solution containing analyte is placed on ENFET while the enzymes are immobilised on the sensor surface. Various methods are used to immobilize the enzyme onto the sensor.

Enzyme activity is defined as the moles of substrate converted per unit time ($mol\ sec^-1$) and is measured in katal [136]. However, enzyme unit $U = \mu mol\ min^{-1}$ is in more frequent practice. A high activity of enzyme leads to fast sensor response. High enzyme activity also indicates a longer shelf life, as a robust enzyme in general tends to survive the harsher environment. Hence while working with enzyme-coupled reaction, one must pay attention to the enzyme activity before reading out the response, so that the result is inferred correctly. We will discuss three primary techniques for enzyme immobilisation.

3.4.1.1 Physical Adsorption

This immobilization technique relies on weak van der walls bonds to attach enzymes on the sensor surface. It involves sensor to be incubated in a solution containing desired enzyme, to allow the physical bonds formation. Loss of several unbound enzyme molecules is the most significant disadvantage of this method. As no chemical modification is required, enzyme activity as close to the native value in biological environment can be expected [137].

3.4.1.2 Covalent Immobilisation

An alternate strategy for enzyme immobilisation is to covalently bound the enzyme on the sensor surface. Using the help of chemical functional groups like carboxylic acid, amines or thiols present in the enzymes covalent bonds can be formed with appropriate chemical moieties on the sensor surface. Although there are additional steps in the sensor fabrication to achieve covalent immobilisation of enzyme, but it is a more stable immobilisation technique when compared to physical adsorption.

There are multiple sites in enzyme at which the covalent bond can be formed. Thus it often becomes practically impossible to choose the perfect site for bond formation. In some unfortunate case the immobilisation can also lead to blocking of the active catalytic site of the enzyme. It is also possible that the enzyme is bound at multiple sites on the surface and hence is not able to catalyze the main biological reaction. In such situations, usually a spacer molecule is used to provide enough space and possibility of conformational change to occur [138].

3.4.1.3 Entrapment

Mixing enzymes into inert polymer matrix was one of the earliest used methods for enzyme immobilisation. Typically enzyme of interest is mixed with an inert matrix such as chitosan [139] among others. However, there exists no universal substrate which would be ideal for every enzyme. Some of the points that must be kept in consideration for enzyme entrapment are as follows:

- The encapsulating membrane should be permeable to the substrate, and product of the biological reaction.

- It should also allow the enzyme to perform conformational change during the reaction and should not deteriorate the enzyme activity.

- The encapsulating membrane should bind the enzyme such that the enzyme remains bounded even upon changing the analyte solution.

All the above points influence the shelf life and number of times the sensor can be used reliably. This enzyme immobilisation strategy suffers from diffusion dynamics of the reactants and products, in the enzyme binding membrane.

3.4.2 Ion selective membrane functionalization

Sensors for ions are another class of biosensor which focus on either single elemental ions or small ionic molecules. These ions play a vital role not just in biological systems but also in environmental, agriculture and industrial processes. The hydrogen ion sensor also known as pH sensor, was the earliest ion sensor fabricated. It depends on selective glass membrane which allows only H^+ ions to move across liquid/glass interface. Thus as discussed in chapter 2, Nernst potential becomes an indicator for hydrogen ion concentration. This laid foundation for other ion based sensor and the quest started to find membranes which could selectively allow specific ions to cross interface. Some naturally occurring molecules which show selectivity for ions, known as ionophores [140] are incorporated into ion sensors.

Similar to enzyme entrapment ionophores are trapped in the membrane composed of the polymer matrix. To allow diffusion of ions through this matrix plasticiser is used. The final physical state of the membrane can range from semi-solid to liquid membranes [141, 142]. A typical membrane composition is $\sim 60 - 67\%$ plasticizer, $\sim 30-33\%$ polymer, $\sim 2-3\%$ ionophore, and some additional lipophilic salts. Typically an organic solvent is used to make a liquid solution containing all the components and referred to as "cocktail". This solution is then ready to be applied on sensor surface. Once the organic solvent evaporates, an ion selective membrane is formed. Considering the IUPAC definition ion sensors constructed in this manner, may not be classified as sensors if the ionophores used to capture ions are not involved in a biochemical process.

3.4.3 Immunosensor immobilization

As discussed in chapter 2, specific binding of antigen to antibody causes a change in refractive index at the interface. Refractive index is directly related to the dielectric constant of material as $\kappa = n^2$, κ is the dielectric constant and n is the refractive index. Alternatively, it could be modelled as, modulation in capacitance term in relation governing I_D, drain current of the transistor [143]. This is not the only mechanism scientific community has attributed to immunoFET. It has been proposed that charge alteration at the electrolyte-semiconductor due to antigen-antibody interaction can be the major factor and is sensed with the field effect device [144]. However, it has been suggested that charge alteration mechanism is doubtful, and cannot be used to explain the sensor response due to lack of ideal polarizable interfaces and the interface charge transfer resistance could very well dominate the overall sensor response [145]. Nevertheless, several immunosensors has been demonstrated even if no single mechanism is attributed clearly to their functioning. The functionalization is usually carried out by immobilising antigens on the semiconducting channel (with or without insulator), or on the gate surface. Similar to enzymes, physical adsorption, as well as a covalent bond can be utilised to immobilise the proteins. Once a uniform film of antigens is formed the sensor is virtually ready to be used.

Chapter 4

Nanomaterial based devices and applications

4.1 Metal-free Electrolyte Gated CNTFET

Single-use sensors offer the highest level of hygiene and do not suffer from cross-contamination. It is important to keep the device cost low enough to justify single-use sensor [146]. A key to achieving this goal is using economical processes and low-cost materials. One of the key costs involved in the realisation of the biosensor is the metal deposition for electrode fabrication. The process itself is time-consuming and requires sophisticated instrumentation. The additional cost is incurred due to the noble metal being used for fabrication of the sensors [147]. To access the feasibility of fully solution processed sensor, electrolyte gated transistor manufactured completely with carbon nanotube were investigated. Carbon nanotube based on their chirality are found in metallic, or semiconducting in nature. Thanks to their superior current carrying capacity multi-walled carbon nanotubes have also been proposed as interconnect material in silicon technology. Aiming at economical fabrication processes, spray deposition system was utilized. Direct spraying of nanomaterial onto the substrate simplified the process to a two-step process.

4.1.1 Material and Methods

For the fabrication of such metal free all carbon electrolyte gated transistor, the multi walled CNTs were used as electrode material. Using sodium dodecyl sulfate

(SDS) as the surfactant [148], aqueous dispersion containing 1 wt% SDS, and 0.1 wt% multi-walled carbon nanotubes (MWCNTs) (obtained from Hanwha Chemical, CM-250) was prepared. To obtain a stable and homogeneous ink, sonication at an average power of 170W for a total of 25 min was performed. This ink was further centrifuged, and only top 80% of supernatant was used.

To pattern the electrodes, lift-off process is used. To get rid of any remaining photoresist after development and to increase the adhesion of carbon nanotubes, oxygen plasma followed by treatment with 3-Aminopropyl triethoxy silane was done. MWCNT was then deposited using spray coating technique. Spray nozzle (Nordson EFD, USA), mounted on an automated motion platform [149] was used to spray the MWCNT dispersion on the patterned photoresist. It was followed by lift-off in acetone. Thus carbon nanotube electrodes on flexible substrates were obtained. As at this stage surfactant is still present on the carbon nanotubes, the samples were treated with deionised water to dissolve away SDS. 15-30 mins water treatment was found optimum for higher yield, as with prolonged treatment time thick films of MWCNT would de-laminate from the substrate. However once treated and annealed, the adhesion was much stronger.

For these devices, 99.9% semiconducting carbon nanotubes were used for transistor channel. As received carbon nanotube dispersion (NanoIntegris) was centrifuged at 15000 rpm for 90 mins and again only top 80% of supernatant was used. This was done to remove any possible bigger bundles. On the substrate with MWCNT electrode, using stencil masks, semiconducting CNTs were sprayed. However this time the density of nanotubes was much less. Proprietary chemicals were used by the manufacturer, to disperse the CNTs. However similar treatment with deionised water recommended by the supplier was used to dissolve the dispersant.

At this moment it is worthwhile to mention that for the patterning of electrodes, etching was also attempted. It left a visible mark of ashed carbon on the substrate. Thus it was not pursued further. Also, the electrical conductivity of such prepared electrodes was less. Similar issues occurred with stencil lithography. Due to longer times required to spray the electrodes, the sharp edges were smeared upon accumulation of sprayed drops along the stencil. This led to a low yield of the devices. However upcoming techniques of the drop-on-demand process such as ink jet printing, and aerosol printing may very well alleviate the issue. Figure 4.1 shows the difference in the nanotube density for MWCNT electrode and the semiconducting channel.

These electrodes were positioned as shown in Figure 4.2.
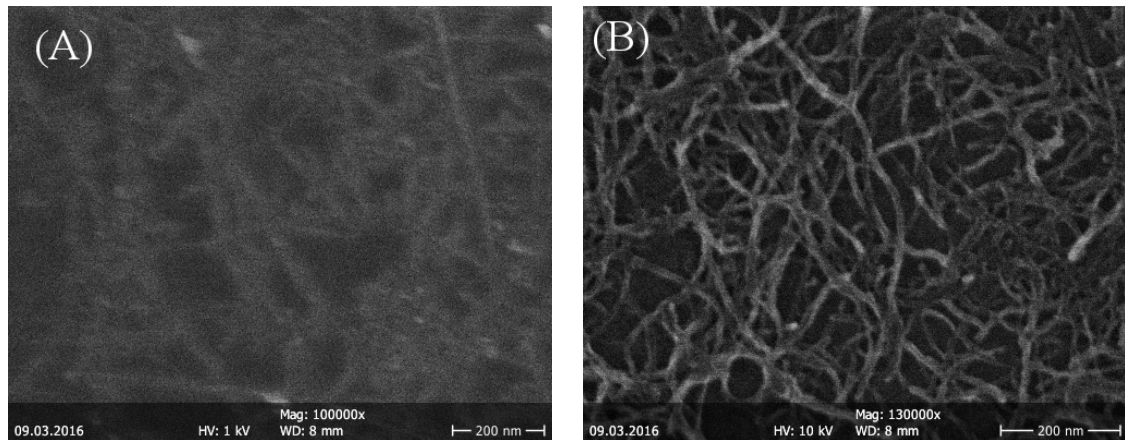
FIGURE 4.1: Scanning electron microscope images for the carbon nanotube films. (A) Semiconducting film, (B) MWCNT film used for electrodes, adapted from [3].
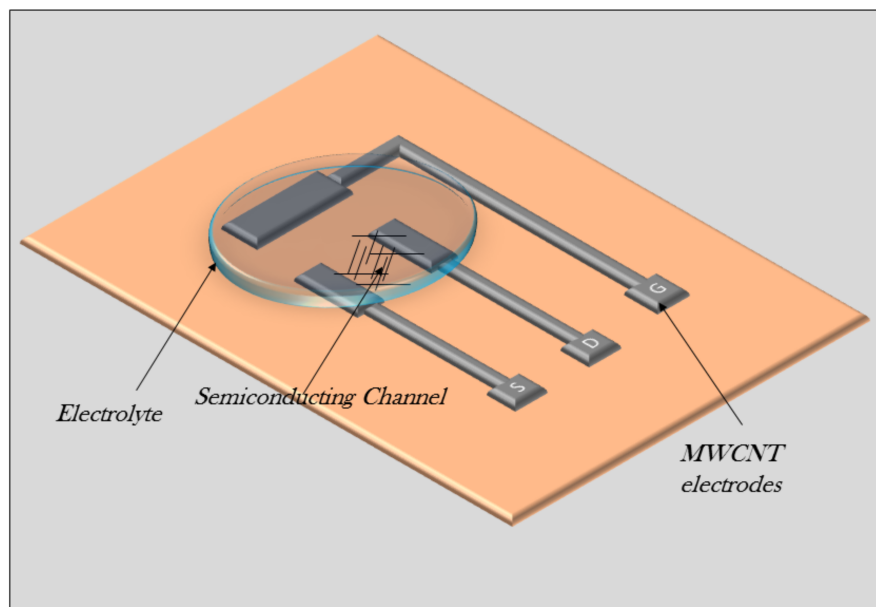
FIGURE 4.2: Design of metal-free fully carbon nanotube electrolyte gated transistor.

All the electrodes were on the same plane and liquid electrolyte covers the gate and the channel simultaneously. This architecture is different from typical MOSFET where the gate is positioned geometrically on a plane parallel to semiconducting channel separated by an insulator. However thanks to the double layer formation at the channel and gate electrode, the gate can be placed anywhere in the volume containing the electrolyte. With the benefit of precision in gate dimension, this architecture is most efficient. Figure 4.3 shows typical transfer and output curves measured for metal free complete carbon CNTFET. The channel length of this particular device was $300\mu m$ and channel width was $700\mu m$. The typical drain
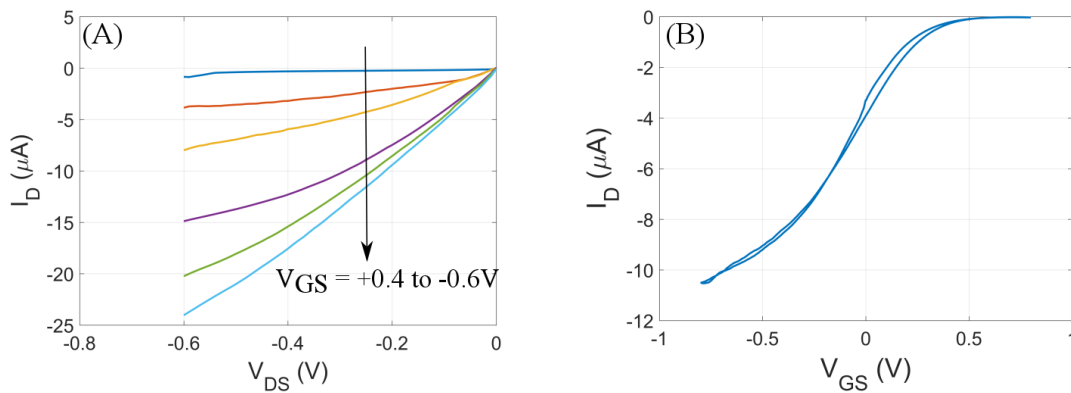
FIGURE 4.3: Electrical characteristics of all carbon nanotube field effect transistor. (A) Output characteristics, (B) transfer characteristics measured at $V_{DS} = -0.2V$, adapted from [3].

current on-off ratio was 2.6 orders of magnitude.

4.1.2 Contact resistance

Choice of electrode material, as mentioned earlier plays a dominant role in determining the economic feasibility of biosensors. However, replacing known materials in favour of economic gain should not harm the device performance. To gain insight, comparison of MWCNT electrodes with gold electrodes was also done. Contact resistance provides an excellent measure to determine the suitability of electrode material used. Transfer length method, first proposed by Shockley [150], was used to extract the contact resistance between the electrode and semiconducting channel [3]. The electrodes were patterned and deposited around semiconducting material at unequal spacing as shown in Figure 4.4(A).

The total resistance measured between any two consecutive electrode contacts can be given as

$$R_T = 2R_C + \frac{R_{sh} L_{ch}}{W} \tag{4.1}$$

Here R_C is the contact resistance at the contact, R_{sh} is the sheet resistance of the semiconducting channel separating the electrodes with L_{ch} as the separation and W as the width of the electrodes. Assuming contact resistance is always same at each electrode-semiconductor interface, if we plot the total resistance as a function of channel length we obtain plot shown in Figure 4.4(B). The y-intercept of the
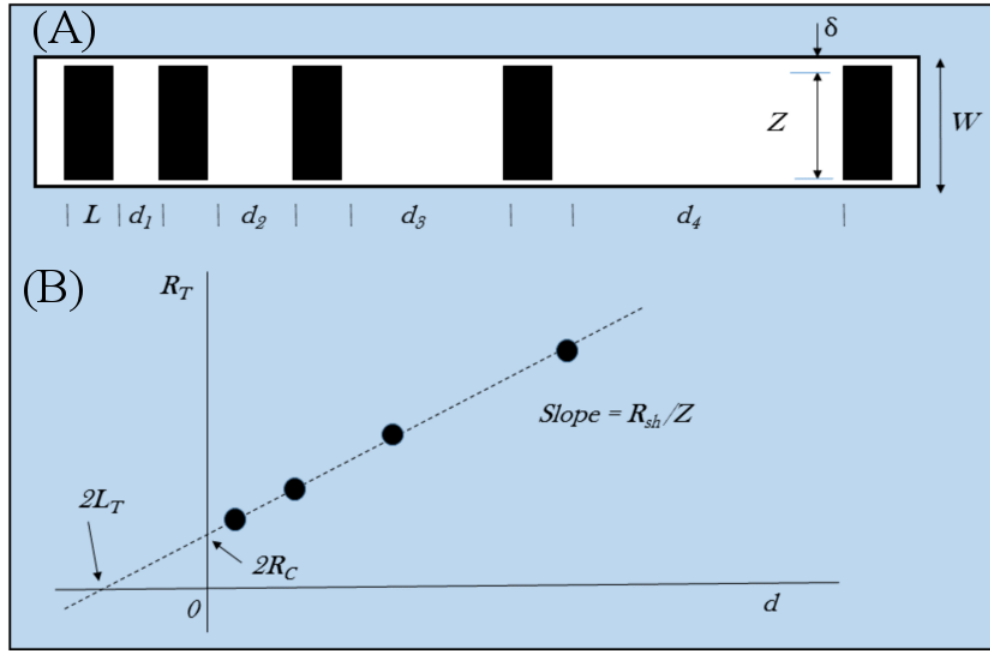
FIGURE 4.4: (A) Test structure for measuring contact resistance and transfer length propsed by W. Shockley. (B) Extraction of transfer length and contact resistance from linear plot of R_T vs d.[4].

linear plot gives the total contact resistance $2R_C$. For large electrodes, we can approximate R_C as below [4].

$$R_C = R_{sh}L_T/W \tag{4.2}$$

and contact length given by

$$L_T = \sqrt{\frac{\rho_C}{R_{sh}}} \tag{4.3}$$

Using above relations, it becomes possible to derive ρ_C from the measured data. Figure 4.5 shows the measurement data of total resistance for electrodes fabricated from MWCNT and gold. The total resistance graph shows that MWCNT electrodes have much lower contact resistance with semiconduting CNTs as compared to gold electrodes.

A fair comparison between contact resistance for the different materials, using this method, is possible only when sheet resistance of the semiconduting channel in both cases is comparable. Random carbon nanotube network pose a challenge in this regard, as each device has different percolation path, leading to variation in sheet resistance.
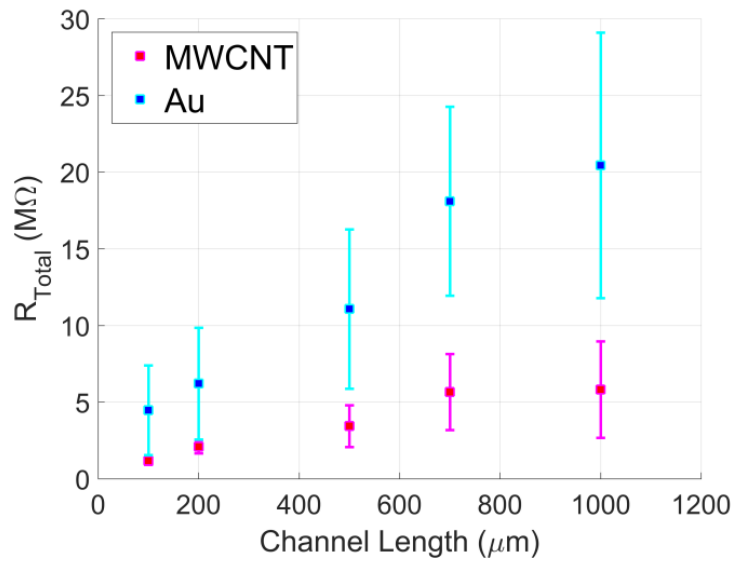
FIGURE 4.5: Comparison of total resistance for CNT and gold electrodes in TLM structure.
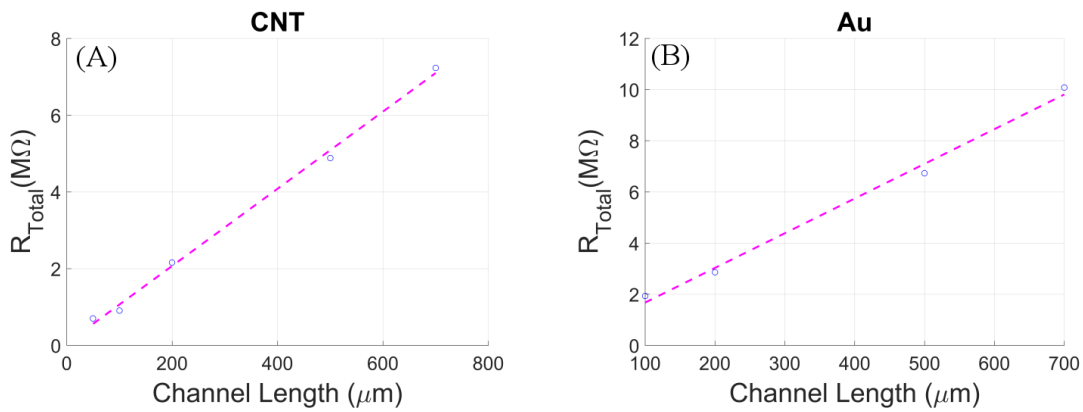
FIGURE 4.6: Comparison of total resistance with devices having same sheet resistance of semiconducting film (A) CNT electrode, (B) gold electrode.

Parameters	R_C	ρ_C	R_{sh}	L_T
All CNTFET	$28.2K\Omega$	$0.237\ \Omega - cm^2$	$3.05\ M\Omega$	$2.8\ \mu m$
Au CNTFET	$156K\Omega$	$5.42\ \Omega - cm^2$	$3.3\ M\Omega$	$11.5\ \mu m$

TABLE 4.1: Data extracted from TLM measurement of an all CNTFET device and a gold contact CNTFET.

Figure 4.6 shows measurement results for two devices which similar sheet resistance values, $3.05M\Omega$ for the MWCNT electrode, and $3.3M\Omega$ for the gold electrode. The data extracted from TLM study is shown in Table 4.1.

4.2 Impact of device geometry on electrolyte gated CNTFET

EGFETs are very attractive devices due to their low operational voltages, thanks to the very high double layer capacitance present at electrolyte-semiconductor and electrolyte-gate interface [151]. It makes them a promising candidate with low power consumption. Sensors based on these devices can operate with less power budget, enabling a long battery life. Thus it is essential to understand the impact of the device architecture on its performance. Comparing transistor with simple two terminal devices, one obvious observation is the requirement of a third terminal. This not only adds to the burden of extra electronic circuitry for sensor reader, but it also occupies an extra space. In the spirit of optimising the sensor layout impact of the gate size on transistor performance is conducted.

The total capacitance at the electrolyte-metal interface is directly proportional to its area. If the fraction of potential available at the semiconductor-electrolyte interface is defined as $V_{G,channel}$ and the external gate bias applied is V_{GS}, then $V_{G,channel}$ is given by the equation 4.4

$$V_{G,channel} = V_{GS}\left(\frac{C_{gate}}{C_{channel} + C_{gate}}\right) \tag{4.4}$$

This assumes a series connection of the two electrolyte double layer capacitors and an infinite series resistance, such that no steady state leakage current flows into the gate terminal. Using Helmholtz capacitance at the interface (assuming high applied bias and high salt concentration), the C_{dl} can be approximated as

$$C_{dl} = \frac{\epsilon\epsilon_0 A}{d} \tag{4.5}$$

using the above equation and rearranging the equation 4.4, we obtain

$$V_{G,channel} = V_{GS}\left(\frac{1}{1 + \frac{A_{channel}}{A_{gate}}}\right) \tag{4.6}$$

Here $A_{channel}$ and A_{gate} represent areas for $C_{channel}$ and, C_{gate} respectively. This gives us design parameter to tune the transistor such that most of the external applied gate bias gets is seen across semiconductor-electrolyte interface. To quantify
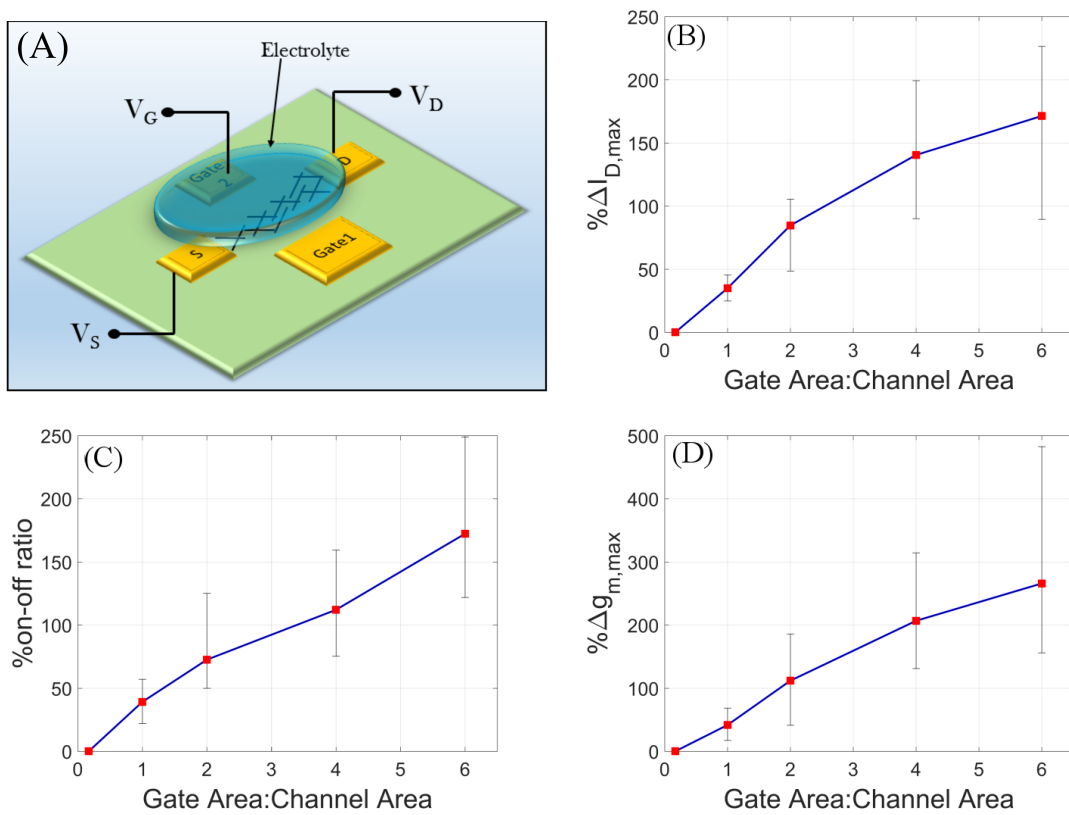
FIGURE 4.7: Analysis of the variation in transistor properties with gate electrode area. (A) Illustration of the device geometry to test the impact of gate area. Percentage change in (B) maximum drain current, (C) on-off ratio and (D) maximum transconductance.

this effect, an experiment is designed such that a single transistor can be gated with gates of different geometrical areas. Figure 4.7(A) shows the illustration of such device.

The gate electrodes are arranged around the semiconducting channel such that their geometrical centre is equidistant from the geometrical centre of the channel. This is done to eliminate any effect of varying distance between the gate and channel, as the electrolyte with finite conductivity can influence the charging time of capacitor.

For this study, the gate electrodes and metal contacts for source and drain were fabricated using lift-off process. 5nm of chromium (Cr) was physically deposited followed by 50 nm of gold (Au) on a polyimide substrate. The channel dimensions were 60 μm as channel length and 3000 μm as channel width. After lift-off the resulting device was further encapsulated using positive photoresist (AZ5214), exposing only gate electrodes. This step is necessary to eliminate any parasitic contribution of contact pads which come in contact with the electrolyte. Transistor

channel comprised of 90% semiconducting carbon nanotube random network and deposited using spray coating method. The different gate:channel areas used in this study were 1:6, 1:1, 2:1, 4:1 and 6:1.

Due to random nature of the semiconducting channel, each device produced is different in terms of channel conductivity. To compare all the devices, percentage changes are calculated relative to device having, A_{Gate}:$A_{channel}$ as 1:6. Figures 4.7 (B), (C) and (D) show the impact of the change in gate area on three major transistor properties namely maximum drain current, on-off ratio and maximum transconductance respectively. As the fraction of external gate voltage available across semiconductor-electrolyte interface increases the transistor performance increases. It implies that having a larger gate area would increase the device performance but at a price of a larger device.

However, in the above example, only the surface area was increased. Thus next step was to keep the geometrical area fixed but rather increase the effective surface area. This was achieved using random MWCNT film as the gate electrode. This study was performed both with and without an underlying gold electrode. Figure 4.8 (A) shows the layout of a device for testing gates with the same geometrical area but different surface areas by having MWCNT on top of them. Figure 4.8 (B) shows the impact of this different architectures on transistor transfer curves. A gate electrode entirely made of MWCNT network has the low current compared to gold gate of same geometrical area. This can be attributed to the increase in RC time constant of the gate capacitor due to increase in resistance. The gate electrode made up of the MWCNTs with underlying gold layer has the maximum current as expected. Thus, we observe that to achieve higher gate current, this strategy demands one additional step after lithography and increases the effort in sensor fabrication. Thus, in favour of ease of fabrication, this technique to increase the gate surface area was not used in sensor studies.

4.3 Carbon nanotube based impedance electrodes

4.3.1 Biocompatibility

One of the simple sensors produced, are used in measuring the impedance of cell culture. This sensor is ideally a pair of electrodes measuring the impedance at a given frequency and voltage level, similar to a conductance sensor. In various
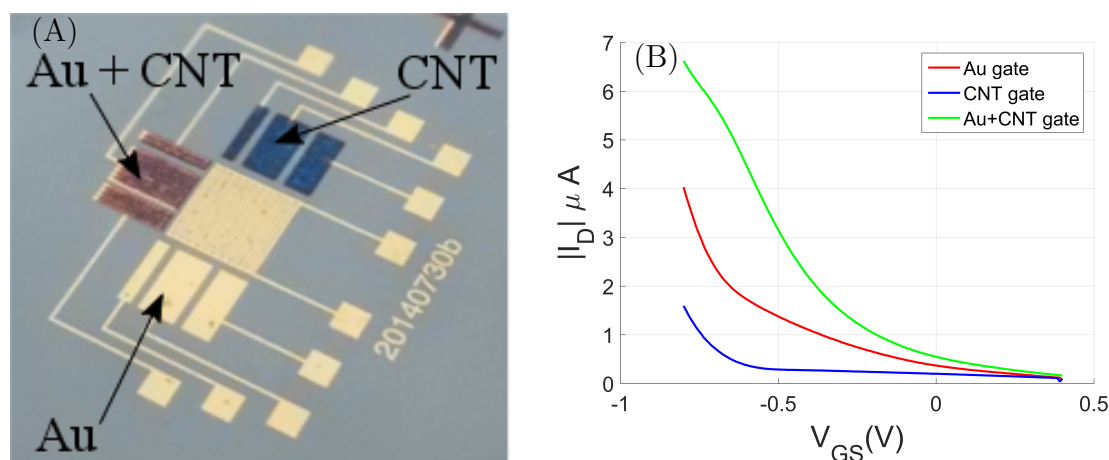
FIGURE 4.8: (A) Device architecture to test the impact of carbon nanotube as gate material on the electrolyte gated CNTFET characteristics. (B) Transfer characteristics of same device measured with different gates.

situations, it is of importance to monitor the cell culture behaviour and observe the cellular parameters such as total cell count, the speed at which the cells are growing and dividing. Furthermore, drugs that are designed to alter the cell growth require that these parameters are monitored continuously. In the past expensive noble metals were mainly used for this purpose. However, later a technique called electrode cell impedance spectroscopy (ECIS) was investigated and proposed to study the effect of cell growth on electrodes by recording the electrical impedance of these electrodes [152, 153].

Noble metals such as gold are utilised in ECIS studies due to their chemical inertness and biocompatibility [154]. Novel materials such as carbon nanotube and graphene also show chemical inertness in aqueous media and are potential candidates for fabrication of electrodes for ECIS [155, 156]. Hence, a study was conducted for their biocompatibility. Using L929 mouse fibroblasts and human umbilical vein endothelial cells (HUVEC), biocompatibility and viability tests were performed. Single-walled carbon nanotubes with one-third tubes as metallic and rest as semiconducting tubes showed similar cell propagation speeds as that of the unmodified substrate [5]. The sheet resistance of the SWCNT film was around $8k\Omega\square$.

Figure 4.9 (A) shows the surface morphology of the SWCNT film measured using atomic force microscope. The intertwined carbon nanotube network forms a dense film. Thus at these densities of CNTs, homogeneous electronic and physical properties are present allowing miniaturisation of the device without changing the
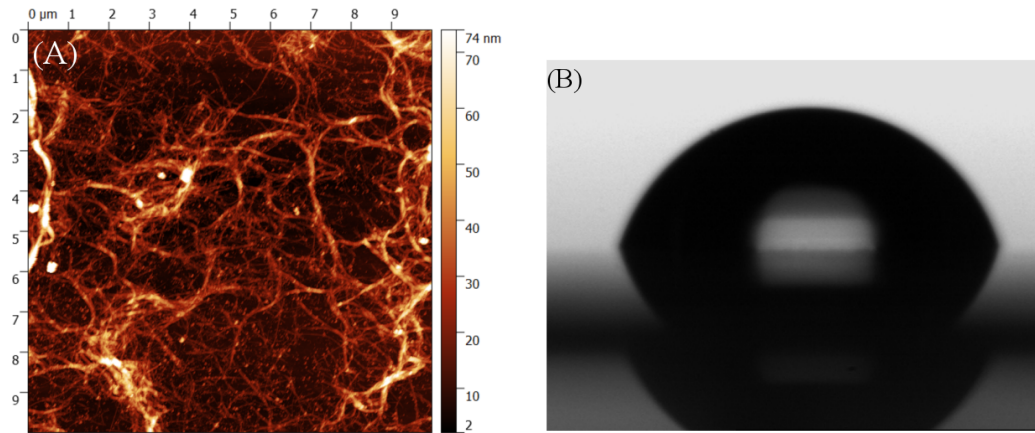
FIGURE 4.9: (A) AFM image of CNT film. (B) Drop of DI-H$_2$O used for contact angle measurements, adapted from [5].

film characteristics. To check the wetting property of the film, contact angle measurement were carried out and the average of 5 such measurements gave contact angle of 69.5 °. Figure 4.9 (B) shows a drop of deionised water for contact angle measurement on the surface of the SWNCT film.

4.3.2 Integration with 3D printing

3D printing technology is currently one of the most trending technology. According to Gartner Inc., a research and advisory firm, 3D printing technology is poised to change business models of several organisations [157]. Among the several advantages of 3D printing, possibly the most exciting one is the ability of produce custom parts. Researchers and engineers have tried to print even biological tissues and cells [158, 159]. On this knowledge, one can envision the integration of 3D printing with nanomaterials for biological applications like biosensor development or even complex systems are artificial tissues. To test this idea, a successful attempt was made to integrate 3D printing with carbon nanotube technology to produce impedance electrodes for monitoring of cell culture. In the preliminary step, the substrate was printed using a semitransparent filament. Once thickness of a few millimetres was achieved, 3D printing process was kept on hold. In the next step, SWCNTs were sprayed using a shadow mask on the printed substrate, and finally 3D printing was again continued.

Figure 4.10 (A) shows the four-well ECIS plate prepared using this technique. This plate was used to monitor the impedance of bakers yeast cell culture. Dry baker yeast was mixed with glucose solution and transferred to the wells of the
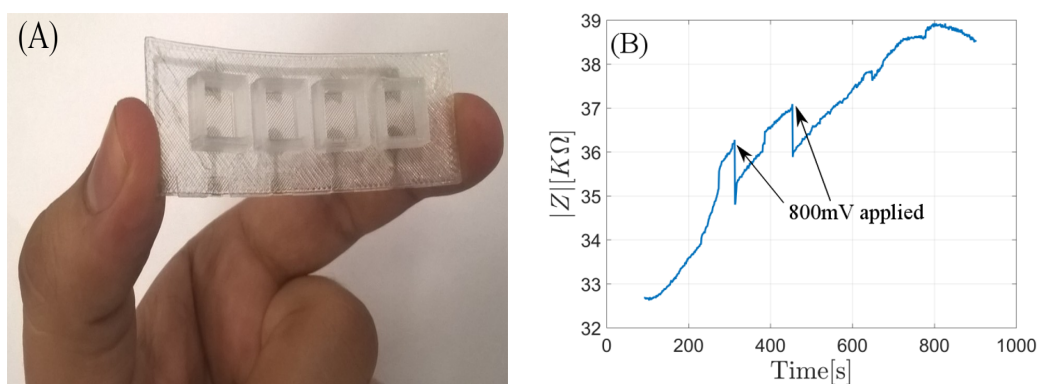
FIGURE 4.10: MWCNT film electrodes for impedance measurement of cell culture on 3D printed substrate. (A) 3D printed wells for cell culture. (B) Recorded impedance as bakers yeast proliferates.
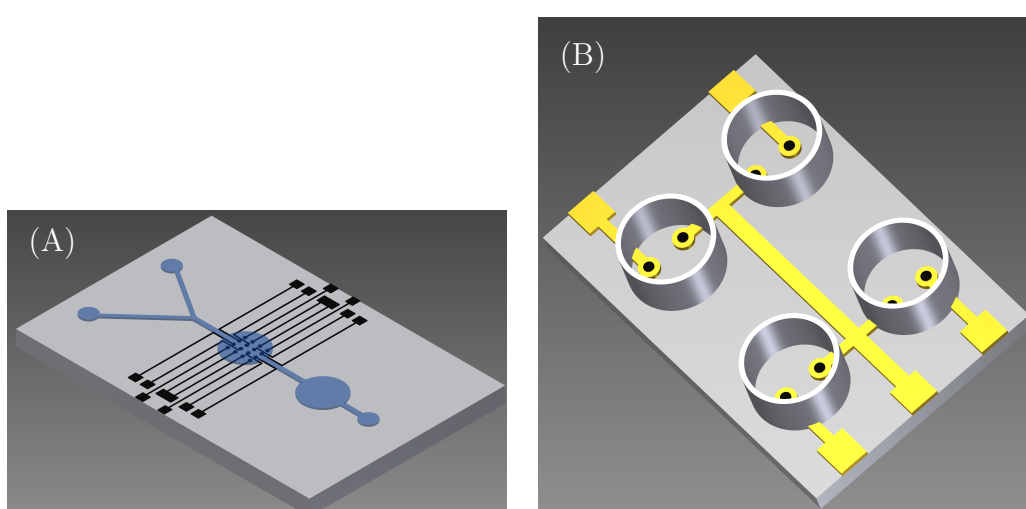
FIGURE 4.11: Possible architectures with fully cnt and hybrid electrodes. (A) Concept to test cell motility, (B) Hybrid electrode design to lower electrode impedance.

as-prepared ECIS test plate. Figure 4.10 (B) shows the increase in impedance as the cell-growth starts. These ECIS plates used for impedance monitoring can also be used to study the healing dynamics of cell culture [160]. To gather information about healing speed of cell culture, wounds were created mechanically, and the recovery was monitored. A high voltage pulse of 1 volts applied for 1 second caused a decrease in the measured impedance due to creation of wounds. Electrical impedance starts to grow after the wounding step. This encourages the use of carbon nanotube as an electrode material for fabrication of ECIS plate.

Figure 4.11 (A) shows the schematic where carbon electrodes are patterned in an array to be used for impedance measurement. Compared to metal film, CNT film has much higher electrical resistance. Measure small changes in cell impedance,
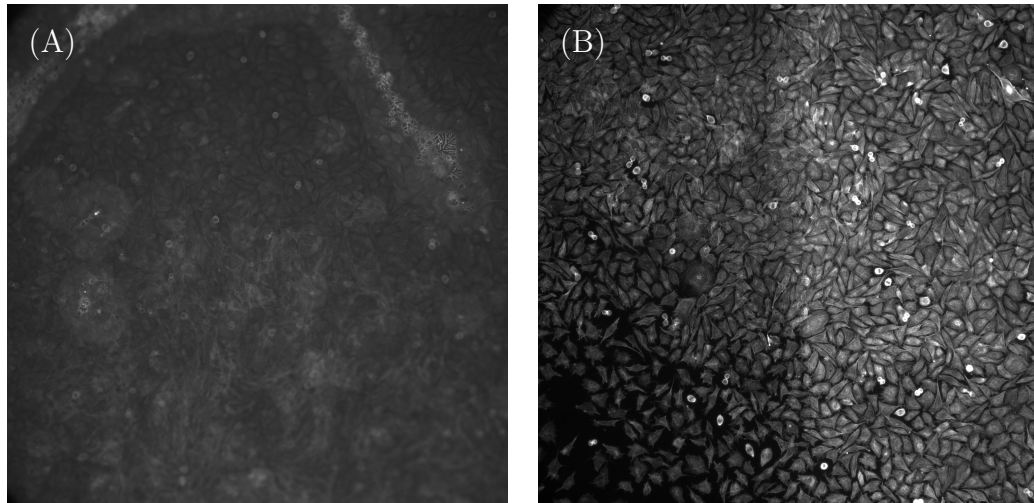
FIGURE 4.12: Optical images of L929 cell cultures on (A) gold electrode and (B) random carbon nanotube film electrode

can pose an issue as the percentage change in total impedance might be smaller than the resolution of measuring equipment. To tackle this problem a hybrid electrode is proposed. Figure 4.11 (B) shows the electrodes made from two different nanomaterials. Majority of the electrode consists of high conductivity material such as silver nanowires, and only the area exposed to cell culture is made from biocompatible carbon nanotubes.

Optical measurements are frequently used in biological research. CNT based electrodes offer superior imaging capability over gold electrodes. Figure 4.12 compares L929 cell cultures on gold and CNT electrodes (Images are provided by ibidi GmbH on the electrodes prepared in the present work).

4.4 Extended gate electrolyte-gated CNTFET

Bringing carbon nanotubes directly in contact with the ions present in electrolyte has an intriguing effect. For example, change in the chemical bonds at the CNT surface is a primary reason for the pH response of CNT based electrolyte gated transistor [161, 162]. Such sensors require intimate contact of carbon nanotubes with the test sample. Change in resistance of carbon nanotube when brought into contact with test sample constitutes a simple chemiresistor. This is the major underlying principle for gas sensors [163, 164]. In case of biosensors built on the same principle, the test sample is replaced by a liquid [163]. In such cases, it

difficult to decide the main reason for the change in sensor response. Following are some potential contributing factors:

1. A chemical reaction between semiconductor and test sample [163].

2. Change in the double layer capacitance at either the gate electrode or the semiconducting surface [143].

3. Change in surface potential due to the presence of bound charged species such as protein or DNA.

It is entirely possible that change due to one factor dominates or even cancels out the contribution due to other factors. In such situations, the sensor would be non-responsive. To remedy this issue, either the semiconductor should be tested in a controlled environment for example by using buffer solutions which maintains the ionic strength and keeps the ion composition constant, or some form of encapsulation must be provided to avoid direct contact with the semiconductor such as insulating oxides [11] or ion selective membranes [12].

To illustrate this effect a carbon nanotube transistor is measured in an electrolyte composed of various concentrations of NaCl prepared in deionised water. As predicted by electrolyte double layer theory, as the ion concentration increases the capacitance at the interface should increase. This should lead to an increase in the absolute value of drain current when same bias levels are applied. Contrary to the expectations, the measured currents are as shown in Figure 4.15 (A), the drain current instead decreases. In fact, as shown in Figure 4.13 this is due to increase in resistance of the CNT film with increase in ion concentration of the electrolyte. Thus the two effects, i.e. increase in the double layer capacitance and the decrease in conductivity of CNT film counteract each other. For eliminating such situations, a different architecture is tested.

4.4.1 Extended gate transistor

Figure 4.14 (A) presents a different device architecture. Here the gate electrode is coupled with a second pair of electrodes. Two separate zones are now available for the electrolyte. The pair consisting of semiconductor and electrode is similar to usual electrolyte gated transistor. The additional second pair of electrodes forms the so-called extended gate. Effectively it is equivalent to placing two double layer capacitor in series with the gate of the transistor.
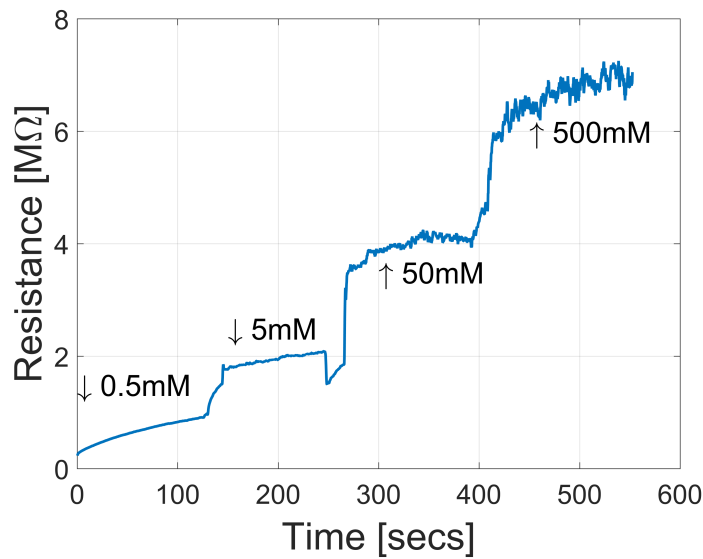
FIGURE 4.13: Variation in the resistance of CNT channel with varying ionic concentration of electrolyte (NaCl) and fixed applied bias.
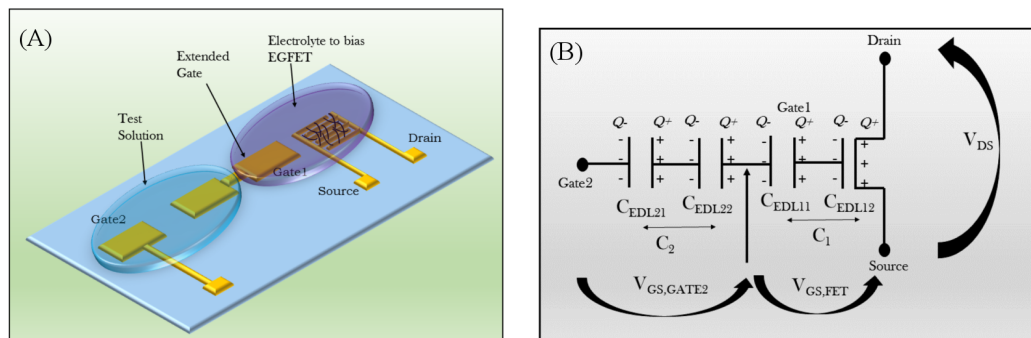
FIGURE 4.14: Extended gate architecture to eliminate issue of reaction with CNTFET. (A) Device architecture, (B) Schematic representation of equivalent electric circuit.

Figure 4.14 (B) shows the equivalent circuit diagram for the presented design. This design provides the advantage of keeping constant electrolyte composition over the semiconducting channel. This benefit comes at the cost of a greater area required for the sensor, extra material usage for electrode fabrication as well as complicated design to contain two separate electrolyte zones. It does, however, help in observing, the anticipated increase in drain current due to increase in ion concentration.

Figure 4.15 (B) presents the same transistor used in measurement of Figure 4.15 (A) but now measured in extended gate configuration. Deionized water is used as the electrolyte for the transistor. Electrolyte over the extended gate is exchanged after a constant time interval, from low concentration to higher and back to low
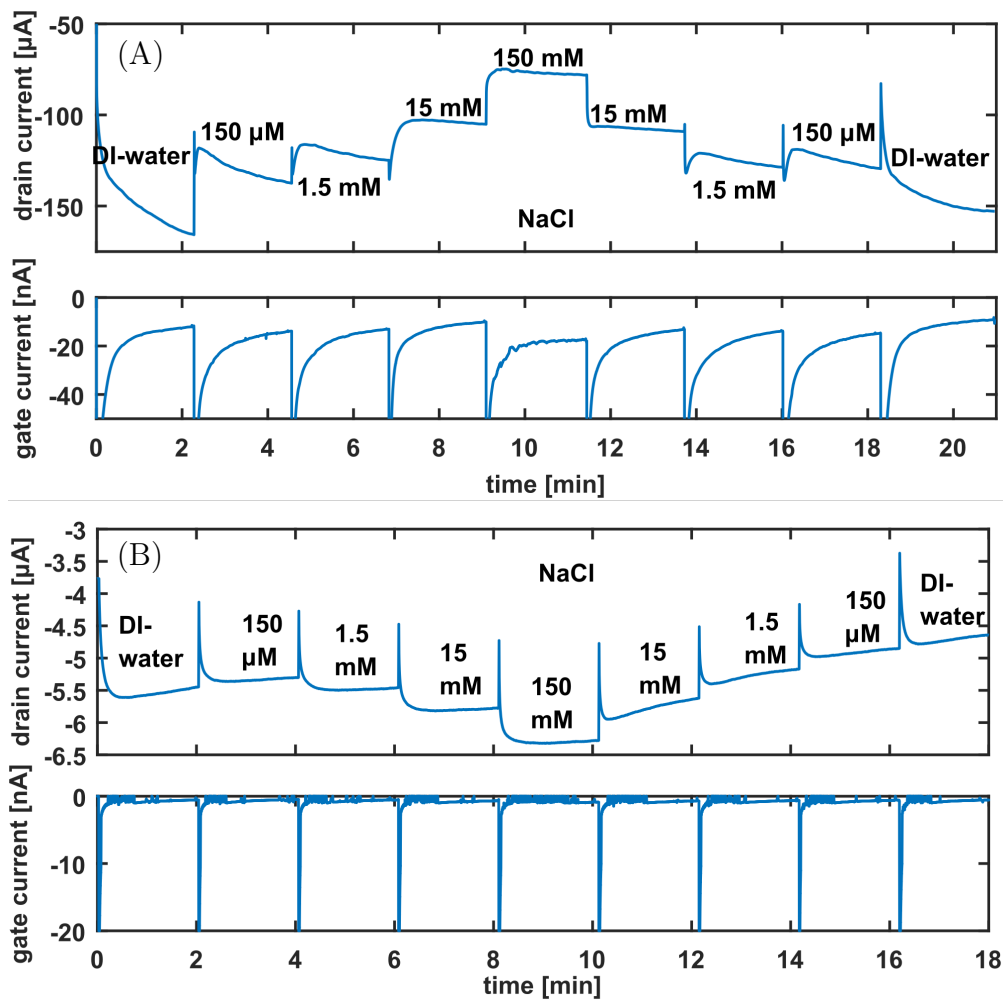
FIGURE 4.15: (A) Online measurement of transistor drain current at constant drain and gate bias. (B) Online drain current measurement of same device with extended gate design. Bias are same in both cases ($V_{DS} = -0.2V$, $V_{GS} = -0.8V$)

ion concentration. A distinct change in the transistor response is visible. Now on increasing the ion concentration the drain current increases. This is in agreement with the fact that double layer capacitance increases with increase in ion concentration of the electrolyte.

Chapter 5

Electrolyte gated CNTFET biosensor

In the previous chapters, we discussed several aspects of electrolyte-gated CNT-FETs. Theoretical background on biosensors and different aspects of EGFETs in biosensors were also presented. In this chapter we discuss in detail the working principle and analyze the results for several different types of biosensors. Different functionalisation schemes were used to attain biosensors for neurotransmitter, sugar molecules, ion and DNA sensing.

5.1 Selective ion sensors

Ions constitute an essential class of chemical species found in the biological system. They play an essential role in various bioprocesses such as stabilising DNA [165], carrying action potential in neurons [166], muscle control [167] and participate in various cell functions [168]. Other than their role as biological entities they also play a major role in several varied systems for example in food processing industry, where ion concentration can be a marker of the attainment of certain processing stage [169]. Change in the ionic levels can have a tremendous ecological impact. For example acidification, an increase in H^+ ion concentration in the ocean may lead to decay of marine life [170]. Ions such as phosphate and nitrate leaching away from farms into water bodies cause an imbalance in aquatic life [171]. Thus the significant interest in developing systems capable of monitoring ions is justifiable.
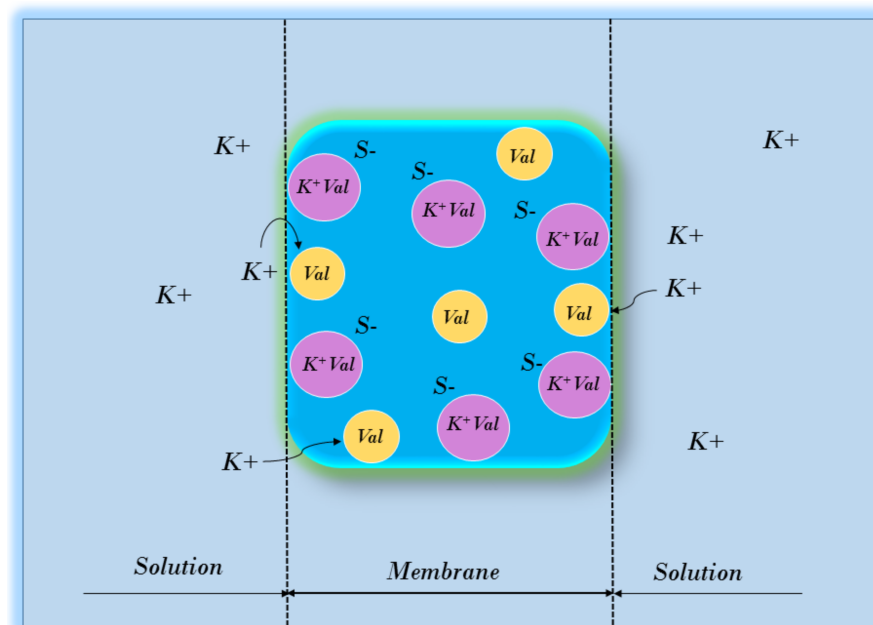
FIGURE 5.1: Movement of ions across a K+ ion selective membrane. Val stands for Valinomycin, ionophore for such a membrane.

Cremer around 1906 recorded the potential difference in acid and base when separated by glass membrane [172]. Later in the 1930s when Arnold Beckman was asked to make a device capable of measuring the acidity of orange juice, he in fact, made the device based on glass membrane [173]. This enabled pH measurement in the field as the device developed was portable. Since then various dopants for glass have been developed to provide a better pH meter. However, the core sensor remains the same. Later, George Eisenman's group developed glass membranes for sodium and potassium sensor [174]. This, however could not be generalised to other ions successfully. Building on the same principle of glass membranes which would allow selective migration of ions, sensors based on polymeric membranes infused with ionophores were developed [175]. These ionophores could selectively allow movement of the target ions from solution into the membrane phase. Figure 5.1 shows the functioning of such a membrane.

Ion sensors have grown from modest pH sensor developed in the early 1900s to automated blood gas analysers [176] capable of detecting significant ions in blood samples in a matter of minutes. Introduction of ion selective field effect transistors (ISFET) in the 1970s marked a new phase in the progress towards development of ion sensors. Site binding model was investigated to explain the new ion sensors viz. ISFETs [177]. In its initial years, ISFETs were thought to be capable of working even without a reference electrode. This was later corrected and the reference electrode was reintroduced [178]. Until now the requirement of reference
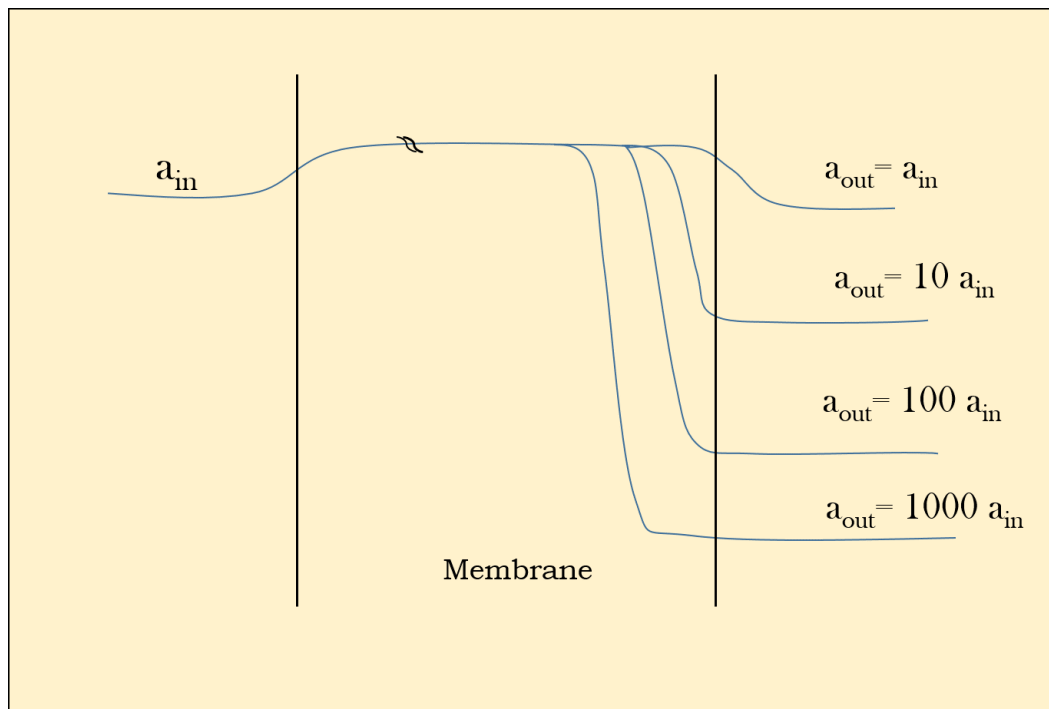
FIGURE 5.2: Potential distribution across a ion-selective membrane.

FIGURE 5.3: Cross-section of an ion-selective field effect transistor.

electrode has hampered the miniaturisation of ion sensors. Ion sensors derive their strength from potentiometric techniques. As illustrated in equation 2.6, any membrane capable of allowing only one ion to exchange with the solution is capable of producing a Nernst potential.

Figure 5.2 shows the potential distribution across an ion-selective membrane. This analogy is not directly applicable to carbon nanotube transistor based sensors, as there is no internal electrolyte solution present. Figure 5.3 presents the cross-section of a ion selective sensor based on electrolyte gated CNTFET.

One remarkable point regarding this sensor is the absence of any internal filling solution. This enables a compact sensor. Such solid state ion sensor fall into the category of coated wire electrode (CWE). These sensors were initially produced with a metallic wire coated with ion-selective membrane [179]. Such sensors suffered from high drift. The reason was attributed to charge built up at the metal-membrane interface. To overcome this issue and facilitate ion to electron transduction, electronically conducting polymers were introduced [180]. As they had high redox capacitance the stability of solid-state electrodes increased. Carbon nanotubes were also used as the ion to electron transducer [181]. However, in the case of carbon nanotube redox reaction is not possible. Instead a high double layer capacitance was attributed for the stability of these sensors. Electrolyte gated CNTFETs thus when coated with ion-selective membrane can be used as ion sensors. If the ionic strength of solution and applied gate bias are high then the double layer capacitor is constant as shown in Figure 3.8. Thus the fraction of gate bias across the double layer capacitor at semiconductor-membrane interface becomes function of primary ion concentration in the test sample.

Several ion sensors were developed in the present work to extend the use of CNTFET sensor platform. All sensors were developed on flexible polyimide substrates. As mentioned in chapter 3, electrolyte gated CNTFET offer two interfaces for functionalisation namely the gate and the channel. Also, it was noted in chapter 4 that undesirable change in conductance happens when carbon nanotubes are directly interfaced with different electrolyte solutions. Thus to encapsulate the carbon nanotubes, and use their high double layer capacitance polymeric ion-selective membranes were used on the semiconducting channel. These membranes were based on polyvinyl chloride (PVC) inert matrix.

The ion selective membranes can be broken down into four main components.

- Ionophore to selectively bind to ion of interest.

- Plasticiser to allow mobility for ions.

- Lipophillic Salt to reduce the resistivity of membrane

- An inert matrix to provide structural support for membrane.

The ionophore is probably the most critical component of the ion selective membrane. The ionophore largely determines the selectivity of the ion sensor. Naturally occurring ionophore valinomycin was first tried out to fabricate ion-selective
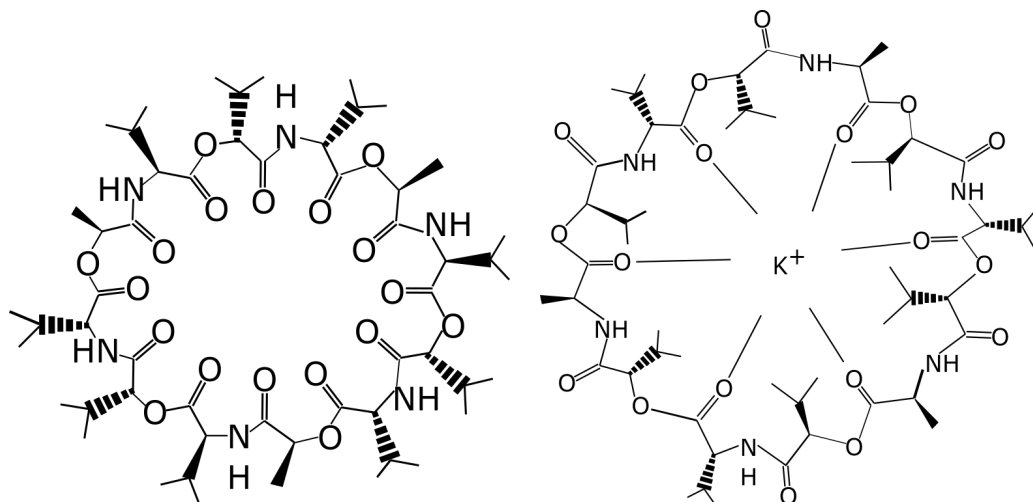
FIGURE 5.4: (A) Valinomycin molecule, (B) Valinomycin and K+ complex.

membranes. Valinomycin in nature is responsible for transport of potassium ion [182]. It is a neutral molecule in itself. Figure 5.4 (A) shows its structure, thanks to its unique size it offers a more stable complex for potassium ion compared to its hydration shell. This complexing phenomenon helps in capturing potassium a hydrophilic ion to be transported from aqueous media to a hydrophobic environment [183]. Figure 5.4 (B) shows valinomycin forming a stable complex with potassium ion.

This idea sparked a quest to search for suitable ion capturing molecules for several different ions of interest. Until now either naturally occurring molecules have been identified or synthetic molecules have been synthesised to cover a broad range of cations [184]. Anions, however, pose a challenge. For example, phosphate ion sensor is still not widely available despite its wide importance and need in the agricultural sector.

Selectivity of ionophores is not ideal, and in fact, ionophore show cross-sensitivity towards interfering ions [185]. Multiple ion sensors systems could be used to increase confidence in the reported sensor value. The selected ionophore is entrapped in an inert polymer matrix to provide mechanical support. The matrix should, however, allow for conformal change and movement of ionophore. To achieve this plasticity, aptly named chemicals called as plasticisers are used [186]. Thus if only these three components were to be used, it would form a reasonably insulating membrane due to lack of any charge carriers within the membrane. This causes a high output impedance and would require even higher input impedance meter. Adding ionic salt directly to the membrane, however, is also not a solution, as those ions would move to more favourable aqueous medium. To counteract this

problem, lipophilic ions were introduced [187]. They maintain the conductivity of the membranes while preserving its ion selective properties. Optimizations regarding the ratio and choice of these components is almost always needed according to the application requirements. Sensor properties such as response time, usable lifetime of the sensor, need for calibration, sensitivity and application area are the main factors to be taken into account while optimising the membrane composition. As of now, it remains more of an art to find the optimum membrane composition.

TABLE 5.1: Composition of ion selective membrane

Ion	Ionophore	PVC	Plasticizer	Lipophilic Salt
K^+	Valinomycin 2.8%	31.6%	64.0% DOS	1.6% NaTFPB
H^+	TDDA 1%	33.2%	65.2% DOS	0.6% KTPB
Na^+	Na ionophore X 0.8%	30.2%	68.8% o-NPOE	0.2% KT-ClPB
Mg^{2+}	Mg ionophore I 0.8%	33.6%	65% o-NPOE	0.6mg KT-ClPB
$NH4^+$	Nonactin 1.8%	36.8%	60.6% DOS	0.8% NaTFPB
PO_4^{2-}	PO_4^{2-} Ionophore 1.9%	32%	65.6% o-NPOE	0.5% NaTFPB

Table 5.1 shows the composition of different ion selective membranes used in the present work. Apart from phosphate membrane, all other membrane solutions were prepared by the group of Prof. Agata Michalska, Faculty of Chemistry, University of Warsaw. 100 mg of these membrane compositions were dissolved in 1 ml of tetra hydrofuran (THF). Once the so-called cocktail was prepared, the sensor surface is cleaned with dry nitrogen. To remove any curvature present in the polyimide substrate, the sensor is temporarily stuck on a flat surface using adhesive tape. Approximately 20 μl of the cocktail solution is drop casted on the semiconductor channel, and the sample is left to dry. Once THF evaporates the boundaries of the polymeric ion-selective membrane are covered with PVC dissolved in THF. This is done to seal the membrane-substrate interface towards moisture penetration. Similarly, all the exposed electrodes are encapsulated using PVC film to avoid any mix potentials. Even with these precautions in the current scheme, it was observed that the membrane would sometimes delaminate, allowing electrolyte to come into direct contact with the semiconducting channel. This results in sensor failure.

Hence a more robust mechanical design would benefit the long-term stability of the sensors. The thickness of the overall membranes obtained was around 80 μm.

To characterize the developed sensors test solutions containing different target ion concentrations are prepared. To eliminate the influence of ionic strength, background salts are used to match the ionic conductivity of all the test solutions.

Figure 5.5 to 5.7 show the online measurements of the sensors developed. Traditionally ISFETs were characterised by measuring threshold shift when operated in saturation regime [188]. This was done mostly to compare ISFET with traditional ion-selective electrodes. However, this is not a necessity and with modern electronics direct drain current can be easily read out at a fixed applied gate and drain bias. Transfer curves are obtained by sweeping the gate bias. As every measuring device needs some settling time the exact sweep rates cannot be guaranteed for all range of drain current measured. This necessitates for large sweep delays to be applied for controlling the sweep rate before progressing to next bias level. This increases the time to record transfer curves. Additionally, the transfer curve is an ambiguous measurement. Hysteresis is usually present in the transistor and causes the threshold voltage to be slightly different for different sweep directions. This presents a dilemma as to which threshold value should be used. Keeping these factors in perspective, it is easier to use drain current recorded at fixed bias levels as a measure of sensor response.

As discussed, table 5.1 presents the composition of different ion selective membranes. After drying of solvent from the ion selective membrane, they are conditioned in 1mM of primary ion concentration typically for 8-10 hours. As shown in Figure 5.5 to 5.6 when the concentration of primary cations increases, the net potential available across the C_{dl} (Figure 3.8) decreases. This decrease in the available bias causes a decrease in the magnitude of drain current. If the similar sensor is used for sensing anions, such as phosphate ions or nitrate ions, the available potential bias across the C_{dl} increases with increasing ion concentration. This consequently increases the drain current with increasing primary anion concentration. Figure 5.7 show the response of phosphate and nitrate sensor respectively and they are in accordance with the above understanding.
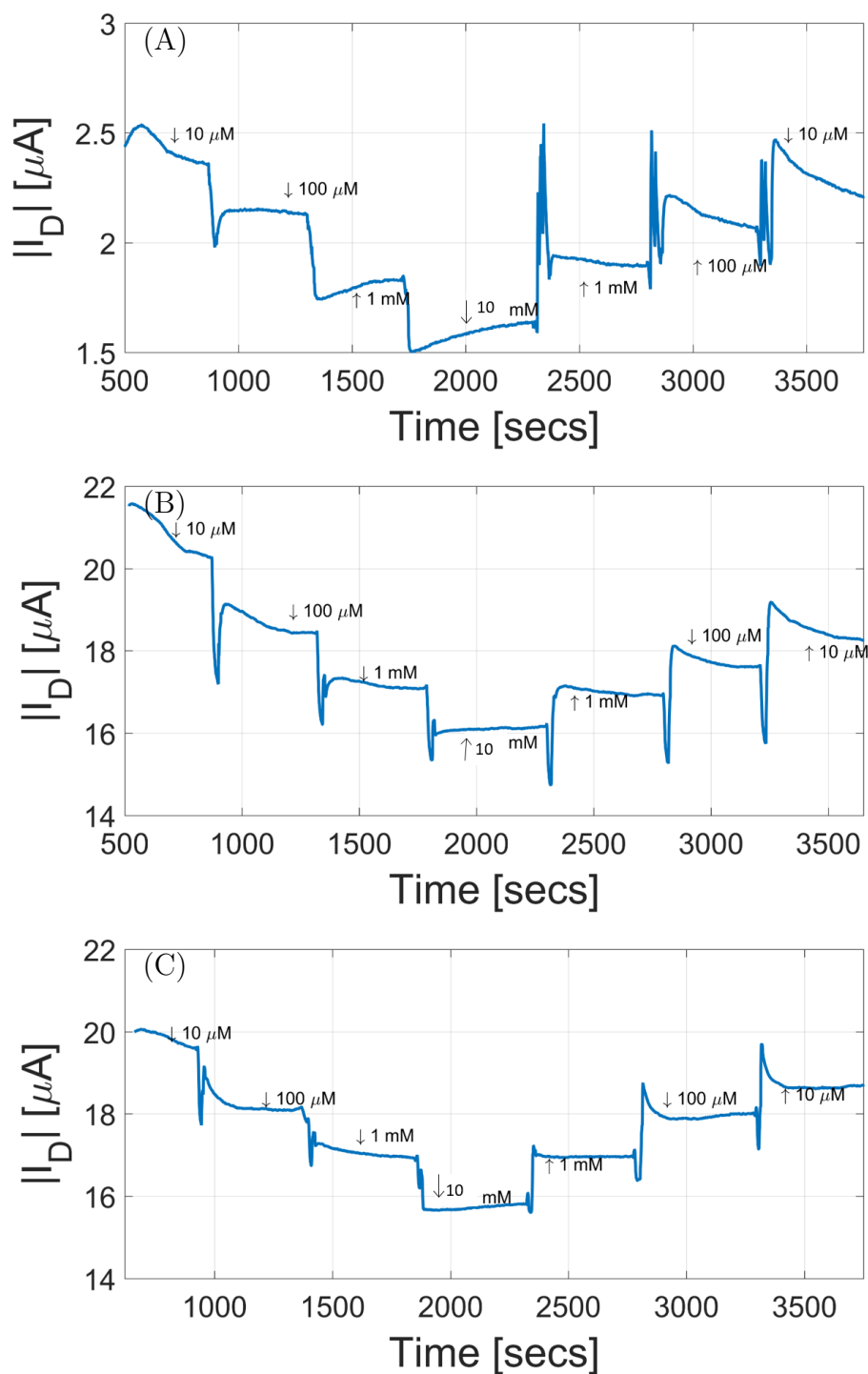
FIGURE 5.5: Ion-selective sensor response measured in $MgCl_2$ background for constant conductivity. Bias for measurement are V_{DS} = -0.8V and V_{GS} = -0.8V. Real time measurement for (A) Na^+ sensor in NaCl, (B) NH_4^+ sensor in NH_4Cl, (C) K^+ sensor in KCl.
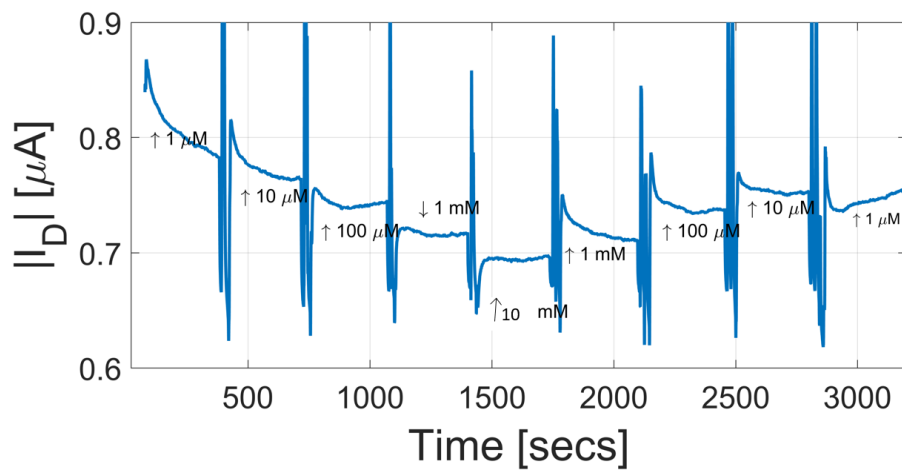
FIGURE 5.6: Ion-selective Mg^{2+} sensor measured in $MgCl_2$ with NaCl background for constant conductivity. Bias for measurement are V_{DS} = -0.8V and V_{GS} = -0.8V.
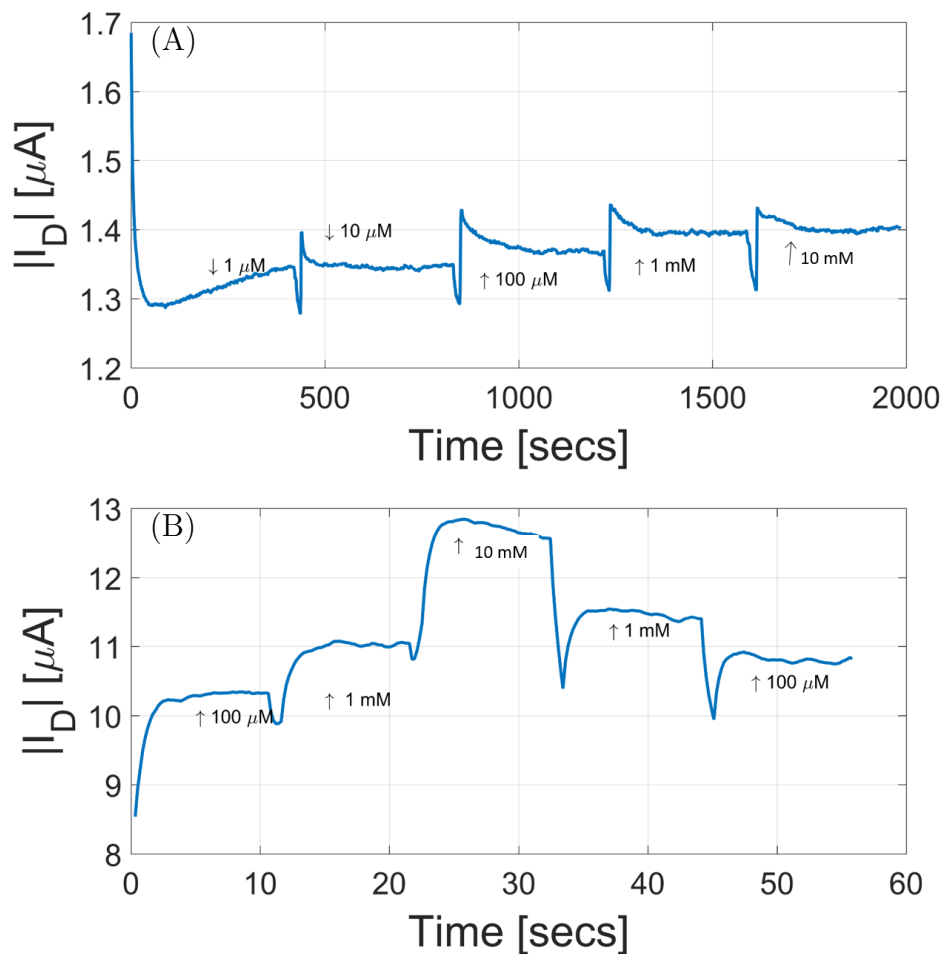
FIGURE 5.7: Anionic ion-selective (A) $NO3^-$ sensor measured in KNO_3 with KCl background for constant conductivity. (B) $PO4^{2-}$ sensor measured in $H_2PO_4{}^-$ with H_2SO_4 background for constant conductivity. Bias for measurement are V_{DS} = -0.8V and V_{GS} = -0.8V.
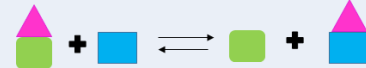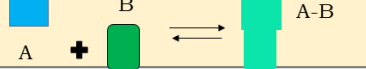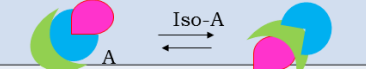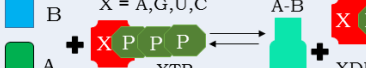
Class	Reaction Type	Important Subclass
1. Oxidoreductases		*Dehydrogenases, Oxidases, Peroxidases, Reductases, Monooxygenases, Dioxygenases*
2. Transferases		*C-Transferases, Glycosyltransferases, Aminotransferases, Phosphotransferases*
3. Hydrolases		*Esterases, Glycosidases, Peptisades, Amidases*
4. Lyases ("synthases")		*C-C-Lyases, C-O-Lyases, C-N-Lyases, C-S-Lyases*
5. Isomerases		*Epimerases, cis trans Isomerases, Intramolecular transferases*
6. Ligases ("synthetases")		*C-C-Ligases, C-O-Ligases, C-N-Ligases, C-S-Ligases*

FIGURE 5.8: Classification of enzymes based on their functions.

5.2 Enzyme based biosensors

Enzymes are biocatalysts responsible for catalysis of almost all the biochemical reactions occurring the living organisms. Figure 5.8 shows their classification based on their function. The use of enzymes in electrochemical biosensor stems from the need to convert neutral species into electroactive components. Oxidoreductase is the most widely used major class of enzymes for such conversions. The design process for enzyme-based sensors starts with a chemical analysis of the substance which needs to be quantified. If the chemical entity of interest can participate in a reaction catalysed by enzyme and results in an electroactive compound, it becomes possible to design an enzymatic sensor. Typically either the chemical of interest is directly oxidised or reduced, and the product is sensed using potentiometric or amperometric methods. For example, using urease urea can be broken down into ammonium ions, and they can be quantified using ammonium ion sensors [189]. Similarly, if the product of a reaction is acid or base, it can change the pH of solution causing a change in conductivity of semiconducting carbon nanotube channel [190]. Hydrogen peroxide is known to oxidise carbon nanotubes and hence change their conductivity [18]. A significant fraction of oxidoreductase enzymes produces hydrogen peroxide. Thus these enzyme-mediated reactions can be used for sensor development.
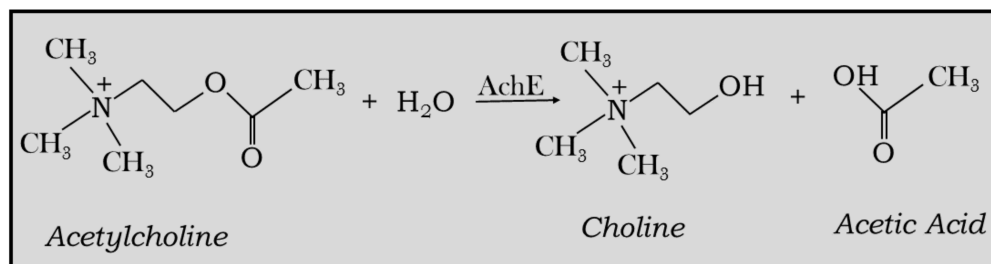
FIGURE 5.9: Acetylcholine hydrolysis by enzyme acetylcholinesterase (AchE).

5.2.1   Acetylcholine biosensor

Acetylcholine is an important neurotransmitter found in central and peripheral nervous system. In the central nervous system, it acts as ion channel gating agent allowing ion channels to open. In the peripheral nervous system, acetylcholine is involved in the muscle movement. The release of acetylcholine in the synaptic cleft formed by the neuron-muscle interface causes sodium ion channels located on the surface of muscle cells to open up and results in muscle contraction [191]. Acetylcholinesterase is an enzyme responsible for removing acetylcholine from the synaptic cleft [192]. If the enzyme fails to remove acetylcholine, it can result in muscle spasm and could become fatal. Several toxins produced naturally by organisms or artificially synthesised work on this principle and inhibit the activity of acetylcholinesterase [193].

The reaction catalysed by enzyme acetylcholinesterase breaks acetylcholine into acetic acid and choline. Figure 5.9 shows the reaction path for conversion of acetylcholine into acetic acid and choline. Biosensor capable of sensing these byproducts could be useful in the determination of acetylcholine itself or to assess enzymatic activity of acetylcholinesterase(AchE). Towards this aim, the electrolyte-gated CNTFET was designed to test the presence of byproducts and later was used to check the enzyme activity of AchE.

An electrolyte gated CNTFET was fabricated on a polyimide substrate [6]. To fabricate the device lift-off process was used to pattern the Cr/Au electrodes. The channel length of the transistor was 50 μm and channel aspect ratio as 900. The semiconducting channel between source and drain was formed by random carbon nanotube network deposited using spray deposition. Sodium dodecyl sulfate (SDS) was used to disperse carbon nanotubes in the aqueous media. After spray deposition, the as-fabricated transistors were placed in around 50 ml of DI water to allow SDS to desorb from the CNT film.
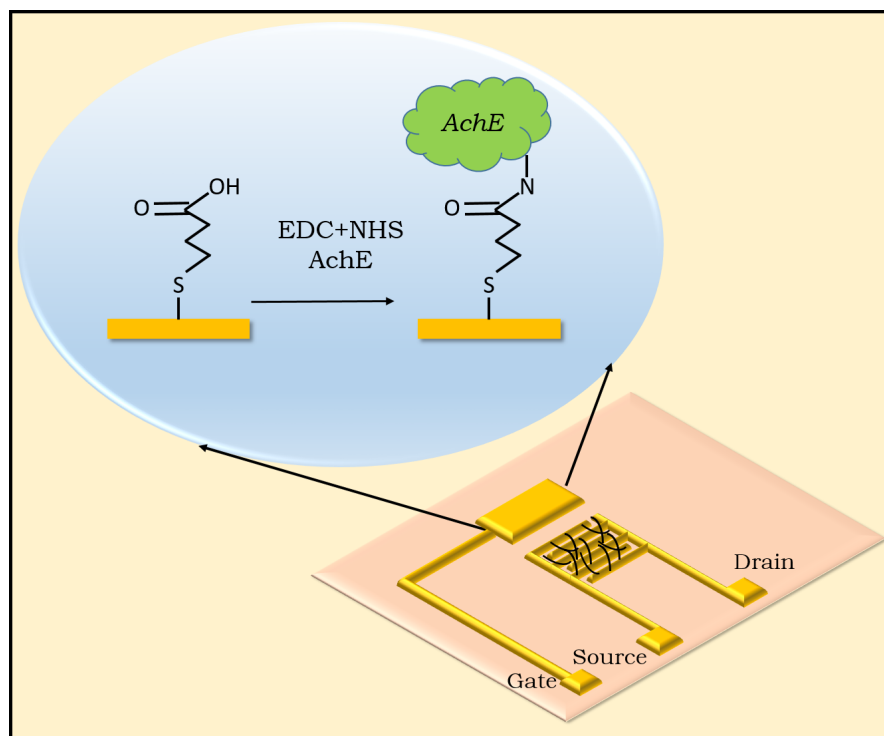
FIGURE 5.10: Functionalization scheme for acetylcholine enzymatic sensor.

5.2.1.1 Sensor functionalisation

A self-assembled monolayer is a uniform layer of molecules formed by a spontaneous chemical reaction on the target surface. It relies on the virtue of chemical properties of the participating surface and the layer forming molecules. Carefully chosen molecules and target surfaces can form a highly ordered layer [194]. The chemical bond between gold and sulfur is a strong bond and is often used to functionalise the gold surface with organic compounds [195]. Mercaptopropionic acid (MPA) was used to form a functional layer over the gate electrode. A ethanol and water solution having water : ethanol ratio as 25:75 was used to prepare a 70 mM MPA solution. On the freshly prepared gate surface, this functionalisation solution was drop casted. The samples with MPA were left overnight to form the self-assembled monolayer. The samples were then rinsed with the same ethanol-water solution [6].

EDC/NHS chemistry is a well known method to immobilize enzymes and other amine containing molecules on carboxyl terminated surfaces [196]. It was used to attach AchE to the carboxyl terminated MPA SAM layer present on the gate electrode. 30 μl of 30mM EDC is mixed with 30 μl of 30mM NHS and is drop cased on gate electrode. This activates the carboxylic group of MPA. Enzyme solution containing 2mg/ml of acetylcholinesterase was prepared in phosphate buffered saline
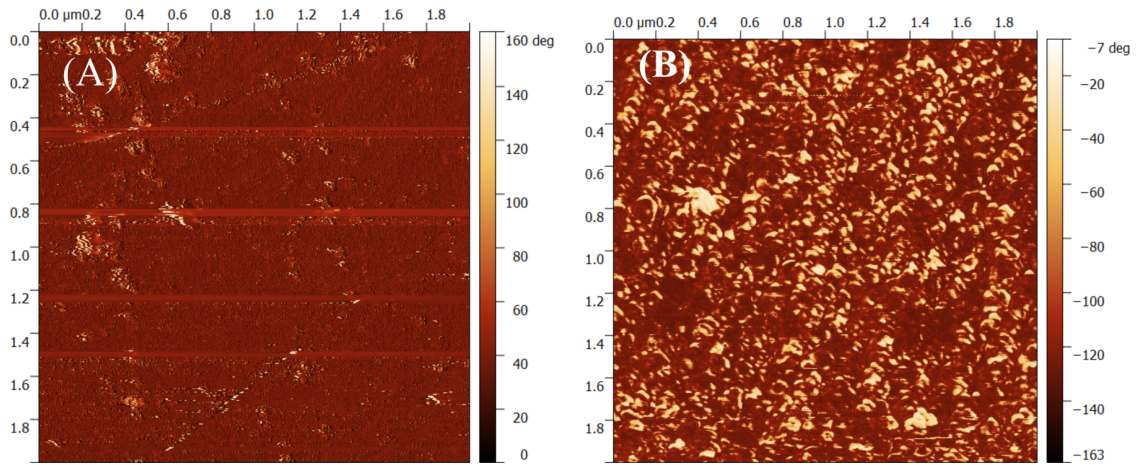
FIGURE 5.11: AFM image showing morphological changes before and after functionalisation of the gold gate. [6]
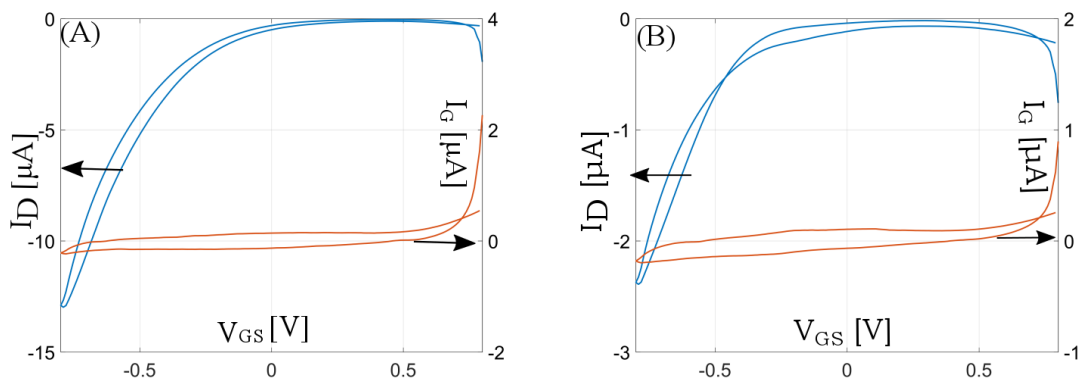
FIGURE 5.12: Transfer (A) before and (B) after functionalisation of the gold gate surface.

(PBS). After washing the activated gold surface with PBS, the enzyme solution was dropped onto the gate electrode and was incubated at room temperature for 12 hours. The samples were finally washed with PBS buffer and stored at 4 degrees until further use. Figure 5.10 shows the functionalisation scheme along with the device architecture. Figure 5.11 shows the AFM image to indicate morphological changes of the gold gate surface before and after functionalisation.

As a standard procedure, the sensors were verified for their electrical functionality. Both before functionalisation and after functionalisation transfer curve were recorded. As anticipated the drain current drops due to the reduction in the gate capacitance after to the formation of a self-assembled monolayer. Figure 5.12 shows the transfer characteristics of the same device before and after functionalisation. For electrical characterisation, 1mM PBS buffer solution was used as an electrolyte. A custom made PDMS chamber is used to contain the electrolyte.
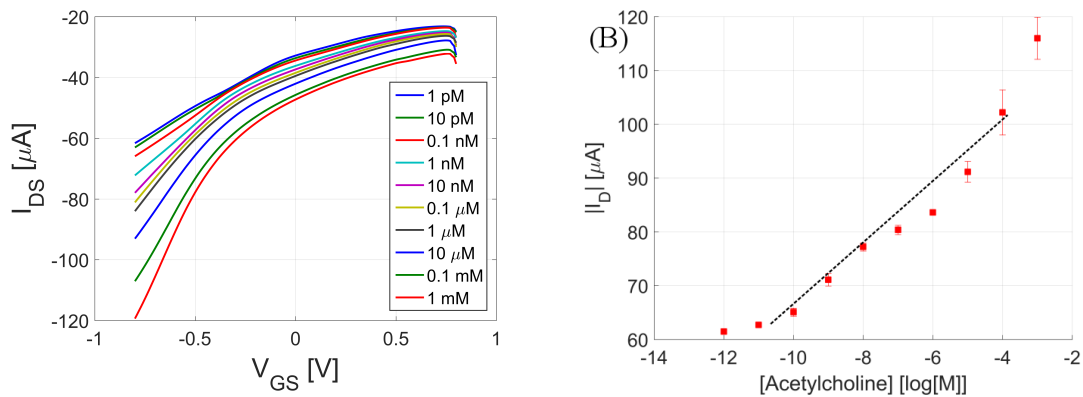
FIGURE 5.13: (A) Transfer curves for different acetylcholine concentrations. (B) Calculating the sensitivity of sensor using linear fit of the maximum current.

Different test solutions with varying concentrations of acetylcholine were prepared; the concentration of solutions range from a lowest concentration of 1 pM to highest concentration of 1 mM. 1mM phosphate buffered saline was used as an electrolyte and buffering agent for sensor characterisation. The sensor response towards acetylcholine is measured by recording transfer characteristics; gate bias is swept from 0.8V to -0.8V w.r.t source, while the drain bias is fixed at -0.2V w.r.t source. These transfer curves were measured three times for each concentration. Figure 5.13 (A) shows the response of the sensor; each transfer curve plotted is average of three measurements at a given concentration. The drain current increased with increase in the acetylcholine concentration. For a given sensor, the sensitivity is defined as the slope of the drain current measured at gate voltage -0.8V vs the acetylcholine concentration. For the sensor data shown in figure 1, it is obtained as 5.7 uA/decade, as shown in Figure 5.13 (B). It should be noted that this is the response of a particular sensor. Due to random nature of percolating carbon nanotube network, each produced sensor may have different sensitivity. In this configuration, before using the sensor, it is essential to perform calibration.

Online measurement is also carried out by keeping the applied bias constant at V_{GS} = -0.8V and V_{DS} = -0.2V. Figure 5.14 (A) shows the sensor's online measurement for a different acetylcholine sensor then that presented in Figure 5.13. Here again, the minimum concentration tested was 1 pM, and acetylcholine concentration was increased until the final concentration reached 1mM. To analyse the selectivity of sensors, two different possible interfering neurotransmitters are tested. Glycine and serine are two small molecules which have been shown to attach to the carbon nanotubes [197]. Such interference is most likely to be present in the real sample. To test the viability of the sensor in the presence of these interfering substances,
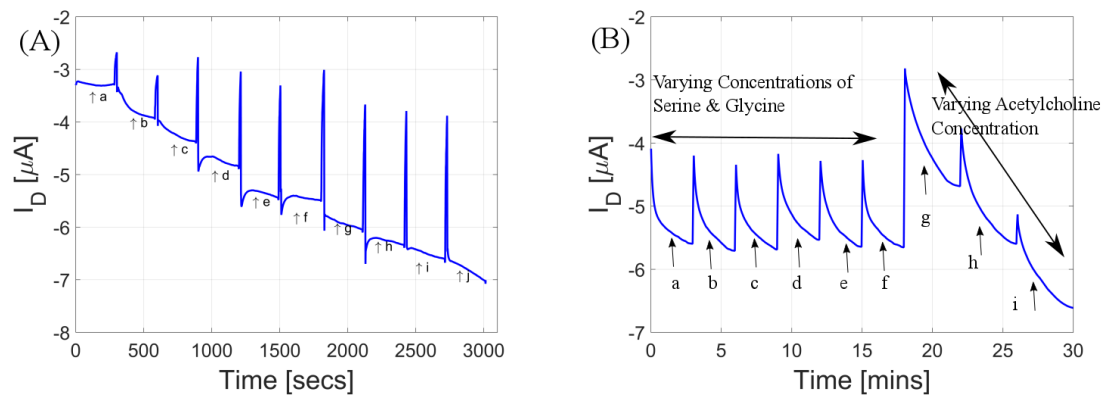
FIGURE 5.14: (A) Real-time response of the sensor from a = 1 pM to j = 1 mM concentration range. (B) Selectivity tests for sensor in the presence of varying concentrations of serine and glycine.

test solutions containing different amounts of glycine and serine are prepared. Table 5.2 shows the composition of these test solutions. The corresponding sensor response is presented in figure 5.14 (B). The sensor shows a higher response due to varying primary analyte than the variation of interfering molecules.

TABLE 5.2: Composition of solutions used for selectivity tests (refer to Figure 5.14)

Individual Concentrations of species (μM)			
Solution	Serine	Glycine	Acetylcholine
a	0.2	20	50
b	2	20	50
c	20	20	50
d	20	0.2	50
e	20	2	50
f	20	20	50
g	20	20	5
h	20	20	50
i	20	20	100

Thanks to their nano dimensions and flexible mechanical properties carbon nanotube allow mechanical bending without significant impact to their electrical properties. This is unlike some bulk crystalline material which deteriorates upon mechanical bending [198]. To test the mechanical properties of the acetylcholine sensors, the sensors were bent to near 90 degrees at a bending radius of 1.7 mm. For the test, the sensor was clamped on one end on a stationary block and on another on a moving block. After every 60 iterations of bending and relaxing, the sensor was measured with 10 nM acetylcholine solution. Figure 5.15 shows the
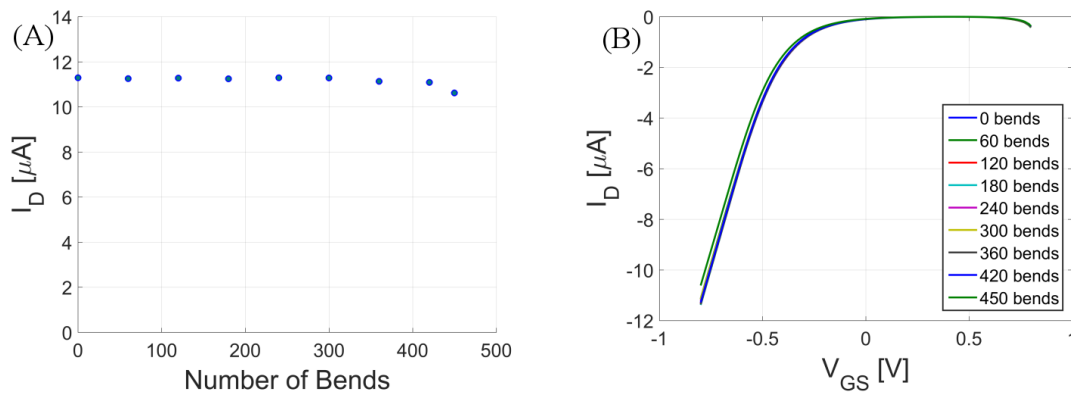
FIGURE 5.15: Mechanical bending tests performed on acetylcholine sensor.

drain current variation with the number of bending cycles as well as the transfer characteristics of the device.

5.2.1.2 Application in pesticide detection

The proposed acetylcholine sensor is based on the breakdown of acetylcholine catalysed by enzyme AchE. As mentioned earlier, excess acetylcholine in the synaptic cleft disrupts muscle activity and breathing. Some of the organophosphates that are actively used in fields indirectly may result in excess acetylcholine when humans or animals are exposed to them. These organophosphates inhibit the enzyme acetylcholinesterase thus leading to a build-up of acetylcholine in the synaptic cleft resulting in a life-threatening situation. Enzyme activity can be monitored by measuring sensor response at a fixed substrate concentration. If the enzyme activity remains same, the same amount of substrate will be consumed in a fixed time period. Therefore the sensor is expected to produce the same response. Based on this understanding, two different concentrations of malathion were prepared in 1mM PBS solution. 5mg/ml and 2mg/ml of malathion test solutions are tested. As a baseline measurement, a sensor is tested with 1nM acetylcholine solution. Then the sensor is exposed to malathion solution for 5 minutes followed by PBS wash and again measured with the 1 nM acetylcholine test solution. Measurement are repeated every 5 minutes alternating between incubation of sensor in malathion and then characterising in 1 nM acetylcholine. The response of sensor decreases due to degradation in enzyme activity. Figure 5.16 shows the transfer curves recorded at every 5 minute interval. Inhibition of the enzyme activity is defined as equation 5.1; the sensor response decreases up to 80% within 20 minutes.
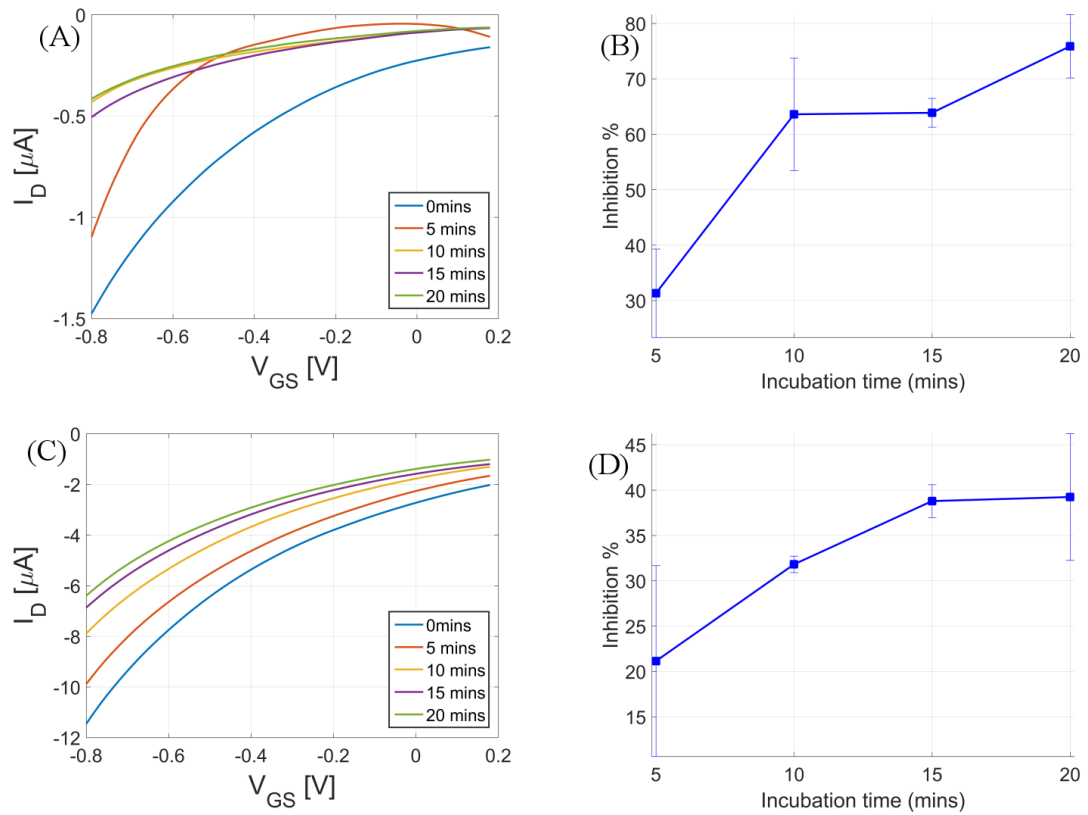
FIGURE 5.16: Enzyme inhibition study in presence of two different concentrations of malathion. Transfer curves for increasing incubation time when the sensor was exposed to (A) 5 mg malathion and (C) 2 mg malathion solutions in phosphate-buffered saline (PBS). Inhibition % of enzyme activity when the sensor was exposed (B) 5 mg malathion and (D) 2 mg malathion solutions in PBS.

$$Inhibition\% = \frac{(I_{DS,Control} - I_{DS})}{I_{DS,Control}} * 100 \qquad (5.1)$$

Similarly, at a lower concentration of malathion at 2mg/ml of up to 40% reduction in sensor response is visible.

This method was further tested with strawberries purchased from local store. Strawberry juice and tap water samples were spiked with 1.35 mg of malathion for 1 ml of solution. Sensor response in these test solutions is shown in Figure 5.17. Thus a systematic decrease in sensor response can signal be used to identify the presence of malathion in food products or water samples.
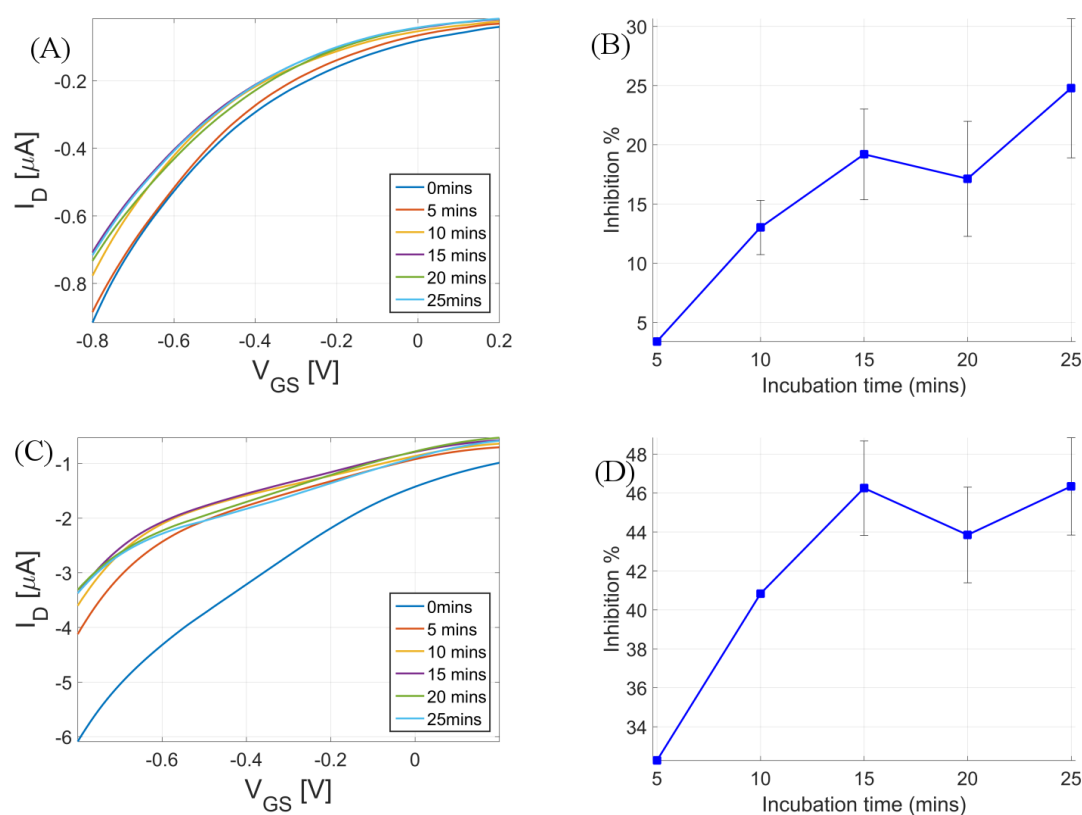
FIGURE 5.17: Real sample analysis for enzyme inhibition. Transfer curves for increasing incubation time when the sensor was exposed to (A) 1.35 mg malathion in 1 ml tap water and (C) 1.35 mg malathion mixed in 1 mL strawberry pulp.

5.2.2 Glucose and Lactate biosensor

Almost 300 million people test their blood glucose every day using a handheld device, yet it is still only a tiny fraction of estimated 1 billion people suffering from blood sugar problems. Bringing down the cost of test equipment and the material is one of the key areas to expand the blood glucose monitoring devices. Measuring glucose in the blood is however not the only use case for glucose sensors. Bioreactors, food processing units and agricultural sectors also require glucose sensors. The glucose meters available in the market are mostly tailored towards blood glucose monitoring. Sensors sensitive to low concentrations are valuable.

Lactate is another biomolecule playing an essential role in muscle movement. Thus it is typically used in the fields of sports monitoring. The level of lactate increases from a few mM in rest state to tens of mM during muscle workout. Its buildup causes acidification of muscle tissue and might lead to tissue break down. Another health related applications for monitoring lactate include diagnosis for liver and
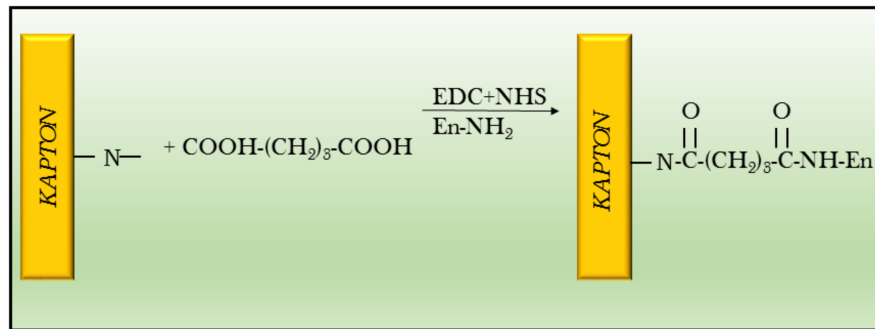
FIGURE 5.18: Functionalization scheme for glucose and lactate sensor.

renal failure, during child birth. Lactate tests are also used for diary, fish and fruits. All the above mentioned use cases warrant a need for affordable lactate sensor.

Building upon the suitability of electrolyte gated CNTFET sensors based on enzyme mediated biosensor, glucose and lactate sensors were investigated. Scheme to functionalise enzyme on the sensor surface is as shown in figure 5.18. Dicarboxylic acid is used to anchor enzyme onto polyimide substrate. For fabrication of the transistor usual lift-off process was used for patterning electrodes with transistor channel length as 50 μm, and channel width/length ratio as 900. 5nm of Cr as adhesion promoter followed by 40 nm of Au is used as the electrode metal. 90% semiconducting carbon nanotubes were spray deposited to form the semiconducting channel. Glutaric acid is used as linker molecule between nitrogen group of polyimide and amine group on enzymes. Mixture containing 30 mg of EDC with 20 mg of NHS in 10 ml MES buffer along with 10 mg of glutaric acid mixed with 100 μl of enzyme solution is dropped onto the channel area. Same concentrations of reagents were used to functionalize glucose as well as lactate sensor. After waiting until the solvent evaporates the samples are washed with MES buffer. At this point the sensors are ready to be tested.

Chemical reactions mediated by the enzymes glucose oxidase and lactate oxidase are given in equation below.

$$\beta\text{-D}-\text{glucose} + O_2 \xrightarrow{\text{GOx}} \text{D}-\text{glucono}-\delta\text{-lactone} + H_2O_2$$

$$\text{L}-\text{lactate} + O_2 \xrightarrow{\text{LOx}} \text{pyruvate} + H_2O_2$$
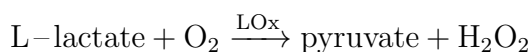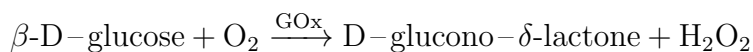
As the byproduct for both sensors is hydrogen peroxide. We assume that production of hydrogen peroxide is responsible for the change in conductance of carbon nanotubes thus resulting in increase in drain current. However, change in pH has also been suggested as a possible cause of sensor response, it however seems to
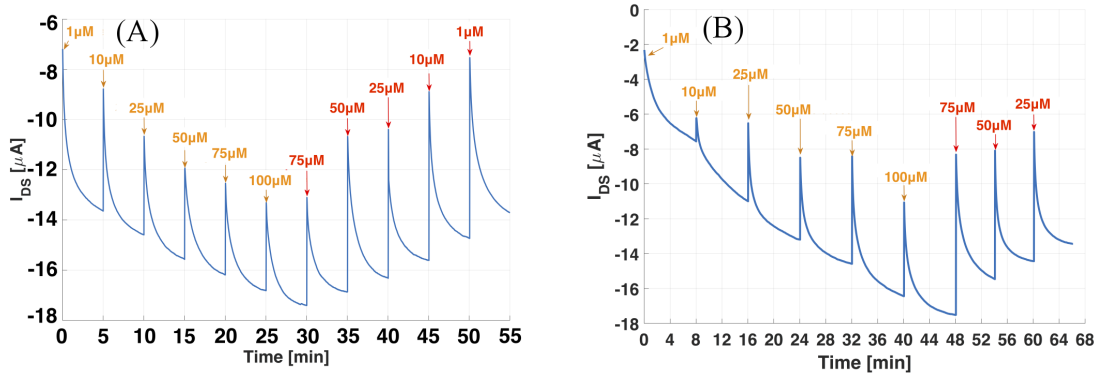
FIGURE 5.19: Real time measurement of (A) lactate and (B) glucose sensor. Adapted from [7].

be less likely as the test solutions are all in PBS buffer and the sensor showed response even in very low concentrations like in range of pico molar. Any change in pH at this concentration is more likely to be buffered. Drain current recorded at bias voltages of V_{GS} = -0.8V and V_{DS} = -0.2V is plotted against concentration of the analytes glucose and lactate. The results are presented in Figure 5.19.

5.3 Non Enzymatic biosensor

5.3.1 Dopamine biosensor

Neurotransmitters play a vital role in well being of humans. They are mainly responsible for information exchange at the synapse between the neurons. Neurotransmitters, however, are not confined to the brain. Several glands and organs produce them in the body. For example, a class of neurotransmitters called catecholamines are produced in adrenal glands [199]. A mechanism called blood brain barrier is believed to prohibit an exchange of molecules in the cerebral fluid with blood. Therefore testing blood neurotransmitter level might not reflect the amount of neurotransmitter present in the brain [200]. Nevertheless the neurotransmitters are indeed found in blood and are tested for various pathological conditions. The diagnose adrenal gland tumour is probably one of the leading examples of such tests.

Dopamine levels in blood or urine sample are determined using mass liquid chromatography coupled with a mass spectrometer. High levels in urine correspond to around 120 pM/L. The cost of equipment is so high that having it as a point of
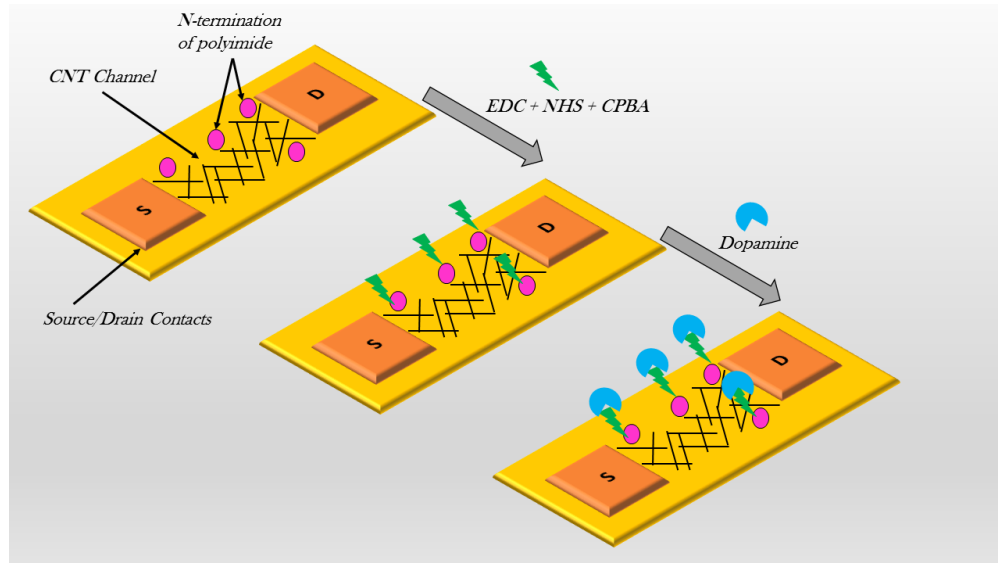
FIGURE 5.20: Functionalization of polyimide surface for dopamine detection.

care diagnostic device is not conceivable at the current state of technology. Similarly, the price per test is also high at around 50 USD. These costs limit their use especially in developing nations or at remote locations. Therefore, electrolyte gated transistor based sensor is developed to test the feasibility of such devices for small biomolecules like dopamine.

The hypothesis for obtaining sensing behaviour is based on the change in the surface charge [201]. If a charged molecule is bound to the semiconductor surface, field effect is attributed to change in conductivity of nanotube. Molecules from catechol family, such as dopamine consist of two hydroxyl (-OH) groups. To capture them cyclic phenylboronic acid has been demonstrated as a good choice [202]. This is favourable as upon binding with dopamine it forms a dipole with the negatively charged site at boron. These features made it possible to verify if electrolyte gated carbon nanotubes can be used for sensing of these molecules. The lift-off process is used to pattern Cr/Au electrodes on the polyimide substrate. The channel length of devices used is 50 μm and the channel width as 80 μm. 90% semiconducting nanotubes are spray deposited using stencil mask. Polyimide surface is functionalised with the help of EDC. CPBA and EDC in 1:1 ratio is drop casted on the channel region and incubated at room temperature for 2 hours. After functionalisation, the samples are rinsed using PBS. Figure shows the functionalization scheme and dopamine binding to form boronic aster.

The as-prepared devices were tested by recording output and transfer characteristics. Keithley 4200 semiconductor characterisation system was used for all the electrical measurements. Different dopamine concentrations were prepared
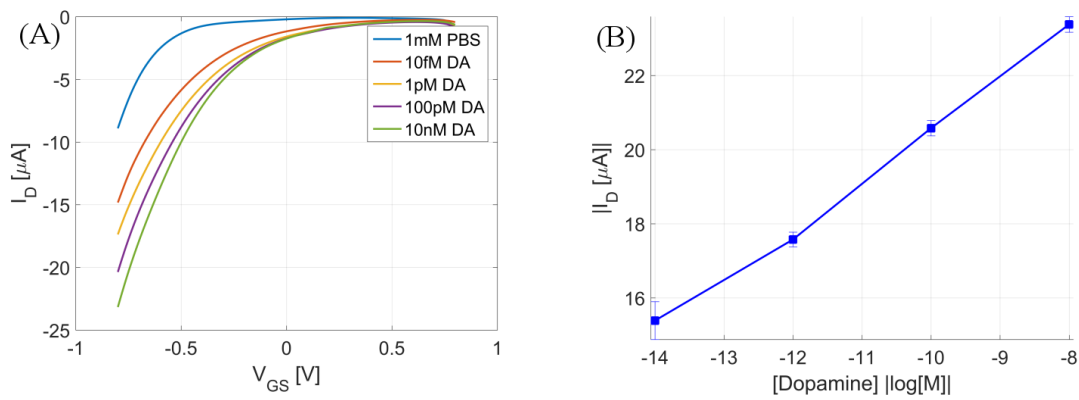
FIGURE 5.21: (A) Transfer curves for different concentrations of dopamine. (B) Maximum current vs concentration of dopamine.

in 1mM PBS buffer solution which was strong enough to maintain pH at 7.3 ± 0.1 while measurements. Solutions with different concentrations of dopamine are tested with increasing concentration from 10fM up to 10 nM. This range is determined while keeping urine dopamine levels in mind. Concentrations more than 120 pM is considered high and is an indication of a possible case tumour. It is important to note that in between measurements, the sensors were not regenerated to free the already bound binding sites. For the present work, as the drain current increases with increase in concentration, it may be safe to assume that mechanism behind this change is the charge of the boronic ester. Figure 5.21 (A) shows the transfer curves recorded at different concentrations of dopamine. Figure 5.21 (B) shows the maximum drain current and associated error bars at each measured concentration.

5.3.2 DNA biosensor

Deoxyribonucleic acid (DNA) biosensor offers unique advantages compared to any other biosensor. This speciality stems from the presence of DNA in every self-reproducing cellular organism. Every organism has a unique DNA and therefore can be used to identify them unambiguously. Sensors based on DNA can detect the presence of a pathogen in agricultural products, water bodies or their spread among animal and human population. It can also be used for identification of a genetic mutation which causes several disorders such as cancer, cystic fibrosis, phenylketonuria among many others. DNA is a polymer built using only four bases namely adenine, thymine, cytosine, and guanine. They can occur in any sequence in DNA of arbitrary length. A single sequence of these base pairs constitutes

what is known as single-stranded DNA (ssDNA). However, nature has evolved the mechanism of storing DNA as two complementary strands bound together with hydrogen bonds formed between adenine and thymine also known as A-T pair and cytosine and guanine or G-C pair. This unique property is the basis of all self-replicating life forms on earth. These base pairs are negatively charged thus imparting a total negative charge to the whole DNA.

There is significant interest in determining the sequence of base pairs of unknown DNA. Cost of this sequencing was more than 500 million USD in 2000. Today a similar sequencing of the human genome sequence is well under 5000 USD. DNA sequencing is most useful in identification of mutations in individuals. The second use case is to recognise the presence of a known DNA sequence. Typically this is done for diagnostic purposes [203].

To identify the presence of a particular DNA sequence, sensor surface is functionalised using a complementary ssDNA capture probe. If the other complementary half of the DNA would exist in the test sample, it would hybridise with the capture probe. Sensors based on this principle are subject of study in current work. DNA sensors based on sensing the charge modification due to DNA hybridisation at the surface of semiconductor have been reported by several groups [204]. DNA also has been shown to bind to carbon nanotubes directly altering their electronic properties [205]. Carbon nanotubes are sensitive to several environmental factors, and hence it is better if the sensitive semiconductor is not interfaced with the test sample where multiple phenomena can occur. DNA is also known to move in the presence of electric field [206]. Reports suggesting screening of DNA by electrolyte typically do not consider the effect of DNA movement with applied bias. Thus negatively charged DNA would repel away from the negatively biased electrode. Keeping this in perspective, the extended gate architecture introduced in chapter 4 can be used for fabrication of DNA sensor.

Thanks to the separation of electrolyte surrounding the semiconducting channel, there is no chance of DNA coming in contact with carbon nanotubes. Another advantage lies in polarity of the electrode that can be functionalised to capture the target ssDNA. Figure 5.22 (A) shows the extended gate CNTFET with capture probe on one of the electrodes. The direction of the electric field inside the functionalised electrode is such that it can attract DNA towards itself thus offering a chance to bring the DNA within the Debye length of the electrolyte. DNA sensors designed with extended gate transistor were tested with sequence given as ATTAGGAACCTTAAGGACTT. The capture probe was functionalised on one
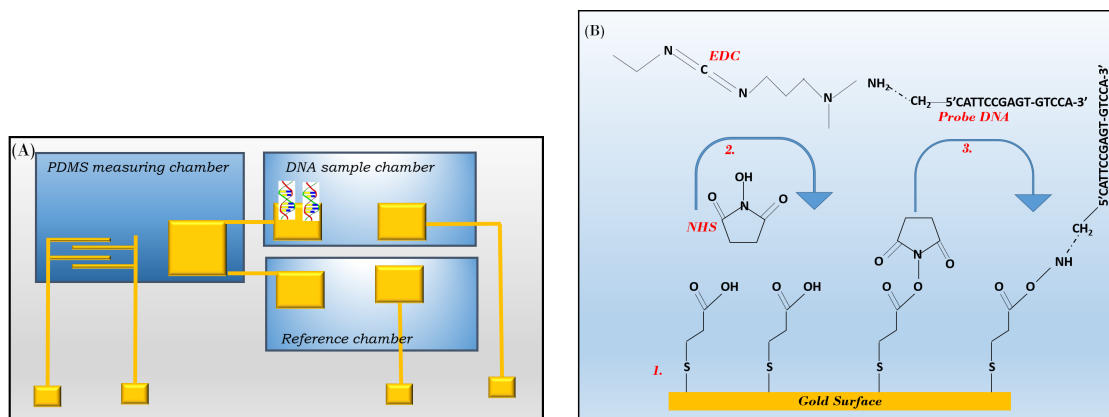
FIGURE 5.22: DNA functionalisation scheme for extended gate FET.
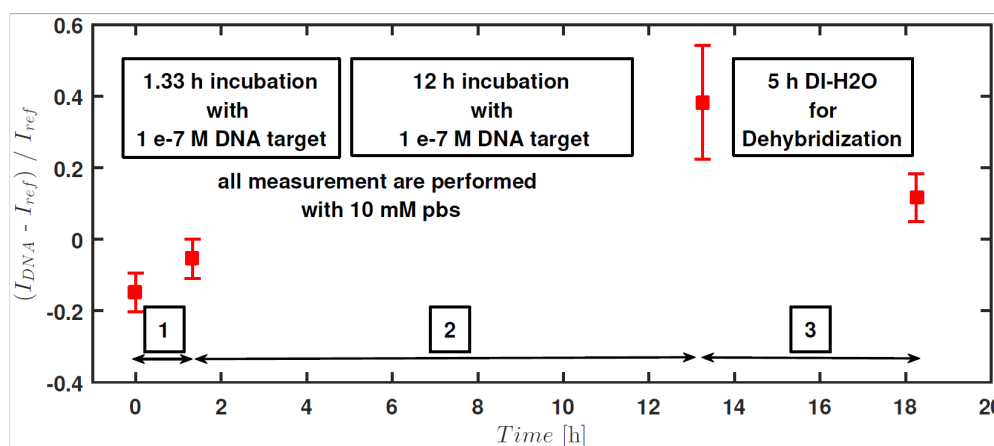
FIGURE 5.23: Response of DNA sensor made using extended gate configuration.

end with an amine group. The extended gate was functionalized with SAM made using mercaptopropionic acid to provide carboxy terminated functional group for further gate modification. For functionalisation of DNA EDC/NHS coupling chemistry was utilised. Figure 5.22 (B) shows the functionalisation scheme for the DNA sensor. Extended gate offers an opportunity to use different gate electrodes with the same transistor.

Hence two electrodes were fabricated as an extended gate, and only one of them was functionalised with capture probe ssDNA. This architecture allows assigning a reference measurement made using the unfunctionalised gate. The drain current is measured at a constant externally applied gate and drain bias. Using reference measurements with unfunctionalised gate reduces the effect of environmental factors influencing the transistor current. The concentration of the target ssDNA was kept at 100 nM. The response of the sensor is measured at different incubation times. The percentage change in drain current of the sensor is presented in figure 5.23 .

At t=0, the drain current of gate functionalised with capture ssDNA is around 40% lower compared to the unfunctionalised gate. This is an indicator of low double layer capacitance due to the presence of SAM layer. However, with DNA hybridisation increase in the drain current is observed. For the measurements, the extended gate is incubated in the complementary test solution without any external bias. After different incubation times, it was washed and connected to the CNTFET for measurements. PBS buffer was used as an electrolyte for both reference gate and DNA capture gate electrodes. This provides a platform for label-free DNA sensing. Further work for improving the sensitivity and investigation for identifying the dominant effect has to be done. Various factors to consider in this study are

- DNA movement under bias.

- The effect of immobilisation on two different surfaces of extended gate architectures.

- The difference in capacitance due to hybridisation under DC bias vs AC measurements at different frequencies.

- Optimising the gate areas to obtain maximum sensitivity.

Chapter 6

Conclusion and outlook

"If we knew what it was we were doing, it would not be called research, would it?"

Albert Einstein

6.1   Conclusion

In this work, we started with an examination of an electrolyte-gated transistor. Using sorted carbon nanotubes with up to 99.9% semiconducting CNTs a random network was tested for its suitability for serving as a semiconducting material for the transistor. Aiming to use cost-effective fabrication process, spray deposition at room temperature was employed. Use of aqueous electrolyte provided high double layer capacitance. This allowed better gate control over the semiconducting channel. Even in a small range of applied bias, the transistors showed acceptable on-off ratio. Use of multi-walled carbon nanotube network, as well as the impact of the geometrical shape of the gate electrode on a planar gate architecture, was systematically studied. The gain in transistor performance by this study was observed. However, this comes at an overall increased device area.

Thanks to their dominant metallic nature, multi-walled carbon nanotubes were tested as an electrode material. Nowadays, conductive electrodes are used in smart bandages or in monitoring of in-vitro cell proliferation. Keeping this application in mind, suitability of multi-walled carbon nanotube electrodes for impedance spectroscopy was verified and biocompatibility of these materials was investigated. To test the electrodes, yeast cells were monitored using impedance electrodes which

89

were fabricated with multi-walled carbon nanotubes. To keep in lieu with the rise of additive manufacturing, integration of spray coated MWCNT electrodes with a 3D printed custom impedance test chip was also demonstrated.

Building on the experience gained in the fabrication process of MWCNT electrodes on flexible substrates, efforts were made to eliminate metal from electrolyte gated transistor architecture. This resulted in fabrication of a metal-free fully carbon nanotube electrolyte gated transistor. These transistors not only had similar characteristics as a traditional metal electrode transistor but in many ways they outperformed their traditional counterparts. This can pave way to bring down the final cost of the transistor. However, as the process required careful manufacturing and optimisations for biofunctionalisation, biosensors based on electrolyte gated CNTFETs were made using gold electrode.

Possibility to work in aqueous electrolyte and sensitive nature of carbon nanotubes offers perfect reasons to consider them for biosensing applications. Sensors for detection of ions in aqueous media were developed. They paved the path for CNTFET based biosensor platform. Several cation sensors for ions such as Potassium, Sodium, Ammonium, Magnesium Calcium were successfully developed. Agriculturally important anion phosphate and nitrate ion sensors were also developed. With these sensors a multi-analyte sensor array capable of measuring macronutrients in the soil or hydroponic system is possible.

Using bound charges near the surface of the semiconductor for sensor application has been proposed and is being explored extensively for nanomaterials. Towards this aim, a sensor for dopamine was developed. Using boronic acid functionalised on the polyimide substrate dopamine in the test sample was captured near carbon nanotube surface. This led to an increase in the drain current due to increase in carbon nanotube conductivity. The developed sensors responded to test concentrations as small as ten femto molar.

Use of enzymes for converting electrically neutral molecules into products that can be used in electrochemical sensors opens up doors for a vast number of physiologically relevant analytes. Glucose and lactate sensors were developed using glucoseoxidase and latateoxidase respectively. Use of enzymes to detect the reaction product is not the only way to utilise them in biosensors. Enzymes play an essential role in sustaining vital functions. By monitoring enzyme activity, toxicity in surroundings can be determined. Based on this principle sensor for detection of widely used organophosphate malathion was demonstrated with the help of spiked strawberry juice and tap water.

Given the sensitive nature of carbon nanotube, their use in a complex environment might lead to unwanted interactions with test solutions. Thus probably like the ion sensors, it is a better approach to encapsulate carbon nanotubes or to not interface them directly with the test sample. To accomplish this goal extended gate transistor was designed. This approach enables constant composition of electrolyte for CNTs. At the same time using multiple extended gates, it is possible to perform measurements relative to an unfunctionalised gate as baseline measurements. This baseline measurement can also take into account the environmental variations such as temperature or light intensity. A DNA sensor using this architecture was demonstrated.

Thus the electrolyte gated transistor offers a platform for biosensors based on different categories of biochemicals. Their excellent electronic and mechanical properties, low-cost fabrication processes can help us to achieve affordable point-of-care diagnostic systems in the near future.

6.2 Outlook

Carbon nanotubes characterised almost thirty years ago still remains in research facilities. Intensive research for their use in beyond CMOS, sensors and mechanical components is still active. Similarly, nearly five decades have passed since the introduction of ISFETs. Despite this extended period, there is a tiny fraction of sensors based on ISFET technology. The search query for "carbon nanotube sensor" yields a staggering 400,000 articles and patents! Still, to the author's best knowledge, successful low cost point-of-care commercial sensors based on them are not available. This reflects the difficulties and lack of mastery over the incredible nanomaterial. The present work adds to the knowledge of biosensors in demonstrating low-cost sensor platform, but much remains to be done. Probably the best way to harness its advantages is to focus the attention on the single use case and develop a complete system for it. This will include multidisciplinary effort including, physical sciences, engineering as well as commercial entities to bring them to the mainstream. History is replete with examples where excellent technological products were overshadowed by inferior solutions due to lack of business adoption. Point-of-care diagnostics present a unique opportunity in this regard as there are many examples where close to nothing exists to fulfill the need. With

the advances in computing technologies, ubiquitous data access and low-cost fabrication technique, the dream of an affordable point-of-care diagnostic system is undoubtedly achievable.

List of Publications

Patents

1. P. Lugli, V.D. Bhatt, and K. Melzer. Electrolyte-gated sensor for species detection. In *European Union Patent Application EP3045902A1 Kind Code: A1, Application number EP3045902A1, International Classes: G01N27/4146; Technische Universität München 2015-01*

2. P. Lugli, V.D. Bhatt, and K. Melzer. Device for analyzing biological substances in a test solution and production method. In *United States Patent Application US 20170097331 Kind Code: A1, Applicatzion no. 15/281772, International Classes: G01N33/487; G01N27/02; G01N33/483, Technische Universität München 2017-04*. FreePatentsOnline.com FPO, Apr 2017

Journal Articles

1. Saumya Joshi, Vijay Deep Bhatt, Ewa Jaworska, Markus Becherer, Krzysztof Maksymiuk, Agata Michalska, and Paolo Lugli. Using Lipophilic Membrane for Enhanced-Performance Aqueous Gated Carbon Nanotube Field Effect Transistors. *Physica Status Solidi (a)*, 1700993:1700993, 2018. ISSN 18626300. doi: 10.1002/pssa.201700993. URL `http://doi.wiley.com/10.1002/pssa.201700993`

2. Saumya Joshi, Vijay Deep Bhatt, Andreas Märtl, Markus Becherer, and Paolo Lugli. Regenerative, highly-sensitive, non-enzymatic dopamine sensor and impact of different buffer systems in dopamine sensing. *Biosensors*, 8 (1):1–10, 2018. ISSN 20796374. doi: 10.3390/bios8010009

3. Vijay Bhatt, Saumya Joshi, Markus Becherer, and Paolo Lugli. Flexible, Low-Cost Sensor Based on Electrolyte Gated Carbon Nanotube Field Effect Transistor for Organo-Phosphate Detection. *Sensors*, 17(6):1147, 2017. ISSN 1424-8220. doi: 10.3390/s17051147. URL `http://www.mdpi.com/1424-8220/17/5/1147`

4. Vijay Deep Bhatt, Saumya Joshi, and Paolo Lugli. Metal-free fully solution-processable flexible electrolyte-gated carbon nanotube field effect transistor. *IEEE Transactions on Electron Devices*, 64(3):1375–1379, 2017. ISSN 00189383. doi: 10.1109/TED.2017.2657882

5. Saumya Joshi, Vijay Deep Bhatt, Hao Wu, Markus Becherer, and Paolo Lugli. Flexible Lactate and Glucose Sensors using Electrolyte-Gated Carbon Nanotube Field Effect Transistor for Non-invasive Real-time Monitoring. *IEEE Sensors Journal*, 17(c):1–1, 2017. ISSN 1530-437X. doi: 10.1109/JSEN.2017.2707521. URL http://ieeexplore.ieee.org/document/7933216/

6. Vijay Deep Bhatt, Shokoufeh Teymouri, Katharina Melzer, Alaa Abdellah, Zeno Guttenberg, and Paolo Lugli. Biocompatibility tests on spray coated carbon nanotube and PEDOT: PSS thin films. *IEEE Transactions on Nanotechnology*, 15(3):373–379, 2016. ISSN 1536125X. doi: 10.1109/TNANO.2016.2535780

7. Simone Colasanti, Vijay Deep Bhatt, Ahmed Abdelhalim, and Paolo Lugli. 3-D Percolative Model-Based Multiscale Simulation of Randomly Aligned Networks of Carbon Nanotubes. *IEEE Transactions on Electron Devices*, 63 (3):1346–1351, 2016. ISSN 00189383. doi: 10.1109/TED.2015.2513012

8. Simone Colasanti, Valentina Robbiano, Florin Christian Loghin, Ahmed Abdelhalim, Vijay Deep Bhatt, Alaa Abdellah, Franco Cacialli, and Paolo Lugli. Experimental and Computational Study on the Temperature Behavior of CNT Networks. *IEEE Transactions on Nanotechnology*, 15(2):171–178, mar 2016. ISSN 1536-125X. doi: 10.1109/TNANO.2015.2510965

9. K. Melzer, V. Deep Bhatt, E. Jaworska, R. Mittermeier, K. Maksymiuk, A. Michalska, and P. Lugli. Enzyme assays using sensor arrays based on ion-selective carbon nanotube field-effect transistors. *Biosensors and Bioelectronics*, 84:7–14, 2016. ISSN 18734235. doi: 10.1016/j.bios.2016.04.077

10. Simone Colasanti, Vijay Deep Bhatt, Ahmed Abdelhalim, and Paolo Lugli. 3-D Percolative Model-Based Multiscale Simulation of Randomly Aligned Networks of Carbon Nanotubes. *IEEE Transactions on Electron Devices*, 63 (3):1346–1351, 2016. ISSN 00189383. doi: 10.1109/TED.2015.2513012

11. Katharina Melzer, Vijay Deep Bhatt, Tobias Schuster, Ewa Jaworska, Krzysztof Maksymiuk, Agata Michalska, Paolo Lugli, and Giuseppe Scarpa. Flexible Electrolyte-Gated Ion-Selective Sensors Based on Carbon Nanotube Networks. *IEEE Sensors Journal*, 15(6):3127–3134, jun 2015. ISSN 1530-437X. doi: 10.1109/JSEN.2014.2362679

12. Qingqing Gong, Vijay Deep Bhatt, Edgar Albert, Alaa Abdellah, Bernhard Fabel, Paolo Lugli, and Giuseppe Scarpa. On the performance of

solution-Processable random network carbon Nanotube Transistors: Unveiling the role of network density and metallic tube content. *IEEE Transactions on Nanotechnology*, 13(6):1181–1185, 2014. ISSN 1536125X. doi: 10.1109/TNANO.2014.2351011

Conference Proceedings

1. Vijay Deep Bhatt, Saumya Joshi, Katharina Melzer, and Paolo Lugli. Flexible dopamine sensor based on electrolyte gated carbon nanotube field effect transistor. *Proceedings - 2016 IEEE Biomedical Circuits and Systems Conference, BioCAS 2016*, 1:38–41, 2017. doi: 10.1109/BioCAS.2016.7833719

2. K. Melzer, V.D. Bhatt, E. Jaworska, K. Maksymiuk, A. Michalska, and P. Lugli. Enzymatic assays based on ion-selective carbon nanotube field-effect transistors. In *Biosensors 2016 26th Anniversary World Congress on Biosensors*. Elsevier B.V., May 2016

3. K. Melzer, V.D. Bhatt, and P. Lugli. Immobilization strategies for enzymatic biosensors based on electrolyte-gated carbon nanotube transistors. In *99th Canadian Chemistry Conference and Exhibition*. Canadian Society for Chemistry, Dalhousie University, Jun 2016. URL `http://abstracts.csc2016.ca/00000882.htm;`

4. K. Melzer, V. D. Bhatt, T. Schuster, E. Jaworska, K. Maksymiuk, A. Michalska, G. Scarpa, and P. Lugli. Multi ion-sensor arrays: Towards an "electronic tongue". In *2016 IEEE 16th International Conference on Nanotechnology (IEEE-NANO)*, pages 475–478. IEEE, aug 2016. ISBN 978-1-5090-1493-4. doi: 10.1109/NANO.2016.7751505. URL `http://ieeexplore.ieee.org/document/7751505/`

5. Vijay Deep Bhatt, Katharina Melzer, Alaa Abdellah, Paolo Lugli, Shokoufeh Teymouri, and Zeno Guttenberg. Biocompatibility tests on spray coated carbon nanotube and PEDOT:PSS thin films. In *2015 IEEE 15th International Conference on Nanotechnology (IEEE-NANO)*, volume 15, pages 5–8. IEEE, jul 2015. ISBN 978-1-4673-8156-7. doi: 10.1109/NANO.2015.7388842. URL `http://ieeexplore.ieee.org/document/7388842/`

6. Simone Colasanti, Vijay Deep Bhatt, Ahmed Abdelhalim, Alaa Abdellah, and Paolo Lugli. A 3D self-consistent percolative model for AC-DC electrical analysis of carbon nanotubes networks. *International Conference on*

Simulation of Semiconductor Processes and Devices, SISPAD, 2015-Octob: 100–103, 2015. ISSN 1946-1569. doi: 10.1109/SISPAD.2015.7292268

7. S. Colasanti, V. Deep Bhatt, A. Abdellah, and P. Lugli. 3D self-consistent percolative model for networks of randomly aligned carbon nanotubes. *Journal of Physics: Conference Series*, 647(1):3–7, 2015. ISSN 17426596. doi: 10.1088/1742-6596/647/1/012018

8. Simone Colasanti, Vijay Deep Bhatt, and Paolo Lugli. 3D modeling of CNT networks for sensing applications. In *2014 10th Conference on Ph.D. Research in Microelectronics and Electronics (PRIME)*, pages 1–4. IEEE, jun 2014. ISBN 978-1-4799-4994-6. doi: 10.1109/PRIME.2014.6872679

Submitted Journal Articles

1. Saumya Joshi, Vijay Bhatt, Ewa Jaworska, Agata Michalska, Krzysztof Maksymiuk, Markus Becherer, Alessio Gagliardi, and Paolo Lugli. Ambient processed, water-stable, aqueous-gated sub-1v n-type carbon nanotube field effect transistor. *Scientific Reports*, March 2018

2. Saumya Joshi, Vijay Deep Bhatt, Himanshi Rani, Markus Becherer, and Paolo Lugli. Understanding the influence of in-plane gate electrode design on electrolyte gated transistor. *Microelectronic Engineering*, Feb 2018

Acknowledgements

"If I have seen further it is by standing on the shoulders of Giants."

Isaac Newton

Numerous people contributed in this thesis making it a wonderful journey. Thanks to the recommendation from Prof. Danilo Demarchi this journey started with the opportunity to work under the guidance of Prof. Paolo Lugli. From the days of master's thesis Prof. Lugli, despite his insanely busy schedule always found time to help and guide me. Often listening to long arguments and half-baked ideas, you always suggested ways to verify them. Thanks for your faith in me and giving me this opportunity.

I would also like to thank Prof. Agata Michalska and Prof. Krzysztof Maksymiuk for in-depth discussions and experiment designs regarding electrochemical methods and numerous ion-selective membranes. I would like to thank Morten and Kathi who probably suffered the most because of me. Thanks for your help in the lab and for sharing office space. Thanks to Florin, Engin and Alaa for helping in spray deposition. For discussions, I would like to thank Aniello & Ahmed. Though we did not shared a lot of lab time I would like to thank Tobi and Robin for introducing me to the facilities at ZNN and great humour during team meetings and discussions.

A big thanks to Markus for helping in every aspect. Your help in research work, advice for future and ever supportive nature have ensured that no roadblocks ever came to the path. Especially your help in arranging lab equipment and optimizing the measurements have encouraged me to ask questions on things which I never thought about, thanks a lot.

Lucia was the first person I met at the institute, and her warm welcome is something which I will never forget. Lucia later followed by Katrin always kept the dreadful paperwork hidden, and reduced it to small notes, and by just signing everything became OK. Similarly, Rosi kept the lab running and restored it no matter how much we broke it. Thank you, Rosi, for patience and procuring the chemicals to make this work possible. I would also like to acknowledge Alan,

Thomas, and Andreas for their measurements and patience to adapt the experiments while working on their master's thesis. I would like to thank Werner in helping me to translate the abstract in Deutsch.

Finally, the one person who shared this journey as a colleague, friend and life partner I can only attempt to thank her. Her action has touched every aspect of this work, without her support, and encouragement probably this work would not be even half of what it is now.

However, naming all the people whom I would like to thank is beyond the practical possibility in these few pages. To fix this problem, I intend to write a separate book where your contributions will be justly stated. For now, please forgive me.

Bibliography

[1] Cynthia G Bard, Allen J and Faulkner, Larry R and Leddy, Johna and Zoski. *Electrochemical methods: fundamentals and applications.–2nd ed.* wiley New York, 2 edition, . ISBN 0-471-04372-9.

[2] Chi-Shuen Lee and H.-S. Philip Wong. Stanford virtual-source carbon nanotube field-effect transistors model, Apr 2015. URL `https://nanohub.org/publications/42/2`.

[3] Vijay Deep Bhatt, Saumya Joshi, and Paolo Lugli. Metal-free fully solution-processable flexible electrolyte-gated carbon nanotube field effect transistor. *IEEE Transactions on Electron Devices*, 64(3):1375–1379, 2017. ISSN 00189383. doi: 10.1109/TED.2017.2657882.

[4] Dieter K Schroder. *MATERIAL AND DEVICE SEMICONDUCTOR MATERIAL AND DEVICE Third Edition*, volume 44. 2006. ISBN 9780471739067. doi: 10.1063/1.2810086. URL `http://www.wiley.com/WileyCDA/WileyTitle/productCd-0471739065.html`.

[5] Vijay Deep Bhatt, Katharina Melzer, Alaa Abdellah, Paolo Lugli, Shokoufeh Teymouri, and Zeno Guttenberg. Biocompatibility tests on spray coated carbon nanotube and PEDOT:PSS thin films. In *2015 IEEE 15th International Conference on Nanotechnology (IEEE-NANO)*, volume 15, pages 5–8. IEEE, jul 2015. ISBN 978-1-4673-8156-7. doi: 10.1109/NANO.2015.7388842. URL `http://ieeexplore.ieee.org/document/7388842/`.

[6] Vijay Deep Bhatt, Saumya Joshi, Markus Becherer, and Paolo Lugli. Flexible, low-cost sensor based on electrolyte gated carbon nanotube field effect transistor for organo-phosphate detection. *Sensors*, 17(5), 2017. ISSN 1424-8220. doi: 10.3390/s17051147. URL `http://www.mdpi.com/1424-8220/17/5/1147`.

[7] Saumya Joshi, Vijay Deep Bhatt, Hao Wu, Markus Becherer, and Paolo Lugli. Flexible Lactate and Glucose Sensors using Electrolyte-Gated Carbon Nanotube Field Effect Transistor for Non-invasive Real-time Monitoring. *IEEE Sensors Journal*, 17(c):1–1, 2017. ISSN 1530-437X. doi: 10. 1109/JSEN.2017.2707521. URL `http://ieeexplore.ieee.org/document/7933216/`.

[8] biosensor. In *IUPAC Compendium of Chemical Terminology*. IUPAC, Research Triangle Park, NC. ISBN 0-9678550-9-8. doi: 10.1351/goldbook. B00663. URL `http://goldbook.iupac.org/B00663.html`.

[9] Prof Ir, P Bergveld Em, and Fac Ee. ISFET , Theory and Practice. (October):1–26, 2003.

[10] Lc C Clark and C Lyons. Electrode systems for continuous monitoring in cardiovascular surgery. *Annals Of The New York Academy Of Sciences*, 102 (1):29–45, 1962. ISSN 00778923. doi: 10.1111/j.1749-6632.1962.tb13623.x. URL `http://onlinelibrary.wiley.com/doi/10.1111/j.1749-6632.1962.tb13623.x/full$\delimiter"026E30F$nhttp://doi.wiley.com/10.1111/j.1749-6632.1962.tb13623.x`.

[11] P. Bergveld. Short Communications: Development of an Ion-Sensitive Solid-State Device for Neurophysiological Measurements. *IEEE Transactions on Biomedical Engineering*, BME-17(1):70–71, 1970. ISSN 15582531. doi: 10. 1109/TBME.1970.4502688.

[12] Stanley D. Moss, Jifi Janata, and Curtis C. Johnson. Potassium Ion-Sensitive Field Effect Transistor. *Analytical Chemistry*, 47(13):2238–2243, 1975. ISSN 15206882. doi: 10.1021/ac60363a005.

[13] M. Zhybak, V. Beni, M.Y. Vagin, E. Dempsey, A.P.F. Turner, and Y. Korpan. Creatinine and urea biosensors based on a novel ammonium ion-selective copper-polyaniline nano-composite. *Biosensors and Bioelectronics*, 77:505–511, mar 2016. ISSN 09565663. doi: 10.1016/j.bios.2015. 10.009. URL `http://dx.doi.org/10.1016/j.bios.2015.10.009http://linkinghub.elsevier.com/retrieve/pii/S0956566315304747`.

[14] Byung-Ki Sohn, Byung-Woog Cho, Chang-soo Kim, and Dae-Hyuk Kwon. ISFET glucose and sucrose sensors by using platinum electrode and photo-crosslinkable polymers. *Sensors and Actuators B: Chemical*, 41(1-3):7–11,

1997. ISSN 09254005. doi: 10.1016/S0925-4005(97)80271-7. URL `http://linkinghub.elsevier.com/retrieve/pii/S0925400597802717`.

[15] Wei Xue and Tianhong Cui. A thin-film transistor based acetylcholine sensor using self-assembled carbon nanotubes and SiO2 nanoparticles. *Sensors and Actuators, B: Chemical*, 134(2):981–987, 2008. ISSN 09254005. doi: 10.1016/j.snb.2008.07.008.

[16] E L Gui, L J Li, K Zhang, Y Xu, X Dong, X Ho, P S Lee, J Kasim, Z X Shen, J A Rogers, and S G Mhaisalkar. DNA sensing by field-effect transistors based on networks of carbon nanotubes. *J Am Chem Soc*, 129(46):14427–14432, 2007. ISSN 0002-7863. doi: 10.1021/ja075176g. URL `http://www.ncbi.nlm.nih.gov/entrez/query.fcgi?cmd=Retrieve{&}db=PubMed{&}dopt=Citation{&}list{_}uids=17973383`.

[17] Jinglei Ping, Ramya Vishnubhotla, Amey Vrudhula, and A. T Charlie Johnson. Scalable Production of High-Sensitivity, Label-Free DNA Biosensors Based on Back-Gated Graphene Field Effect Transistors. *ACS Nano*, 10(9): 8700–8704, 2016. ISSN 1936086X. doi: 10.1021/acsnano.6b04110.

[18] Ying Wang, Wanzhi Wei, Jinxiang Zeng, Xiaoying Liu, and Xiandong Zeng. Fabrication of a copper nanoparticle/chitosan/carbon nanotube-modified glassy carbon electrode for electrochemical sensing of hydrogen peroxide and glucose. *Microchimica Acta*, 160(1):253–260, Jan 2008. ISSN 1436-5073. doi: 10.1007/s00604-007-0844-6. URL `https://doi.org/10.1007/s00604-007-0844-6`.

[19] Ali Düzgün, Hassan Imran, Kalle Levon, and F. Xavier Rius. Protein Detection with Potentiometric Aptasensors: A Comparative Study between Polyaniline and Single-Walled Carbon Nanotubes Transducers. *The Scientific World Journal*, 2013:1–8, 2013. ISSN 1537-744X. doi: 10.1155/2013/282756. URL `http://www.hindawi.com/journals/tswj/2013/282756/`.

[20] Apon Numnuam, Karin Y. Chumbimuni-Torres, Yun Xiang, Ralph Bash, Panote Thavarungkul, Proespichaya Kanatharana, Ernö Pretsch, Joseph Wang, and Eric Bakker. Potentiometric detection of DNA hybridization. *Journal of the American Chemical Society*, 130(2):410–411, 2008. ISSN 00027863. doi: 10.1021/ja0775467.

[21] Hiroaki Suzuki, Hisanori Shiroishi, Satoshi Sasaki, and Isao Karube. Microfabricated liquid junction ag/agcl reference electrode and its application to a one-chip potentiometric sensor. *Analytical Chemistry*, 71(22):5069–5075, 1999. doi: 10.1021/ac990437t. URL https://doi.org/10.1021/ac990437t.

[22] Fabio Baldessari. Electrokinetics in nanochannels: Part i. electric double layer overlap and channel-to-well equilibrium. *Journal of Colloid and Interface Science*, 325(2):526 – 538, 2008. ISSN 0021-9797. doi: https://doi.org/10.1016/j.jcis.2008.06.007. URL http://www.sciencedirect.com/science/article/pii/S0021979708007406.

[23] F. Schlögl. Chemical reaction models for non-equilibrium phase transitions. *Zeitschrift für Physik*, 253(2):147–161, Apr 1972. ISSN 0044-3328. doi: 10.1007/BF01379769. URL https://doi.org/10.1007/BF01379769.

[24] Cynthia G Bard, Allen J and Faulkner, Larry R and Leddy, Johna and Zoski. *Electrochemical methods: fundamentals and applications.* wiley New York, 2 edition, . ISBN 0-471-04372-9.

[25] Joseph H. Flynn and Leo A. Wall. A quick, direct method for the determination of activation energy from thermogravimetric data. *Journal of Polymer Science Part B: Polymer Letters*, 4(5):323–328. doi: 10.1002/pol.1966.110040504. URL https://onlinelibrary.wiley.com/doi/abs/10.1002/pol.1966.110040504.

[26] X.J. Chen, K.A. Khor, and S.H. Chan. Electrochemical behavior of la(sr)mno3 electrode under cathodic and anodic polarization. *Solid State Ionics*, 167(3):379 – 387, 2004. ISSN 0167-2738. doi: https://doi.org/10.1016/j.ssi.2003.08.049. URL http://www.sciencedirect.com/science/article/pii/S016727380300393X.

[27] S. J. Updike and G. P. Hicks. The enzyme electrode. *Nature*, 214(5092):986–988, 1967. ISSN 00280836. doi: 10.1038/214986a0.

[28] Asha Chaubey and B. D. Malhotra. Mediated biosensors. *Biosensors and Bioelectronics*, 17(6-7):441–456, 2002. ISSN 09565663. doi: 10.1016/S0956-5663(01)00313-X.

[29] Jie Liu and Joseph Wang. A Novel Improved Design for the First-generation Glucose Biosensor. *Food Technology and Biotechnology*, 39(1):55–58, 2001. ISSN 13309862.

[30] Golam Faruque Khan, Masaki Ohwa, and Wolfgang Wernet. Design of a stable charge transfer complex electrode for a third-generation amperometric glucose sensor. *Analytical Chemistry*, 68(17):2939–2945, 1996. doi: 10.1021/ ac9510393. URL `https://doi.org/10.1021/ac9510393`. PMID: 8794929.

[31] Geng huang Wu, Yan fang Wu, Xi wei Liu, Ming cong Rong, Xiao mei Chen, and Xi Chen. An electrochemical ascorbic acid sensor based on palladium nanoparticles supported on graphene oxide. *Analytica Chimica Acta*, 745: 33–37, 2012. ISSN 00032670. doi: 10.1016/j.aca.2012.07.034. URL `http://dx.doi.org/10.1016/j.aca.2012.07.034`.

[32] Xuan Zhu, Xiaofeng Wang, Chen Zhang, Xiaoqi Wang, and Qing Gu. A riboswitch sensor to determine vitamin B12 in fermented foods. *Food Chemistry*, 175:523–528, 2015. ISSN 18737072. doi: 10.1016/j.foodchem.2014.11. 163. URL `http://dx.doi.org/10.1016/j.foodchem.2014.11.163`.

[33] Taher Alizadeh and Somayeh Amjadi. Indirect voltammetric determination of nicotinic acid by using a graphite paste electrode modified with reduced graphene oxide and a molecularly imprinted polymer. pages 2687–2695, 2017. ISSN 0026-3672. doi: 10.1007/s00604-017-2296-y.

[34] Takao Hibi and Mitsugi Senda. Enzymatic Assay of Histamine by Amperometric Detection of H2O2 with Peroxide based Sensor, 2000.

[35] Hao Tang, Peng Lin, Helen L W Chan, and Feng Yan. Highly sensitive dopamine biosensors based on organic electrochemical transistors. *Biosensors and Bioelectronics*, 26(11):4559–4563, 2011. ISSN 09565663. doi: 10.1016/j.bios.2011.05.025. URL `http://dx.doi.org/10.1016/j.bios.2011.05.025`.

[36] John D. Elsworth and Robert H. Roth. Dopamine Synthesis, Uptake, Metabolism, and Receptors: Relevance to Gene Therapy of Parkinson's Disease. *Experimental Neurology*, 144(1):4–9, 1997. ISSN 00144886. doi: 10.1006/exnr.1996.6379. URL `http://linkinghub.elsevier.com/retrieve/pii/S0014488696963797`.

[37] Jong-Hoon Kim, Jonathan M. Auerbach, José A. Rodríguez-Gómez, Iván Velasco, Denise Gavin, Nadya Lumelsky, Sang-Hun Lee, John Nguyen, Rosario Sánchez-Pernaute, Krys Bankiewicz, and Ron McKay. Dopamine neurons derived from embryonic stem cells function in an animal model of Parkinson's disease. *Nature*, 418(6893):50–56, 2002. ISSN 0028-0836. doi: 10.1038/nature00900. URL `http://www.nature.com/doifinder/10.1038/nature00900`.

[38] Maite Sanz Alaejos and Francisco Jorge García Montelongo. Application of amperometric biosensors to the determination of vitamins and α-amino acids. *Chemical Reviews*, 104(7):3239–3265, 2004. ISSN 00092665. doi: 10.1021/cr0304471.

[39] John P. Hart and Stephen A. Wring. Recent developments in the design and application of screen-printed electrochemical sensors for biomedical, environmental and industrial analyses. *TrAC Trends in Analytical Chemistry*, 16(2):89 – 103, 1997. ISSN 0165-9936. doi: https://doi.org/10.1016/S0165-9936(96)00097-0. URL `http://www.sciencedirect.com/science/article/pii/S0165993696000970`.

[40] Dario Kriz, Maria Kempe, and Klaus Mosbach. Introduction of molecularly imprinted polymers as recognition elements in conductometric chemical sensors. *Sensors and Actuators B: Chemical*, 33(1):178 – 181, 1996. ISSN 0925-4005. doi: https://doi.org/10.1016/0925-4005(96)80094-3. URL `http://www.sciencedirect.com/science/article/pii/0925400596800943`. Eurosensors IX.

[41] Pengguang Yu and Shaojun Dong. The fabrication and performance of an Ag/AgCl reference electrode in human serum. *Analytica Chimica Acta*, 330 (2-3):167–174, 1996. ISSN 00032670. doi: 10.1016/0003-2670(96)00162-6.

[42] Shahriar Jamasb. An analytical technique for counteracting drift in ion-selective field effect transistors (ISFETs). *IEEE Sensors Journal*, 4(6):795–801, 2004. ISSN 1530437X. doi: 10.1109/JSEN.2004.833148.

[43] Sergey M. Borisov and Otto S. Wolfbeis. Optical biosensors. *Chemical Reviews*, 108(2):423–461, 2008. doi: 10.1021/cr068105t. URL `https://doi.org/10.1021/cr068105t`. PMID: 18229952.

[44] Bo Liedberg, Claes Nylander, and Ingemar Lunström. Surface plasmon resonance for gas detection and biosensing. *Sensors and actuators*, 4:299–304, 1983.

[45] Alan Saghatelian, Kevin M. Guckian, Desiree A. Thayer, and M. Reza Ghadiri. DNA detection and signal amplification via an engineered allosteric enzyme. *Journal of the American Chemical Society*, 125(2):344–345, 2003. ISSN 00027863. doi: 10.1021/ja027885u.

[46] A. A. Maradudin and G. I. Stegeman. *Surface Acoustic Waves*, pages 5–35. Springer Berlin Heidelberg, Berlin, Heidelberg, 1991. ISBN 978-3-642-75785-3. doi: 10.1007/978-3-642-75785-3_2. URL https://doi.org/10.1007/978-3-642-75785-3_2.

[47] W E Bulst, G Fischerauer, and L Reindl. State of the Art in Wireless Sensing with Surface Acoustic Waves. *Industrial Electronics, IEEE Transactions on*, 48(2):265–271, 2001. ISSN 02780046. doi: 10.1109/41.915404.

[48] Friederike J. Gruhl and Kerstin Länge. Surface Acoustic Wave (SAW) Biosensor for Rapid and Label-Free Detection of Penicillin G in Milk. *Food Analytical Methods*, 7(2):430–437, 2014. ISSN 19369751. doi: 10.1007/s12161-013-9642-4.

[49] Kerstin Länge, Bastian E. Rapp, and Michael Rapp. Surface acoustic wave biosensors: A review. *Analytical and Bioanalytical Chemistry*, 391(5):1509–1519, 2008. ISSN 16182642. doi: 10.1007/s00216-008-1911-5.

[50] Christiane Ziegler. Cantilever-based biosensors. *Analytical and Bioanalytical Chemistry*, 379(7):946–959, Aug 2004. ISSN 1618-2650. doi: 10.1007/s00216-004-2694-y. URL https://doi.org/10.1007/s00216-004-2694-y.

[51] A. Amjad, I. A. Mirza, S. A. Abbasi, U. Farwa, N. Malik, and F. Zia. A standardized framework for the validation and verification of clinical molecular genetic tests. *Iranian Journal of Microbiology*, 3(4):189–193, 2011. ISSN 20083289. doi: 10.1038/ejhg.2010.101.

[52] Keith J. Laidler. The development of the Arrhenius equation. *Journal of Chemical Education*, 61(6):494, 1984. ISSN 0021-9584. doi: 10.1021/ed061p494. URL http://pubs.acs.org/doi/abs/10.1021/ed061p494.

[53] Holger Klapproth, Sonja Bednar, Johannes Baader, Mirko Lehmann, Ingo Freund, Thomas Brandstetter, and Jürgen Rühe. Development of a multi-analyte CMOS sensor for point-of-care testing. *Sensing and Bio-Sensing Research*, 5:117–122, 2015. ISSN 22141804. doi: 10.1016/j.sbsr.2015.08.004. URL `http://dx.doi.org/10.1016/j.sbsr.2015.08.004`.

[54] Hi Gyu Moon, Youngmo Jung, Soo Deok Han, Young Seok Shim, Beomju Shin, Taikjin Lee, Jin Sang Kim, Seok Lee, Seong Chan Jun, Hyung Ho Park, Chulki Kim, and Chong Yun Kang. Chemiresistive Electronic Nose toward Detection of Biomarkers in Exhaled Breath. *ACS Applied Materials and Interfaces*, 8(32):20969–20976, 2016. ISSN 19448252. doi: 10.1021/acsami.6b03256.

[55] K. Melzer, V. D. Bhatt, T. Schuster, E. Jaworska, K. Maksymiuk, A. Michalska, G. Scarpa, and P. Lugli. Multi ion-sensor arrays: Towards an "electronic tongue". In *2016 IEEE 16th International Conference on Nanotechnology (IEEE-NANO)*, pages 475–478. IEEE, aug 2016. ISBN 978-1-5090-1493-4. doi: 10.1109/NANO.2016.7751505. URL `http://ieeexplore.ieee.org/document/7751505/`.

[56] Kota Shiba, Ryo Tamura, Gaku Imamura, and Genki Yoshikawa. Data-driven nanomechanical sensing: Specific information extraction from a complex system. *Scientific Reports*, 7(1):1–12, 2017. ISSN 20452322. doi: 10.1038/s41598-017-03875-7.

[57] Saskia K Van Bergen, Irina B Bakaltcheva, Jeffrey S Lundgren, and Lisa C Shriver-Lake. On-site detection of explosives in groundwater with a fiber optic biosensor. *Environmental science & technology*, 34(4):704–708, 2000.

[58] Antonios Perdikaris, Nikos Alexandropoulos, and Spiridon Kintzios. Development of a Novel, Ultra-rapid Biosensor for the Qualitative Detection of Hepatitis B Virus-associated Antigens and Anti-HBV, Based on "Membrane-engineered" Fibroblast Cells with Virus-Specific Antibodies and Antigens. *Sensors*, 9(3):2176–2186, mar 2009. ISSN 1424-8220. doi: 10.3390/s90302176. URL `http://www.mdpi.com/1424-8220/9/3/2176/`.

[59] Ivan Martin, Bojana Obradovic, Lisa E. Freed, and Gordana Vunjak-Novakovic. Method for quantitative analysis of glycosaminoglycan distribution in cultured natural and engineered cartilage. *Annals of Biomedical*

Engineering, 27(5):656–662, Sep 1999. ISSN 1573-9686. doi: 10.1114/1.205. URL https://doi.org/10.1114/1.205.

[60] Victoria Pribul and T Wooley. Point of care testing. *Surgery*, 31(2):84–86, 2013. ISSN 02639319. doi: 10.1016/j.mpsur.2012.12.002. URL http://dx.doi.org/10.1016/j.mpsur.2012.12.002.

[61] Rosanna W Peeling, King K Holmes, David Mabey, and Allan Ronald. Rapid tests for sexually transmitted infections (stis): the way forward. *Sexually transmitted infections*, 82(suppl 5):v1–v6, 2006.

[62] Brian Blau McIntyre, Nick Ingelbrecht. forecast wearable electronic devices worldwide, 2017. URL https://www.gartner.com/doc/3778064/forecast-wearable-electronic-devices-worldwide.

[63] P. R. Nair and M. A. Alam. Performance limits of nanobiosensors. *Applied Physics Letters*, 88(23):98–101, 2006. ISSN 00036951. doi: 10.1063/1.2211310.

[64] Meining Zhang, Kuanping Gong, Hongwu Zhang, and Lanqun Mao. Layer-by-layer assembled carbon nanotubes for selective determination of dopamine in the presence of ascorbic acid. *Biosensors and Bioelectronics*, 20(7):1270–1276, 2005. ISSN 09565663. doi: 10.1016/j.bios.2004.04.018.

[65] Wencai Zhu, Ting Chen, Xuemei Ma, Houyi Ma, and Shenhao Chen. Highly sensitive and selective detection of dopamine based on hollow gold nanoparticles-graphene nanocomposite modified electrode. *Colloids and Surfaces B: Biointerfaces*, 111:321–326, 2013. ISSN 09277765. doi: 10.1016/j.colsurfb.2013.06.026. URL http://dx.doi.org/10.1016/j.colsurfb.2013.06.026.

[66] Ying Chih Wang, Anna L. Stevens, and Jongyoon Han. Million-fold preconcentration of proteins and peptides by nanofluidic filter. *Analytical Chemistry*, 77(14):4293–4299, 2005. ISSN 00032700. doi: 10.1021/ac050321z.

[67] Yurena Seguí Femenias, Ueli Angst, Francesco Caruso, and Bernhard Elsener. Ag/AgCl ion-selective electrodes in neutral and alkaline environments containing interfering ions. *Materials and Structures/Materiaux et Constructions*, 49(7):2637–2651, 2016. ISSN 13595997. doi: 10.1617/s11527-015-0673-8.

[68] William Waddell and Roger Bates. Intracellular pH. *Physiological reviews*, 49(2), 1969.

[69] Eleftherios P. Diamandis. Theranos phenomenon: promises and fallacies. *Clinical Chemistry and Laboratory Medicine (CCLM)*, 53(7): 989–993, jan 2015. ISSN 1437-4331. doi: 10.1515/cclm-2015-0356. URL https://www.degruyter.com/view/j/cclm.2015.53.issue-7/cclm-2015-0356/cclm-2015-0356.xml.

[70] LV Radushkevich and VM Lukyanovich. O strukture ugleroda, obrazujucegosja pri termiceskom razlozenii okisi ugleroda na zeleznom kontakte. *Zurn Fisic Chim*, 26(1):88–95, 1952.

[71] Sumio Iijima. Helical microtubules of graphitic carbon. *Nature*, 354(6348): 56–58, nov 1991. ISSN 0028-0836. doi: 10.1038/354056a0. URL http://www.nature.com/doifinder/10.1038/354056a0.

[72] MFL De Volder, SH Tawfick, RH Baughman, and AJ Hart. Carbon nanotubes: present and future commercial applications. *Science*, 339(February): 535–539, 2013. ISSN 10959203. doi: 10.1126/science.1222453. URL http://www.sciencemag.org/content/339/6119/535.short.

[73] M. Mitchell Waldrop. The chips are down for Moore's law. *Nature*, 530 (7589):144–147, 2016. ISSN 0028-0836. doi: 10.1038/530144a. URL http://www.nature.com/doifinder/10.1038/530144a.

[74] Millie S. Dresselhaus, G. Dresselhaus, R. Saito, and A. Jorio. Raman spectroscopy of carbon nanotubes. *Physics Reports*, 409(2):47–99, 2005. ISSN 03701573. doi: 10.1016/j.physrep.2004.10.006.

[75] KS Novoselov, AK Geim, and SV Morozov. Electric field effect in atomically thin carbon films. *Science*, 22:2–6, 2004. URL http://www.sciencemag.org/content/306/5696/666.short.

[76] Michael S Arnold, Alexander a Green, James F Hulvat, Samuel I Stupp, and Mark C Hersam. Sorting carbon nanotubes by electronic structure using density differentiation. *Nature nanotechnology*, 1(1):60–5, October 2006. ISSN 1748-3395. doi: 10.1038/nnano.2006.52. URL http://www.ncbi.nlm.nih.gov/pubmed/18654143.

[77] Mildred S. Dresselhaus, Ado Jorio, Mario Hofmann, Gene Dresselhaus, and Riichiro Saito. Perspectives on carbon nanotubes and graphene Raman spectroscopy. *Nano Letters*, 10(3):751–758, 2010. ISSN 15306984. doi: 10.1021/nl904286r.

[78] R Saito, T Takeya, T Kimura, G Dresselhaus, and M S Dresselhaus. Raman intensity of single-wall carbon nanotubes. 57(7):4145–4153, 1998.

[79] P. M. Ajayan. Nanotubes from Carbon. *Chemical Reviews*, 99(7):1787–1800, 1999. ISSN 0009-2665. doi: 10.1021/cr970102g. URL `http://pubs.acs.org/doi/abs/10.1021/cr970102g`.

[80] Elena Starodub, Aaron Bostwick, Luca Moreschini, Shu Nie, Farid El Ga-baly, Kevin F. McCarty, and Eli Rotenberg. In-plane orientation effects on the electronic structure, stability, and Raman scattering of monolayer graphene on Ir(111). *Physical Review B*, 83(12):125428, 2011. ISSN 1098-0121. doi: 10.1103/PhysRevB.83.125428. URL `https://link.aps.org/doi/10.1103/PhysRevB.83.125428`.

[81] A. Moisala, Q. Li, I.A. Kinloch, and A.H. Windle. Thermal and electrical conductivity of single- and multi-walled carbon nanotube-epoxy composites. *Composites Science and Technology*, 66(10):1285 – 1288, 2006. ISSN 0266-3538. doi: https://doi.org/10.1016/j.compscitech.2005.10.016. URL `http://www.sciencedirect.com/science/article/pii/S0266353805003969`.

[82] Elham Abbasi, Sedigheh Fekri Aval, Abolfazl Akbarzadeh, Morteza Milani, and Hamid Tayefi Nasrabadi. Dendrimers:synthesis,applications, and properties. *Nanoscale Research Letters*, 9(1):247–256, 2014. ISSN 1556-276X. doi: 10.1186/1556-276X-9-247.

[83] M. José-Yacamán, M. Miki-Yoshida, L. Rendón, and J. G. Santiesteban. Catalytic growth of carbon microtubules with fullerene structure. *Applied Physics Letters*, 62(6):657–659, 1993. ISSN 00036951. doi: 10.1063/1.108857.

[84] P M and Ajayan and T W Ebbesen. Nanometre-size tubes of carbon. *Reports on Progress in Physics*, 60:1025–1062, 1997.

[85] L. Chico, Vincent H. Crespi, Lorin X. Benedict, Steven G. Louie, and Marvin L. Cohen. Pure carbon nanoscale devices: Nanotube heterojunctions. *Physical Review Letters*, 76(6):971–974, 1996. ISSN 10797114. doi: 10.1103/PhysRevLett.76.971.

[86] P. X. Hou, S. Bai, Q. H. Yang, C. Liu, and H. M. Cheng. Multi-step purification of carbon nanotubes. *Carbon*, 40(1):81–85, 2002. ISSN 00086223. doi: 10.1016/S0008-6223(01)00075-6.

[87] A. Thess, R. Lee, P. Nikolaev, H. Dai, P. Petit, J. Robert, C. Xu, Y. H. Lee, S. G. Kim, A. G. Rinzler, D. T. Colbert, G. E. Scuseria, D. Tomanek, J. E. Fischer, and R. E. Smalley. Crystalline Ropes of Metallic Carbon Nanotubes. *Science*, 273(5274):483–487, 1996. ISSN 0036-8075. doi: 10. 1126/science.273.5274.483. URL http://www.sciencemag.org/cgi/doi/10.1126/science.273.5274.483.

[88] F. Kreupl, A. P. Graham, G. S. Duesberg, W. Steinhögl, M. Liebau, E. Unger, and W. Hönlein. Carbon nanotubes in interconnect applications. *Microelectronic Engineering*, 64(1-4):399–408, 2002. ISSN 01679317. doi: 10.1016/S0167-9317(02)00814-6.

[89] Ninette Stürzl, Frank Hennrich, Sergei Lebedkin, and Manfred M. Kappes. Near monochiral single-walled carbon nanotube dispersions in organic solvents. *Journal of Physical Chemistry C*, 113(33):14628–14632, 2009. ISSN 19327447. doi: 10.1021/jp902788y.

[90] Thomas Ebbesen. Carbon Nanotubes. *Annu. Rev. Mater. Sci.*, 24:235–64, 1994.

[91] Fei Xiao, Faqiong Zhao, Jiangwen Li, Liqin Liu, and Baizhao Zeng. Characterization of hydrophobic ionic liquid-carbon nanotubes-gold nanoparticles composite film coated electrode and the simultaneous voltammetric determination of guanine and adenine. *Electrochimica Acta*, 53(26):7781–7788, 2008. ISSN 00134686. doi: 10.1016/j.electacta.2008.05.053.

[92] Peng-Cheng Ma, Naveed A. Siddiqui, Gad Marom, and Jang-Kyo Kim. Dispersion and functionalization of carbon nanotubes for polymer-based nanocomposites: A review. *Composites Part A: Applied Science and Manufacturing*, 41(10):1345 – 1367, 2010. ISSN 1359-835X. doi: https://doi.org/10.1016/j.compositesa.2010.07.003. URL http://www.sciencedirect.com/science/article/pii/S1359835X10002009.

[93] R. Andrews and M. C. Weisenberger. Carbon nanotube polymer composites. *Current Opinion in Solid State and Materials Science*, 8(1):31–37, 2004. ISSN 13590286. doi: 10.1016/j.cossms.2003.10.006.

[94] Jing Kong, Hyongsok T. Soh, Alan M. Cassell, Calvin F. Quate, and Hongjie Dai. Synthesis of individual singlewalled carbon nanotubes on patterned silicon wafers. *Nature*, 395(October):878–881, 1998. ISSN 0028-0836. doi: 10.1038/nature02458.1.

[95] Ding Wang, Pengcheng Song, Changhong Liu, Wei Wu, and Shoushan Fan. Highly oriented carbon nanotube papers made of aligned carbon nanotubes. *Nanotechnology*, 19(7), 2008. ISSN 09574484. doi: 10.1088/0957-4484/19/7/075609.

[96] Kunitoshi Yamamoto, Seiji Akita, and Yoshikazu Nakayama. Orientation an durification of carbon nanotubes using ac electrophoresis. *J. Phys. D: Appl. Phys.*, 31:L34, 1998.

[97] Takeshi Kawano, Heather C. Chiamori, Marcel Suter, Qin Zhou, Brian D. Sosnowchik, and Liwei Lin. An electrothermal carbon nanotube gas sensor. *Nano Letters*, 7(12):3686–3690, 2007. doi: 10.1021/nl071964s. URL `https://doi.org/10.1021/nl071964s`. PMID: 18001108.

[98] Coskun Kocabas, Moonsub Shim, and John A. Rogers. Spatially selective guided growth of high-coverage arrays and random networks of single-walled carbon nanotubes and their integration into electronic devices. *Journal of the American Chemical Society*, 128(14):4540–4541, 2006. doi: 10.1021/ja0603150. URL `https://doi.org/10.1021/ja0603150`. PMID: 16594668.

[99] Qing Cao and John A. Rogers. Random networks and aligned arrays of single-walled carbon nanotubes for electronic device applications. *Nano Research*, 1(4):259–272, Oct 2008. ISSN 1998-0000. doi: 10.1007/s12274-008-8033-4. URL `https://doi.org/10.1007/s12274-008-8033-4`.

[100] Seong Jun Kang, Coskun Kocabas, Taner Ozel, Moonsub Shim, Ninad Pimparkar, Muhammad A. Alam, Slava V. Rotkin, and John A. Rogers. High-performance electronics using dense, perfectly aligned arrays of single-walled carbon nanotubes. *Nature Nanotechnology*, 2(4):230–236, 2007. ISSN 17483395. doi: 10.1038/nnano.2007.77.

[101] Melissa Mushrush, Antonio Facchetti, Michael Lefenfeld, Howard E. Katz, and Tobin J. Marks. Easily processable phenylene thiophene based organic

field-effect transistors and solution fabricated nonvolatile transistor memory elements. *Journal of the American Chemical Society*, 125(31):9414–9423, 2003. doi: 10.1021/ja035143a. URL `https://doi.org/10.1021/ja035143a`. PMID: 12889972.

[102] Yi-Kuei Chang and Franklin Chau-Nan Hong. The fabrication of zno nanowire field-effect transistors by roll-transfer printing. *Nanotechnology*, 20(19):195302, 2009. URL `http://stacks.iop.org/0957-4484/20/i=19/a=195302`.

[103] Brian White, Sarbajit Banerjee, Stephen O'Brien, Nicholas J. Turro, and Irving P. Herman. Zeta-potential measurements of surfactant-wrapped individual single-walled carbon nanotubes. *Journal of Physical Chemistry C*, 111(37):13684–13690, 2007. ISSN 19327447. doi: 10.1021/jp070853e.

[104] Panagiotis Angelikopoulos, Andrei Gromov, Ailsa Leen, Oleg Nerushev, Henry Bock, and Eleanor E B Campbell. Dispersing Individual Single-Wall Carbon Nanotubes in Aqueous Surfactant Solutions below the cmc. *J. Phys. Chem.*, 114:2–9, 2010.

[105] Ming Zheng, Anand Jagota, Ellen D. Semke, Bruce A. Diner, Robert S McLean, Steve R. Lustig, Raymond E. Richardson, and Nancy G. Tassi. DNA-assisted dispersion and separation of carbon nanotubes. *Nature materials*, 2(5):338–342, 2003. ISSN 1476-1122. doi: 10.1038/nmat877M4-Citavi. URL `http://dx.doi.org/10.1038/nmat877$\delimiter"026E30F$nhttp://www.ncbi.nlm.nih.gov/pubmed/12692536$\delimiter"026E30F$nE:$\delimiter"026E30F$Literatur$\delimiter"026E30F$Citavi$\delimiter"026E30F$CarbonNanotubes$\delimiter"026E30F$CitaviAttachments$\delimiter"026E30F$Zheng, Jagotaetal2003-DNA-assisteddispersionandseparation.pdf`.

[106] Junrong Yu, Nadia Grossiord, Cor E. Koning, and Joachim Loos. Controlling the dispersion of multi-wall carbon nanotubes in aqueous surfactant solution. *Carbon*, 45(3):618 – 623, 2007. ISSN 0008-6223. doi: https://doi.org/10.1016/j.carbon.2006.10.010. URL `http://www.sciencedirect.com/science/article/pii/S0008622306005306`.

[107] Simon M Sze and Kwok K Ng. *Physics of semiconductor devices*. John wiley & sons, 2006.

[108] H. Helmholtz. Ueber einige Gesetze der Vertheilung elektrischer Ströme in körperlichen Leitern mit Anwendung auf die thierisch-elektrischen Versuche. *Annalen der Physik und Chemie*, 165(6):211–233, 1853. ISSN 00033804. doi: 10.1002/andp.18531650603. URL `http://doi.wiley.com/10.1002/andp.18531650603`.

[109] David E. Yates, Samuel Levine, and Thomas W. Healy. Site-binding model of the electrical double layer at the oxide/water interface. *J. Chem. Soc., Faraday Trans. 1*, 70:1807–1818, 1974. doi: 10.1039/F19747001807. URL `http://dx.doi.org/10.1039/F19747001807`.

[110] Hans-Jürgen Butt. Measuring electrostatic, van der waals, and hydration forces in electrolyte solutions with an atomic force microscope. *Biophysical Journal*, 60(6):1438 – 1444, 1991. ISSN 0006-3495. doi: https://doi.org/10.1016/S0006-3495(91)82180-4. URL `http://www.sciencedirect.com/science/article/pii/S0006349591821804`.

[111] Grace Dansoa Tabi, Benjamin Nketia-Yawson, So-Huei Kang, Chang-duk Yang, and Yong-Young Noh. High performance p-type chlorinated-benzothiadiazole-based polymer electrolyte gated organic field-effect transistors. *Organic Electronics*, 54:255 – 260, 2018. ISSN 1566-1199. doi: https://doi.org/10.1016/j.orgel.2018.01.003. URL `http://www.sciencedirect.com/science/article/pii/S156611991830003X`.

[112] L. H. Hess, M. V. Hauf, M. Seifert, F. Speck, T. Seyller, M. Stutzmann, I. D. Sharp, and J. A. Garrido. High-transconductance graphene solution-gated field effect transistors. *Applied Physics Letters*, 99(3):033503, 2011. doi: 10.1063/1.3614445. URL `https://doi.org/10.1063/1.3614445`.

[113] Jonathan D. Yuen, Anoop S. Dhoot, Ebinazar B. Namdas, Nelson E. Coates, Martin Heeney, Iain McCulloch, Daniel Moses, and Alan J. Heeger. Electrochemical doping in electrolyte-gated polymer transistors. *Journal of the American Chemical Society*, 129(46):14367–14371, 2007. doi: 10.1021/ja0749845. URL `https://doi.org/10.1021/ja0749845`. PMID: 17967016.

[114] Ki Ho Park, Manish Chhowalla, Zafar Iqbal, and Federico Sesti. Single-walled Carbon Nanotubes Are a New Class of Ion Channel Blockers. *Journal of Biological Chemistry*, 278(50):50212–50216, 2003. ISSN 00219258. doi: 10.1074/jbc.M310216200.

[115] S. Ono, K. Miwa, S. Seki, and J. Takeya. A comparative study of organic single-crystal transistors gated with various ionic-liquid electrolytes. *Applied Physics Letters*, 94(6):1–4, 2009. ISSN 00036951. doi: 10.1063/1.3079401.

[116] Jaan Männik, Iddo Heller, Anne M. Janssens, Serge G. Lemay, and Cees Dekker. Charge noise in liquid-gated single-wall carbon nanotube transistors. *Nano Letters*, 8(2):685–688, 2008. ISSN 15306984. doi: 10.1021/nl073271h.

[117] Iddo Heller, Sohail Chatoor, Jaan Männik, Marcel A.G. Zevenbergen, Cees Dekker, and Serge G. Lemay. Influence of electrolyte composition on liquid-gated carbon nanotube and graphene transistors. *Journal of the American Chemical Society*, 132(48):17149–17156, 2010. ISSN 00027863. doi: 10.1021/ja104850n.

[118] H. J. Li, W. G. Lu, J. J. Li, X. D. Bai, and C. Z. Gu. Multichannel ballistic transport in multiwall carbon nanotubes. *Phys. Rev. Lett.*, 95:086601, Aug 2005. doi: 10.1103/PhysRevLett.95.086601. URL `https://link.aps.org/doi/10.1103/PhysRevLett.95.086601`.

[119] Luis E. F. Foa Torres and Stephan Roche. Inelastic quantum transport and peierls-like mechanism in carbon nanotubes. *Phys. Rev. Lett.*, 97:076804, Aug 2006. doi: 10.1103/PhysRevLett.97.076804. URL `https://link.aps.org/doi/10.1103/PhysRevLett.97.076804`.

[120] Jie Deng and H.-S. Philip Wong. A Compact SPICE Model for Carbon-Nanotube Field-Effect Transistors Including Nonidealities and Its Application—Part I: Model of the Intrinsic Channel Region. *IEEE Transactions on Electron Devices*, 54(12):3186–3194, 2007. ISSN 0018-9383. doi: 10.1109/TED.2007.909030. URL `http://ieeexplore.ieee.org/document/4383021/`.

[121] Simone Colasanti. *Modeling and Simulation of Carbon Nanotubes Networks: Toward a Multiscale Approach*. Dissertation, Technische Universität München, München, 2016.

[122] Tadayuki Matsuo and Kensall D. Wise. An Integrated Field-Effect Electrode for Biopotential Recording. *IEEE Transactions on Biomedical Engineering*, BME-21(6):485–487, 1974. ISSN 15582531. doi: 10.1109/TBME.1974.324338.

[123] Jří Janata. *Principles of Chemical Sensors*. 2009. ISBN 9780387699301. doi: 10.1007/b136378.

[124] Hyuk Jin Lee, Uk Sun Hong, Dong Kwon Lee, Jae Ho Shin, Hakhyun Nam, and Geun Sig Cha. Solvent-processible polymer membrane-based liquid junction-free reference electrode. *Analytical Chemistry*, 70(16):3377–3383, 1998. doi: 10.1021/ac980265k. URL `https://doi.org/10.1021/ac980265k`.

[125] Renata Mamińska, Artur Dybko, and Wojciech Wróblewski. All-solid-state miniaturised planar reference electrodes based on ionic liquids. *Sensors and Actuators B: Chemical*, 115(1):552–557, may 2006. ISSN 09254005. doi: 10.1016/j.snb.2005.10.018. URL `http://linkinghub.elsevier.com/retrieve/pii/S0925400505008476`.

[126] Luisa Torsi, Maria Magliulo, Kyriaki Manoli, and Gerardo Palazzo. Organic field-effect transistor sensors: a tutorial review. *Chemical Society Reviews*, 42(22):8612, 2013. ISSN 0306-0012. doi: 10.1039/c3cs60127g. URL `http://xlink.rsc.org/?DOI=c3cs60127g`.

[127] Chenguang Lu, Qiang Fu, Shaoming Huang, and Jie Liu. Polymer electrolyte-gated carbon nanotube field-effect transistor. *Nano Letters*, 4(4):623–627, 2004. ISSN 15306984. doi: 10.1021/nl049937e.

[128] Aaron D. Franklin, Damon B. Farmer, and Wilfried Haensch. Defining and overcoming the contact resistance challenge in scaled carbon nanotube transistors. *ACS Nano*, 8(7):7333–7339, 2014. doi: 10.1021/nn5024363. URL `https://doi.org/10.1021/nn5024363`. PMID: 24999536.

[129] John A. Defranco, Bradley S. Schmidt, Michal Lipson, and George G. Malliaras. Photolithographic patterning of organic electronic materials. *Organic Electronics: physics, materials, applications*, 7(1):22–28, 2006. ISSN 15661199. doi: 10.1016/j.orgel.2005.10.002.

[130] Amit Kumar, Hans A. Biebuyck, and George M. Whitesides. Patterning self-assembled monolayers: Applications in materials science. *Langmuir*, 10(5):1498–1511, 1994. doi: 10.1021/la00017a030. URL `https://doi.org/10.1021/la00017a030`.

[131] A. R. Champagne, A. J. Couture, F. Kuemmeth, and D. C. Ralph. Nanometer-scale scanning sensors fabricated using stencil lithography. *Applied Physics Letters*, 82(7):1111–1113, 2003. ISSN 00036951. doi: 10.1063/1.1554483.

[132] Suresh Kumar Raman Pillai and Mary B. Chan-Park. High-performance printed carbon nanotube thin-film transistors array fabricated by a non-lithography technique using hafnium oxide passivation layer and mask. *ACS Applied Materials & Interfaces*, 4(12):7047–7054, 2012. doi: 10.1021/am302431e. URL https://doi.org/10.1021/am302431e. PMID: 23194001.

[133] R. Yakimova, G. Steinhoff, R.M. Petoral, C. Vahlberg, V. Khranovskyy, G.R. Yazdi, K. Uvdal, and A. Lloyd Spetz. Novel material concepts of transducers for chemical and biosensors. *Biosensors and Bioelectronics*, 22(12):2780 – 2785, 2007. ISSN 0956-5663. doi: https://doi.org/10.1016/j.bios.2006.12.032. URL http://www.sciencedirect.com/science/article/pii/S095656630600618X. Chem and Biosensing Transistors: from materials to systems.

[134] Marvin J Johnson. Aerobic Microbial Growth at Low Oxygen Concentrations. *Microbiology*, 94(1):101–108, 1967.

[135] Andrei B. Kharitonov, Maya Zayats, Amir Lichtenstein, Eugenii Katz, and Itamar Willner. Enzyme monolayer-functionalized field-effect transistors for biosensor applications. *Sensors and Actuators, B: Chemical*, 70(1-3):222–231, 2000. ISSN 09254005. doi: 10.1016/S0925-4005(00)00573-6.

[136] NC-IUB. Units of enzyme activity. *European Journal of Biochemistry*, 97:319–320, 1979. ISSN 0201-8470. doi: 10.1111/j.1432-1033.1979.tb13116.x.

[137] E. M I M Ekanayake, D. M G Preethichandra, and Keiichi Kaneto. Polypyrrole nanotube array sensor for enhanced adsorption of glucose oxidase in glucose biosensors. *Biosensors and Bioelectronics*, 23(1):107–113, 2007. ISSN 09565663. doi: 10.1016/j.bios.2007.03.022.

[138] R. A. Williams and H. W. Blanch. Covalent immobilization of protein monolayers for biosensor applications. *Biosensors and Bioelectronics*, 9(2):159–167, 1994. ISSN 09565663. doi: 10.1016/0956-5663(94)80108-8.

[139] Bin Zhou, Jia Sun, Xiao Han, Jie Jiang, and Qing Wan. Low-voltage organic/inorganic hybrid transparent thin-film transistors gated by chitosan-based proton conductors. *IEEE Electron Device Letters*, 32(11):1549–1551, 2011. ISSN 07413106. doi: 10.1109/LED.2011.2164612.

[140] Vinod Kumar Gupta, Suresh Jain, and Sudeshna Chandra. Chemical sensor for lanthanum(III) determination using aza-crown as ionophore in poly(vinyl chloride) matrix. *Analytica Chimica Acta*, 486(2):199–207, 2003. ISSN 00032670. doi: 10.1016/S0003-2670(03)00506-3.

[141] Jeong Hoon Lee, Yong-Ak Song, and Jongyoon Han. Multiplexed proteomic sample preconcentration device using surface-patterned ion-selective membrane. *Lab on a Chip*, 8(4):596, 2008. ISSN 1473-0197. doi: 10.1039/b717900f. URL http://xlink.rsc.org/?DOI=b717900f.

[142] A. Craggs, G. J Moody, and J. D. R. Thomas. Matrix Membrane Ion-Selective Electrodes. *Journal of Chemical Education*, 51(8):541–544, 1974.

[143] Mohammad Yusuf Mulla, Elena Tuccori, Maria Magliulo, Gianluca Lattanzi, Gerardo Palazzo, Krishna Persaud, and Luisa Torsi. Capacitance-modulated transistor detects odorant binding protein chiral interactions. *Nature Communications*, 6:1–9, 2015. ISSN 20411723. doi: 10.1038/ncomms7010. URL http://dx.doi.org/10.1038/ncomms7010.

[144] Geunbae Lim and Shuichi Shoji. An Extended Gate Field Effect Transistor Based Protein Sensor. (111):3–6, 2005.

[145] J. Janata. Graphene Bio-Field-Effect Transistor Myth. *ECS Solid State Letters*, 1(6):M29–M31, 2012. ISSN 2162-8742. doi: 10.1149/2.014206ssl. URL http://ssl.ecsdl.org/cgi/doi/10.1149/2.014206ssl.

[146] Daniel R. Thévenot, Klara Toth, Richard A. Durst, and George S. Wilson. Electrochemical biosensors: recommended definitions and classification1international union of pure and applied chemistry: Physical chemistry division, commission i.7 (biophysical chemistry); analytical chemistry division, commission v.5 (electroanalytical chemistry).1. *Biosensors and Bioelectronics*, 16(1):121 – 131, 2001. ISSN 0956-5663. doi: https://doi.org/10.1016/S0956-5663(01)00115-4. URL http://www.sciencedirect.com/science/article/pii/S0956566301001154.

[147] Hui Wu, Liangbing Hu, Michael W. Rowell, Desheng Kong, Judy J. Cha, James R. McDonough, Jia Zhu, Yuan Yang, Michael D. McGehee, and Yi Cui. Electrospun metal nanofiber webs as high-performance transparent electrode. *Nano Letters*, 10(10):4242–4248, 2010. doi: 10.1021/nl102725k. URL `https://doi.org/10.1021/nl102725k`. PMID: 20738115.

[148] Linda Vaisman, H. Daniel Wagner, and Gad Marom. The role of surfactants in dispersion of carbon nanotubes. *Advances in Colloid and Interface Science*, 128-130:37 – 46, 2006. ISSN 0001-8686. doi: https://doi.org/10.1016/j.cis.2006.11.007. URL `http://www.sciencedirect.com/science/article/pii/S0001868606002065`. In Honor of Professor Nissim Garti's 60th Birthday.

[149] A. M. Munzer, M. Heimgreiter, K. Melzer, A. Weise, B. Fabel, A. Abdellah, P. Lugli, and G. Scarpa. Back-gated spray-deposited carbon nanotube thin film transistors operated in electrolytic solutions: an assessment towards future biosensing applications. *J. Mater. Chem. B*, 1:3797–3802, 2013. doi: 10.1039/C3TB20170H. URL `http://dx.doi.org/10.1039/C3TB20170H`.

[150] W. Shockley. Research and Investigation of Inverse Epitaxial UHF Power Transistors. Rep. No. AFAL-TDR-64-207. Technical report, Air Force Avionics Lab., Wright-Patterson Air Force Base, OH, 1964.

[151] Seung-Hyun Hur, Myung-Han Yoon, Anshu Gaur, Moonsub Shim, Antonio Facchetti, Tobin J. Marks, and John A. Rogers. Organic nanodielectrics for low voltage carbon nanotube thin film transistors and complementary logic gates. *Journal of the American Chemical Society*, 127(40):13808–13809, 2005. doi: 10.1021/ja0553203. URL `https://doi.org/10.1021/ja0553203`. PMID: 16201799.

[152] I. Giaever and C. R. Keese. Monitoring fibroblast behavior in tissue culture with an applied electric field. *Proceedings of the National Academy of Sciences*, 81(12):3761–3764, 1984. ISSN 0027-8424. doi: 10.1073/pnas.81.12.3761. URL `http://www.pnas.org/cgi/doi/10.1073/pnas.81.12.3761`.

[153] I Giaever and C R Keese. Micromotion of mammalian cells measured electrically. *Proceedings of the National Academy of Sciences of the United States of America*, 88(17):7896–7900, 1991. ISSN 0027-8424. doi: 10.1073/pnas.88.17.7896.

[154] Silke Arndt, Jochen Seebach, Katherina Psathaki, Hans-Joachim Galla, and Joachim Wegener. Bioelectrical impedance assay to monitor changes in cell shape during apoptosis. *Biosensors and Bioelectronics*, 19(6):583 – 594, 2004. ISSN 0956-5663. doi: https://doi.org/10.1016/S0956-5663(03)00269-0. URL `http://www.sciencedirect.com/science/article/pii/S0956566303002690`.

[155] V. Datsyuk, M. Kalyva, K. Papagelis, J. Parthenios, D. Tasis, A. Siokou, I. Kallitsis, and C. Galiotis. Chemical oxidation of multiwalled carbon nanotubes. *Carbon*, 46(6):833 – 840, 2008. ISSN 0008-6223. doi: https://doi.org/10.1016/j.carbon.2008.02.012. URL `http://www.sciencedirect.com/science/article/pii/S0008622308000717`.

[156] Jinming Cai, Pascal Ruffieux, Rached Jaafar, Marco Bieri, Thomas Braun, Stephan Blankenburg, Matthias Muoth, Ari P. Seitsonen, Moussa Saleh, Xinliang Feng, Klaus Müllen, and Roman Fasel. Atomically precise bottom-up fabrication of graphene nanoribbons. *Nature*, 466(7305):470–473, 2010. ISSN 00280836. doi: 10.1038/nature09211.

[157] Gartner. Gartner predicts 2018: 3d printing changes business models, December 2017. URL `https://blogs.gartner.com/pete-basiliere/2017/12/12/gartner-predicts-2018-3d-printing-changes-business-models/`.

[158] Falguni Pati, Dong Heon Ha, Jinah Jang, Hyun Ho Han, Jong Won Rhie, and Dong Woo Cho. Biomimetic 3D tissue printing for soft tissue regeneration. *Biomaterials*, 62:164–175, 2015. ISSN 18785905. doi: 10.1016/j.biomaterials.2015.05.043. URL `http://dx.doi.org/10.1016/j.biomaterials.2015.05.043`.

[159] Hyun Wook Kang, Sang Jin Lee, In Kap Ko, Carlos Kengla, James J. Yoo, and Anthony Atala. A 3D bioprinting system to produce human-scale tissue constructs with structural integrity. *Nature Biotechnology*, 34(3):312–319, 2016. ISSN 15461696. doi: 10.1038/nbt.3413. URL `http://dx.doi.org/10.1038/nbt.3413`.

[160] Robert W Holley. Control of growth of mammalian cells in cell culture. *Nature*, 258:735–737, 1975.

[161] Wei Zhao, Chulho Song, and Pehr E. Pehrsson. Water-soluble and optically pH-sensitive single-walled carbon nanotubes from surface modification. *Journal of the American Chemical Society*, 124(42):12418–12419, 2002. ISSN 00027863. doi: 10.1021/ja027861n.

[162] Jing Kong, Nathan R Franklin, Chongwu Zhou, Michael G Chapline, Shu Peng, Kyeongjae Cho, and Hongjie Dai. Nanotube molecular wires as sensors. *Science*, 287(January):622–625, 2000. doi: 10.1126/science.287.5453.622.

[163] Ashish Modi, Nikhil Koratkar, Eric Lass, Bingqing Wei, and Pulickel M. Ajayan. Miniaturized gas ionization sensors using carbon nanotubes. *Nature*, 424(6945):171–174, 2003. ISSN 00280836. doi: 10.1038/nature01777.

[164] Ni Luh Wulan Septiani and Brian Yuliarto. Review—The Development of Gas Sensor Based on Carbon Nanotubes. *Journal of The Electrochemical Society*, 163(3):B97–B106, 2016. ISSN 0013-4651. doi: 10.1149/2.0591603jes. URL `http://jes.ecsdl.org/lookup/doi/10.1149/2.0591603jes`.

[165] Michael Fothergill, Myron F. Goodman, John Petruska, and Arieh Warshel. Structure-energy analysis of the role of metal ions in phosphodiester bond hydrolysis by dna polymerase i. *Journal of the American Chemical Society*, 117(47):11619–11627, 1995. doi: 10.1021/ja00152a001. URL `https://doi.org/10.1021/ja00152a001`.

[166] C H Luo and Y Rudy. A dynamic model of the cardiac ventricular action potential. i. simulations of ionic currents and concentration changes. *Circulation Research*, 74(6):1071–1096, 1994. ISSN 0009-7330. doi: 10.1161/01.RES.74.6.1071. URL `http://circres.ahajournals.org/content/74/6/1071`.

[167] F. Hayashi and J. Lipski. The role of inhibitory amino acids in control of respiratory motor output in an arterially perfused rat. *Respiration Physiology*, 89(1):47 – 63, 1992. ISSN 0034-5687. doi: https://doi.org/10.1016/0034-5687(92)90070-D. URL `http://www.sciencedirect.com/science/article/pii/003456879290070D`.

[168] Steve F. Perry. The chloride cell:structure and function in the gills of freshwater fishes. *Annual Review of Physiology*, 59(1):325–347, 1997.

doi: 10.1146/annurev.physiol.59.1.325. URL `https://doi.org/10.1146/annurev.physiol.59.1.325`. PMID: 9074767.

[169] M. F. San Martín, G. V. Barbosa-Cánovas, and B. G. Swanson. Food processing by high hydrostatic pressure. *Critical Reviews in Food Science and Nutrition*, 42(6):627–645, 2002. doi: 10.1080/20024091054274. URL `https://doi.org/10.1080/20024091054274`. PMID: 12487422.

[170] O.C Zafiriou. Chemistry of superoxide ion-radical in seawater and uncatalyzed dismutation kinetics studied by pulse radiolysis. *Marine Chemistry*, 30:31 – 43, 1990. ISSN 0304-4203. doi: https://doi.org/10.1016/0304-4203(90)90060-P. URL `http://www.sciencedirect.com/science/article/pii/030442039090060P`.

[171] F.J Cook, W Hicks, E.A Gardner, G.D Carlin, and D.W Froggatt. Export of acidity in drainage water from acid sulphate soils. *Marine Pollution Bulletin*, 41(7):319 – 326, 2000. ISSN 0025-326X. doi: https://doi.org/10.1016/S0025-326X(00)00138-7. URL `http://www.sciencedirect.com/science/article/pii/S0025326X00001387`. Sources, Fates and Consequences of Pollutants in the Great Barrier Reef.

[172] Max Cremer. Über die Ursache der elektromotorischen Eigenschaften der Gewebe, zugleich ein Beitrag zur Lehre von polyphasischen Elektrolytketten. *Z. Biologie*, 47:542, 1906.

[173] Arnold Beckman. Apparatus for testing acidity, May 3 1936. US Patent US2058761A.

[174] George Eisenman. Apparatus for testing acidity, May 3 1962. US Patent US3041252A.

[175] Chun-Ze Lai, Secil S. Koseoglu, Elizabeth C. Lugert, Paul G. Boswell, József Rábai, Timothy P. Lodge, and Philippe Bühlmann. Fluorous polymeric membranes for ionophore-based ion-selective potentiometry: How inert is teflon af? *Journal of the American Chemical Society*, 131(4):1598–1606, 2009. doi: 10.1021/ja808047x. URL `https://doi.org/10.1021/ja808047x`. PMID: 19133768.

[176] Shuichi Shoji, Masayoshi Esashi, and Tadayuki Matsuo. Prototype miniature blood gas analyser fabricated on a silicon wafer. *Sensors and Actuators*, 14(2):101 – 107, 1988. ISSN 0250-6874. doi: https://doi.org/10.1016/

0250-6874(88)80057-X. URL `http://www.sciencedirect.com/science/article/pii/025068748880057X`.

[177] R.E.G. van Hal, J.C.T. Eijkel, and P. Bergveld. A novel description of isfet sensitivity with the buffer capacity and double-layer capacitance as key parameters. *Sensors and Actuators B: Chemical*, 24(1):201 – 205, 1995. ISSN 0925-4005. doi: https://doi.org/10.1016/0925-4005(95)85043-0. URL `http://www.sciencedirect.com/science/article/pii/0925400595850430`.

[178] T. Murakami, S. Nakamoto, J. Kimura, T. Kuriyama, and I. Karube. A micro planar ampehometric glucose sensor using an isfet as a reference electrode. *Analytical Letters*, 19(19-20):1973–1986, 1986. doi: 10.1080/00032718608064540. URL `https://doi.org/10.1080/00032718608064540`.

[179] Jianhua Liu, Yoshitaka Masuda, Eiichi Sekido, Shin-Ichi Wakida, and Kazuo Hiiro. Phosphate ion-sensitive coated-wire/field-effect transistor electrode based on cobalt phthalocyanine with poly(vinyl chloride) as the membrane matrix. *Analytica Chimica Acta*, 224:145 – 151, 1989. ISSN 0003-2670. doi: https://doi.org/10.1016/S0003-2670(00)83455-8. URL `http://www.sciencedirect.com/science/article/pii/S0003267000834558`.

[180] Bansi D. Malhotra, Asha Chaubey, and S.P. Singh. Prospects of conducting polymers in biosensors. *Analytica Chimica Acta*, 578(1):59 – 74, 2006. ISSN 0003-2670. doi: https://doi.org/10.1016/j.aca.2006.04.055. URL `http://www.sciencedirect.com/science/article/pii/S0003267006008889`. Pacifichem SI.

[181] Cristina C. Cid, Jordi Riu, Alicia Maroto, and F. Xavier Rius. Ion-sensitive field effect transistors using carbon nanotubes as the transducing layer. *Analyst*, 133:1001–1004, 2008. doi: 10.1039/B800862K. URL `http://dx.doi.org/10.1039/B800862K`.

[182] Mary Pinkerton, L.K. Steinrauf, and Phillip Dawkins. The molecular structure and some transport properties of valinomycin. *Biochemical and Biophysical Research Communications*, 35(4):512 – 518, 1969. ISSN 0006-291X. doi: https://doi.org/10.1016/0006-291X(69)90376-3. URL `http://www.sciencedirect.com/science/article/pii/0006291X69903763`.

[183] Katarina NeupertLaves and Max Dobler. The Crystal Structure of a K+ Complex of Valinomycin. *Helvetica Chimica Acta*, 58(2):432–442, 1975. ISSN 15222675. doi: 10.1002/hlca.19750580212.

[184] Eric Bakker, Ernö Pretsch, and Philippe Bühlmann. Selectivity of potentiometric ion sensors. *Analytical Chemistry*, 72(6):1127–1133, 2000. doi: 10.1021/ac991146n. URL `https://doi.org/10.1021/ac991146n`. PMID: 10740849.

[185] Andrey Legin, Sergey Makarychev-Mikhailov, Olga Goryacheva, Dmitry Kirsanov, and Yuri Vlasov. Cross-sensitive chemical sensors based on tetraphenylporphyrin and phthalocyanine. *Analytica Chimica Acta*, 457 (2):297 – 303, 2002. ISSN 0003-2670. doi: https://doi.org/10.1016/S0003-2670(02)00052-1. URL `http://www.sciencedirect.com/science/article/pii/S0003267002000521`.

[186] Rudolf Eugster, Thomas Rosatzin, Bruno Rusterholz, Barbara Aebersold, Urs Pedrazza, Denise Rüegg, Angela Schmid, Ursula E. Spichiger, and Wilhelm Simon. Plasticizers for liquid polymeric membranes of ion-selective chemical sensors. *Analytica Chimica Acta*, 289(1):1 – 13, 1994. ISSN 0003-2670. doi: https://doi.org/10.1016/0003-2670(94)80001-4. URL `http://www.sciencedirect.com/science/article/pii/0003267094800014`.

[187] Thomas Rosatzin, Eric Bakker, Koji Suzuki, and Wilhelm Simon. Lipophilic and immobilized anionic additives in solvent polymeric membranes of cation-selective chemical sensors. *Analytica Chimica Acta*, 280(2):197 – 208, 1993. ISSN 0003-2670. doi: https://doi.org/10.1016/0003-2670(93)85122-Z. URL `http://www.sciencedirect.com/science/article/pii/000326709385122Z`.

[188] Shahriar Jamasb, Scott D Collins, and Rosemary L Smith. A Physical Model for Threshold Voltage Instability in Si3N4-Gate H+-Sensitive FET's (pH ISFET's). *IEEE Transactions on Electron Devices*, 45(6):1239–1245, 1998. ISSN 00189383. doi: 10.1109/16.678525.

[189] Anne Senillou, Nicole Jaffrezic-Renault, Claude Martelet, and Serge Cosnier. A miniaturized urea sensor based on the integration of both ammonium based urea enzyme field effect transistor and a reference field effect

transistor in a single chip. *Talanta*, 50(1):219 – 226, 1999. ISSN 0039-9140. doi: https://doi.org/10.1016/S0039-9140(99)00122-8. URL `http://www.sciencedirect.com/science/article/pii/S0039914099001228`.

[190] Dongjin Lee and Tianhong Cui. Low-cost, transparent, and flexible single-walled carbon nanotube nanocomposite based ion-sensitive field-effect transistors for ph/glucose sensing. *Biosensors and Bioelectronics*, 25(10):2259 – 2264, 2010. ISSN 0956-5663. doi: https://doi.org/10.1016/j.bios.2010.03.003. URL `http://www.sciencedirect.com/science/article/pii/S0956566310001211`.

[191] F. C. Macintosh. The distribution of acetylcholine in the peripheral and the central nervous system. *The Journal of Physiology*, 99(4):436–442. doi: 10.1113/jphysiol.1941.sp003913. URL `https://physoc.onlinelibrary.wiley.com/doi/abs/10.1113/jphysiol.1941.sp003913`.

[192] Daniel M. Quinn. Acetylcholinesterase: enzyme structure, reaction dynamics, and virtual transition states. *Chemical Reviews*, 87(5):955–979, 1987. doi: 10.1021/cr00081a005. URL `https://doi.org/10.1021/cr00081a005`.

[193] Jose M. Barbosa Filho, Karina C. Paula Medeiros, Margareth de Fatima F.M. Diniz, Leonia M. Batista, Petronio F. Athayde-Filho, Marcelo S. Silva, Emidio V.L. da Cunha, Jackson R.G. Silva Almeida, and Lucindo J. Quintans-Junior. Natural products inhibitors of the enzyme acetylcholinesterase. *Revista Brasileira de Farmacognosia*, 16:258 – 285, 06 2006. ISSN 0102-695X. URL `http://www.scielo.br/scielo.php?script=sci_arttext&pid=S0102-695X2006000200021&nrm=iso`.

[194] Abraham Ulman. Formation and structure of self-assembled monolayers. *Chemical Reviews*, 96(4):1533–1554, 1996. doi: 10.1021/cr9502357. URL `https://doi.org/10.1021/cr9502357`. PMID: 11848802.

[195] Lou Strong and George M. Whitesides. Structures of self-assembled monolayer films of organosulfur compounds adsorbed on gold single crystals: electron diffraction studies. *Langmuir*, 4(3):546–558, 1988. doi: 10.1021/la00081a009. URL `https://doi.org/10.1021/la00081a009`.

[196] Marcel J. E. Fischer. *Amine Coupling Through EDC/NHS: A Practical Approach*, pages 55–73. Humana Press, Totowa, NJ, 2010. ISBN 978-1-60761-670-2. doi: 10.1007/978-1-60761-670-2_3. URL https://doi.org/10.1007/978-1-60761-670-2_3.

[197] Xin Sun, Han Shao, Ke Xiang, Ya Yan, Xiang Yu, Diansen Li, Wutian Wu, Libing Zhou, Kwok-Fai So, Yi Ren, Seeram Ramakrishna, Ang Li, and Liumin He. Poly(dopamine)-modified carbon nanotube multilayered film and its effects on macrophages. *Carbon*, 113:176 – 191, 2017. ISSN 0008-6223. doi: https://doi.org/10.1016/j.carbon.2016.11.040. URL http://www.sciencedirect.com/science/article/pii/S0008622316310144.

[198] Diletta Sciti, Mylène Brach, and Alida Bellosi. Long-term oxidation behavior and mechanical strength degradation of a pressurelessly sintered zrb2–mosi2 ceramic. *Scripta Materialia*, 53(11):1297 – 1302, 2005. ISSN 1359-6462. doi: https://doi.org/10.1016/j.scriptamat.2005.07.026. URL http://www.sciencedirect.com/science/article/pii/S1359646205004549.

[199] SM Southwick, S Paige, CA Morgan, JD Bremner, JH Krystal, and DS Charney. Neurotransmitter alterations in ptsd: catecholamines and serotonin. *Seminars in clinical neuropsychiatry*, 4(4):242—248, October 1999. ISSN 1084-3612. doi: 10.153/scnp00400242. URL https://doi.org/10.153/SCNP00400242.

[200] Hans C. Lou, Lars Edvinsson, and Eric T. MacKenzie. The concept of coupling blood flow to brain function: Revision required? *Annals of Neurology*, 22(3):289–297. doi: 10.1002/ana.410220302. URL https://onlinelibrary.wiley.com/doi/abs/10.1002/ana.410220302.

[201] Hao Tang, Peng Lin, Helen L.W. Chan, and Feng Yan. Highly sensitive dopamine biosensors based on organic electrochemical transistors. *Biosensors and Bioelectronics*, 26(11):4559 – 4563, 2011. ISSN 0956-5663. doi: https://doi.org/10.1016/j.bios.2011.05.025. URL http://www.sciencedirect.com/science/article/pii/S0956566311003228.

[202] Chih-Heng Lin, Cheng-Yun Hsiao, Cheng-Hsiung Hung, Yen-Ren Lo, Cheng-Che Lee, Chun-Jung Su, Horng-Chin Lin, Fu-Hsiang Ko, Tiao-Yuan Huang, and Yuh-Shyong Yang. Ultrasensitive detection of dopamine using a

polysilicon nanowire field-effect transistor. *Chem. Commun.*, pages 5749–5751, 2008. doi: 10.1039/B812968A. URL `http://dx.doi.org/10.1039/B812968A`.

[203] MD Adams, JM Kelley, JD Gocayne, M Dubnick, MH Polymeropoulos, H Xiao, CR Merril, A Wu, B Olde, RF Moreno, and al. et. Complementary dna sequencing: expressed sequence tags and human genome project. *Science*, 252(5013):1651–1656, 1991. ISSN 0036-8075. doi: 10.1126/science.2047873. URL `http://science.sciencemag.org/content/252/5013/1651`.

[204] Chaker Tlili, Hafsa Korri-Youssoufi, Laurence Ponsonnet, Claude Martelet, and Nicole J. Jaffrezic-Renault. Electrochemical impedance probing of dna hybridisation on oligonucleotide-functionalised polypyrrole. *Talanta*, 68(1): 131 – 137, 2005. ISSN 0039-9140. doi: https://doi.org/10.1016/j.talanta.2005.04.069. URL `http://www.sciencedirect.com/science/article/pii/S0039914005002572`.

[205] Sobhi Daniel, Talasila Prasada Rao, Kota Sreenivasa Rao, Sikhakolli Usha Rani, G.R.K. Naidu, Hea-Yeon Lee, and Tomoji Kawai. A review of dna functionalized/grafted carbon nanotubes and their characterization. *Sensors and Actuators B: Chemical*, 122(2):672 – 682, 2007. ISSN 0925-4005. doi: https://doi.org/10.1016/j.snb.2006.06.014. URL `http://www.sciencedirect.com/science/article/pii/S0925400506004527`.

[206] Charles L. Asbury and Ger van den Engh. Trapping of dna in nonuniform oscillating electric fields. *Biophysical Journal*, 74(2):1024 – 1030, 1998. ISSN 0006-3495. doi: https://doi.org/10.1016/S0006-3495(98)74027-5. URL `http://www.sciencedirect.com/science/article/pii/S0006349598740275`.

[207] P. Lugli, V.D. Bhatt, and K. Melzer. Electrolyte-gated sensor for species detection. In *European Union Patent Application EP3045902A1 Kind Code: A1, Application number EP3045902A1, International Classes: G01N27/4146; Technische Universität München 2015-01*.

[208] P. Lugli, V.D. Bhatt, and K. Melzer. Device for analyzing biological substances in a test solution and production method. In *United States Patent Application US 20170097331 Kind Code: A1, Applicatzion no. 15/281772,*

International Classes: G01N33/487; G01N27/02; G01N33/483, Technische Universität München 2017-04. FreePatentsOnline.com FPO, Apr 2017.

[209] Saumya Joshi, Vijay Deep Bhatt, Ewa Jaworska, Markus Becherer, Krzysztof Maksymiuk, Agata Michalska, and Paolo Lugli. Using Lipophilic Membrane for Enhanced-Performance Aqueous Gated Carbon Nanotube Field Effect Transistors. *Physica Status Solidi (a)*, 1700993:1700993, 2018. ISSN 18626300. doi: 10.1002/pssa.201700993. URL `http://doi.wiley.com/10.1002/pssa.201700993`.

[210] Saumya Joshi, Vijay Deep Bhatt, Andreas Märtl, Markus Becherer, and Paolo Lugli. Regenerative, highly-sensitive, non-enzymatic dopamine sensor and impact of different buffer systems in dopamine sensing. *Biosensors*, 8 (1):1–10, 2018. ISSN 20796374. doi: 10.3390/bios8010009.

[211] Vijay Bhatt, Saumya Joshi, Markus Becherer, and Paolo Lugli. Flexible, Low-Cost Sensor Based on Electrolyte Gated Carbon Nanotube Field Effect Transistor for Organo-Phosphate Detection. *Sensors*, 17(6):1147, 2017. ISSN 1424-8220. doi: 10.3390/s17051147. URL `http://www.mdpi.com/1424-8220/17/5/1147`.

[212] Vijay Deep Bhatt, Shokoufeh Teymouri, Katharina Melzer, Alaa Abdellah, Zeno Guttenberg, and Paolo Lugli. Biocompatibility tests on spray coated carbon nanotube and PEDOT: PSS thin films. *IEEE Transactions on Nanotechnology*, 15(3):373–379, 2016. ISSN 1536125X. doi: 10.1109/TNANO.2016.2535780.

[213] Simone Colasanti, Vijay Deep Bhatt, Ahmed Abdelhalim, and Paolo Lugli. 3-D Percolative Model-Based Multiscale Simulation of Randomly Aligned Networks of Carbon Nanotubes. *IEEE Transactions on Electron Devices*, 63 (3):1346–1351, 2016. ISSN 00189383. doi: 10.1109/TED.2015.2513012.

[214] Simone Colasanti, Valentina Robbiano, Florin Christian Loghin, Ahmed Abdelhalim, Vijay Deep Bhatt, Alaa Abdellah, Franco Cacialli, and Paolo Lugli. Experimental and Computational Study on the Temperature Behavior of CNT Networks. *IEEE Transactions on Nanotechnology*, 15(2):171–178, mar 2016. ISSN 1536-125X. doi: 10.1109/TNANO.2015.2510965.

[215] K. Melzer, V. Deep Bhatt, E. Jaworska, R. Mittermeier, K. Maksymiuk, A. Michalska, and P. Lugli. Enzyme assays using sensor arrays based on

ion-selective carbon nanotube field-effect transistors. *Biosensors and Bioelectronics*, 84:7–14, 2016. ISSN 18734235. doi: 10.1016/j.bios.2016.04.077.

[216] Katharina Melzer, Vijay Deep Bhatt, Tobias Schuster, Ewa Jaworska, Krzysztof Maksymiuk, Agata Michalska, Paolo Lugli, and Giuseppe Scarpa. Flexible Electrolyte-Gated Ion-Selective Sensors Based on Carbon Nanotube Networks. *IEEE Sensors Journal*, 15(6):3127–3134, jun 2015. ISSN 1530-437X. doi: 10.1109/JSEN.2014.2362679.

[217] Qingqing Gong, Vijay Deep Bhatt, Edgar Albert, Alaa Abdellah, Bernhard Fabel, Paolo Lugli, and Giuseppe Scarpa. On the performance of solution-Processable random network carbon Nanotube Transistors: Unveiling the role of network density and metallic tube content. *IEEE Transactions on Nanotechnology*, 13(6):1181–1185, 2014. ISSN 1536125X. doi: 10.1109/TNANO.2014.2351011.

[218] Vijay Deep Bhatt, Saumya Joshi, Katharina Melzer, and Paolo Lugli. Flexible dopamine sensor based on electrolyte gated carbon nanotube field effect transistor. *Proceedings - 2016 IEEE Biomedical Circuits and Systems Conference, BioCAS 2016*, 1:38–41, 2017. doi: 10.1109/BioCAS.2016.7833719.

[219] K. Melzer, V.D. Bhatt, E. Jaworska, K. Maksymiuk, A. Michalska, and P. Lugli. Enzymatic assays based on ion-selective carbon nanotube field-effect transistors. In *Biosensors 2016 26th Anniversary World Congress on Biosensors*. Elsevier B.V., May 2016.

[220] K. Melzer, V.D. Bhatt, and P. Lugli. Immobilization strategies for enzymatic biosensors based on electrolyte-gated carbon nanotube transistors. In *99th Canadian Chemistry Conference and Exhibition*. Canadian Society for Chemistry, Dalhousie University, Jun 2016. URL `http://abstracts.csc2016.ca/00000882.htm;`.

[221] Vijay Deep Bhatt, Katharina Melzer, Alaa Abdellah, Paolo Lugli, Shokoufeh Teymouri, and Zeno Guttenberg. Biocompatibility tests on spray coated carbon nanotube and PEDOT:PSS thin films. In *2015 IEEE 15th International Conference on Nanotechnology (IEEE-NANO)*, volume 15, pages 5–8. IEEE, jul 2015. ISBN 978-1-4673-8156-7. doi: 10.1109/NANO.2015.7388842. URL `http://ieeexplore.ieee.org/document/7388842/`.

[222] Simone Colasanti, Vijay Deep Bhatt, Ahmed Abdelhalim, Alaa Abdellah, and Paolo Lugli. A 3D self-consistent percolative model for AC-DC electrical analysis of carbon nanotubes networks. *International Conference on Simulation of Semiconductor Processes and Devices, SISPAD*, 2015-Octob: 100–103, 2015. ISSN 1946-1569. doi: 10.1109/SISPAD.2015.7292268.

[223] S. Colasanti, V. Deep Bhatt, A. Abdellah, and P. Lugli. 3D self-consistent percolative model for networks of randomly aligned carbon nanotubes. *Journal of Physics: Conference Series*, 647(1):3–7, 2015. ISSN 17426596. doi: 10.1088/1742-6596/647/1/012018.

[224] Simone Colasanti, Vijay Deep Bhatt, and Paolo Lugli. 3D modeling of CNT networks for sensing applications. In *2014 10th Conference on Ph.D. Research in Microelectronics and Electronics (PRIME)*, pages 1–4. IEEE, jun 2014. ISBN 978-1-4799-4994-6. doi: 10.1109/PRIME.2014.6872679.

[225] Saumya Joshi, Vijay Bhatt, Ewa Jaworska, Agata Michalska, Krzysztof Maksymiuk, Markus Becherer, Alessio Gagliardi, and Paolo Lugli. Ambient processed, water-stable, aqueous-gated sub-1v n-type carbon nanotube field effect transistor. *Scientific Reports*, March 2018.

[226] Saumya Joshi, Vijay Deep Bhatt, Himanshi Rani, Markus Becherer, and Paolo Lugli. Understanding the influence of in-plane gate electrode design on electrolyte gated transistor. *Microelectronic Engineering*, Feb 2018.